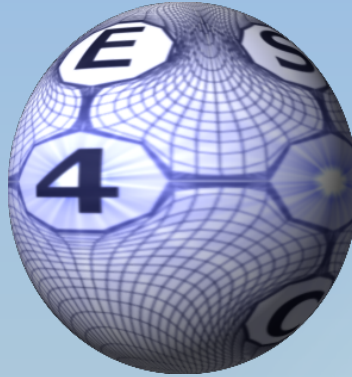
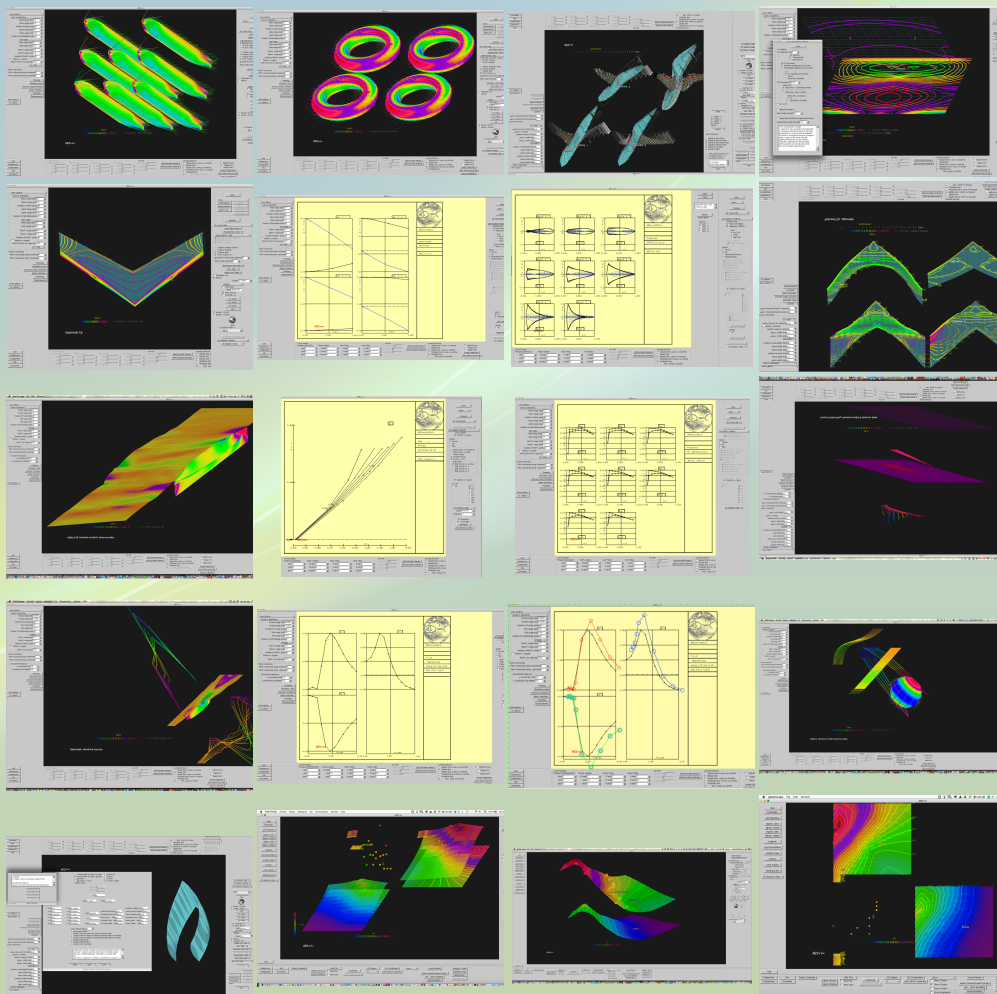


Modelling, prediction and analysis of subsonic & supersonic (hypersonic)  
steady & unsteady aerodynamics, free surface hydrodynamics and aeroacoustics  
for oscillating and deforming aircraft and watercraft



Michael H.L. Hounjet



No part of this report may be reproduced and/or disclosed, in any form or by any means  
without the prior written permission of AES4AC B.V. ([www.aes4ac.com](http://www.aes4ac.com))







## Contents

<b>Summary</b>	<b>6</b>
<b>Introduction</b>	<b>8</b>
<b>Mathematical models</b>	<b>10</b>
<i>Aerodynamic model</i>	10
Flow equation	10
Boundary equations	11
Planar wakes	12
Flexible and rotating surfaces	12
Gusts	12
Solid Walls	12
Symmetry & Anti-Symmetry	13
Runway	13
Transonic flow	13
Permeability	13
Characteristics quantities	13
Mach number adaptation.	15
Quantities of Interest	16
Elementary solutions:	16
<i>Hydrodynamic model</i>	17
Flow equation	17
Boundary equations	18
Planar wakes	19
Flexible and rotating surfaces	19
Waves	19
Solid Walls	19
Symmetry & Anti-Symmetry	19
Permeability	19
Characteristics quantities	20
Quantities of Interest	21
Elementary solutions:	22
<i>Aeroacoustics model</i>	26
Flow equation	26
Boundary equations	27
Flexible and rotating surfaces	27
Gusts	27
Solid Walls	28
Symmetry & Anti-Symmetry	28
Incident Waves	28
Characteristic quantities	28
Quantities of Interest	29
Elementary solutions:	29
<b>Solution method</b>	<b>31</b>
<i>Integral equation method</i>	31
<i>Gradient free boundary volume method</i>	33
<i>Kutta condition</i>	35
<i>Potential Influence Coefficients</i>	36
Aerodynamic influence coefficients	37
Hydrodynamic influence coefficients	38

Aeroacoustics influence coefficients	38
<i>Solution method</i>	38
<i>Downwash</i>	39
<i>The outputs</i>	40
<b>Warping</b>	<b>41</b>
<i>Volume spline/Mollifying method or VSIC (Volume Spline Injection Continuation) method</i>	42
<i>The volume spline method</i>	43
<i>The mollifier or the VSIC method</i>	46
Mollifier demo	47
<b>Digital model description</b>	<b>50</b>
<i>Geometry</i>	50
Geometric Input file	50
Patch types	51
Lift Carry Over strips	52
Wakes	52
Static Geometry	52
Connection of Patches	53
<i>Dynamics Geometry</i>	56
<i>General modes file format</i>	56
Regular Vibration Input file	56
<i>Polynomial modes file</i>	57
<i>Flow Dynamics</i>	58
<i>Outputs</i>	58
<i>File outputs</i>	58
<i>Efficiency</i>	59
<b>Examples of applications</b>	<b>60</b>
<i>Aerodynamic examples</i>	61
A set of donuts	61
A set of payloads	61
Change of geometry	62
Warping on a wing fuselage	62
Approximate transonic modelling	63
Wing 445.6 Steady	64
Wing 445.6 unsteady	66
<i>Hydrodynamic examples</i>	68
The Wigley Hull	68
The submerged sphere	69
The submerged Delta wing of Rene Coene	70
A submerged spheroid	71
<i>Aeroacoustics example</i>	73
<b>Summary of the AES=O= method</b>	<b>74</b>
<i>I: Steady and Unsteady Aerodynamics</i>	74
<i>II: Steady and Unsteady Hydrodynamics</i>	74
<i>III: aeroacoustics</i>	75
<b>Installation</b>	<b>76</b>
<b>How to Run and Use information</b>	<b>77</b>
<i>License validation</i>	80
<i>Left Sidebar</i>	81
Case Parameters	85
Configuration Parameters	87



Downwash	97
<i>Left Sidebar Bottom</i>	113
Preferences Button > Preferences window.	113
<i>Bottom bar</i>	116
Bottom bar right row	116
Bottom bar mid row (Aerodynamics&Aeroacoustics)	116
Bottom bar mid row (Hydrodynamics)	116
<i>Right sidebar</i>	118
Mode Selector Button> Modes window	122
GAF Selector Button> GAF window	122
<b>Running AES=O=</b>	<b>132</b>
<i>The Input files</i>	132
The .prefs_aes=o= file	132
Table 33 .prefs_aes=o= file	134
The aes=o=.cnf file	134
<i>Outputs</i>	135
<b>An aerodynamic demo application</b>	<b>136</b>
<b>Conclusions</b>	<b>151</b>
<b>Bibliography</b>	<b>152</b>
<b>Appendix AES4AC B.V.</b>	<b>155</b>
<b>List of Figures</b>	<b>156</b>
<b>List of Tables</b>	<b>159</b>

## Summary

AES=O= performs the prediction & analysis of compressible steady & unsteady aerodynamics (subsonic & supersonic), incompressible hydrodynamics (implicitly and explicitly including free surfaces) and aeroacoustic quantities of interest for multipart deformed/trimmed and oscillating Aircraft & Watercraft configurations.

### *Flow equations*

Hydrodynamics, Aerodynamics and unsteady aerodynamics/aeroacoustics are modelled with the Laplace, the Prandl Glauert equation and the well-known equation of acoustics, respectively. The latter becomes the convective Helmholtz equation for Mach number is zero.

### *Methodology*

The true surface gradient free Boundary Volume Method (BVM) [1] for potential flows.

### *Configurations*

Realistic geometries (wings/T-tails/ Winglets/ fuselages/ payloads/ ships/ submarines et cetera (thick and thin))

### *Specifics*

Effects of symmetry, anti-symmetry, runway, sea bottom, free surfaces and observer surfaces are modelled. A permeability model for supersonic inlets/outlets & bluff body parts modelling and a shockwave model for approximate transonic modelling [2] is included. A Mach number correction model for approximate hypersonic flow ([3]) is embedded. Hydrodynamic configurations beneath a free surface can be modelled with explicit surfaces (Rankine [4]) applying the linearized free surface boundary condition or implicitly (Havelock [5, 6]) with elementary solutions that satisfy the linearized free-surface boundary condition and radiation conditions.

### *Oscillations, deformations, seedings*

Rigid motions and sub-rigid (effectors) motions/deformations are modelled including arbitrary elastic (e.g. FEM modals) motions/deformations of the configurations. Arbitrary deformation is warped by efficient volume spline class methods<sup>1</sup>. The flow field might include gusts & waves & scattered sound fields.

### *Time behaviour*

The time behaviour of oscillating configuration parts or unsteady flow elements (gusts, waves) is not restricted to harmonic oscillations and extended to exponentially undamped motions [7]. Also the H method [8] is embedded to analytically extend data for harmonic oscillations to data for exponentially undamped motions.

### *Potential flow*

The potential flow field is composed with a superposition of distributions of elementary potential solutions of the governing equations at selected surfaces of the configuration and/or free surfaces and/or a shock surface. Constant source and/or constant/linear doublet singularities can be applied at the surface of the configuration or at the camber surface.<sup>2</sup>

---

<sup>1</sup> As a bonus, the mollifier/VSIC method has been described and demonstrated

<sup>2</sup> An AES=3= type modelling can also be adopted in lifting surface mode (Doublet Lattice in subsonic flow. Potential Gradient or Constant pressure model in supersonic flow).



### *Gradient free Boundary Volume Method*

The gradient free Boundary Volume Method [1] is the method of solution. The scalar potential due to distributions of elementary solutions (sources, doublets) is evaluated at discrete points at wetted surfaces and at ghost surfaces located a relatively small distance from them. The strength of the distributions is obtained by imposing boundary conditions with a flux-balance model in incompressible/subsonic flow and characteristic differentiation for supersonic flow using the potential values at the discrete points avoiding analytical gradients, collocation and tedious dealing with the integration and derivatives of the elementary solutions.

### *Application inputs*

The input model is composed of patches describing the configuration, observer patches (interference analysis), patches describing the free-surface for hydrodynamic modelling (explicit Rankine model), and patches describing a shock interface. The deformation/oscillation is prescribed for each patch. Incident sea waves, the incident sound potential, a geometry correction (representing boundary layer/edge effects), a trim vector (+static deformation and effector settings) can be set. Structural data (geometry & mode shapes et cetera) is efficiently warped to the aerodynamic configuration geometry by means of Hounjet's well-known volume spline [9] [10, 11] methods.

### *Application outputs*

The main quantities of interest are pressure and force<sup>3</sup>/generalised force coefficients. They are available as data file, excel file and on screen graphical output. The pressure coefficient distribution can be factored with a correction (Mach (Froude) number, frequency and position dependent!) to accommodate for missing transonic, boundary layer and edge effects. The pressure coefficients are obtained at the center of panel leading and trailing edges and used in the calculation of generalized forces. At subsonic edges of lifting surfaces care has been taken to deal with the singular behaviour of the pressure and to integrate the pressures consistent with the evaluation of forces by global methods.

### *Execution*

Efficiency is offered by storage of warpings for reuse, accommodating follow on stages of a design cycle (Mach/Froude number and/or frequency changes) and by storage of the solution matrices for reuse accommodating follow on stages of a design cycle (mode shape changes). Also it is made possible to coarsen the paneling in one button click to reduce computational work. Calculations can also be performed in batch. The input and output data can be interactively inspected/analysed. The patches can be edited/generated on the fly.

---

• <sup>3</sup> Suction Force modelling (Exact induced drag on lifting surfaces)

## Introduction

The **AES=O=** method, developed by AES4AC B.V. (see Appendix AES4AC) is directed to the prediction of steady and unsteady linearized potential flow aero(hydro)dynamics (forces & pressures) on arbitrary thin & thick (2D & 3D) deformed/trimmed and oscillating Aircraft and watercraft configurations with a broad application range of Mach number, Froude number, frequency, angle of attack/slip, trim and sinkage, vibration modes, sea waves, scattered waves & gust modes.

In particular **AES=O=** calculates 3 types of physics:

1. *Aerodynamics*: Steady and unsteady pressures and forces on arbitrary aircraft structures for subsonic ( $Mach=0..1$  and supersonic/hypersonic ( $Mach = 1..$ ) speeds governed by the thin-aerofoil equations (Laplace, Prandl-Glauert)<sup>4</sup>. The structures are deformed and/or trimmed and/or oscillating with arbitrary oscillating vibration modes or placed in arbitrary oscillating flows characterized by the divergence rate (exponential growing motions) and the reduced frequency (oscillating sinusoidal motions). Also, transonic effects can be approximately modelled ([2]) and hypersonic effects ([3]). Accurate Suction Force modelling (correct induced drag on lifting surfaces).
2. *Hydrodynamics*: Steady and unsteady pressures and forces on arbitrary watercraft structures for incompressible ( $Mach=0$ ) speeds governed by the Laplace equation moving in the vicinity of free surfaces and/or sidewalls and sea bottoms. The structures are oscillating with arbitrary oscillating vibration modes or placed in arbitrary oscillating flows characterized by the divergence rate and the reduced frequency. Efficient integration of Havelock sources & doublets (implicit linearized free-surface BC) for Froude  $\geq 0$  and frequency  $\geq 0$  with a unique efficient proprietor integration method (Telles [12]-Filon et cetera). Alternatively, the free surface can be taken into account with a Rankine explicit model. Also, trim and sinkage is taken into account.
3. *Aeroacoustics*: pressures on arbitrary structures governed by the well-known equation of acoustical theory which becomes the convective Helmholtz equation [13] at Mach number zero. Easy modelling of incident sound potential & impedance distributions.

The **AES=O=** modeling is based on the unique true surface gradient free Boundary Volume Method (BVM) method for realistic geometry and lifting surface methods. ([1]). The BVM method is a strict potential formulation, imposing boundary condition with a flux-balance model in subsonic flow and characteristic differentiation for supersonic flow. It uses the evaluation of the potential at the A/C surface and at a virtual surface located a relatively small distance from it.

Constant source and/or constant doublet distributions of singularities can be applied at the A/C surface or at the camber surface.

---

<sup>4</sup> The well-known equation of acoustical theory is applied for the unsteady case



Other characteristics are:

- The geometry of the structure is modelled with components(patch). Each component is composed of quadrilaterals (panels).
- Symmetric, anti-symmetric, runway, sea bottom, wall models and free surface Rankine models.
- Shock patches for approximate transonic flow.
- Observer surfaces for interference analysis.
- Permeability model for inlets/outlets & bluff body parts modelling.
- Rigid, sub-rigid (effectors) & arbitrary motions/deformations, gusts & waves.
- Geometry correction (Mach (Froude) number, angle of attack, Reynolds number & position dependent!) to accommodate boundary layer and edge effects.
- Trim vector to model static deformation and effector settings.
- H continuation of harmonic generalised forces (ref )
- 3D inspection/analysis of panelling, trim state (static deformation & effector settings), displacement modes, pressure distribution & warping.
- And more



## Mathematical models

This chapters presents the mathematical models.

### Aerodynamic model

The aerodynamics is modelled with the thin-aerofoil potential flow equations for subsonic and supersonic flow (without strong shockwaves) conditions. The potential flow is considered around an oscillating body, which is a superposition on a uniform flow with free-stream velocity or on the flow about the steady body. Alternatively the potential flow is considered around a steady body, which is a superposition on a uniform flow with free-stream velocity and incoming gusts. The vorticity is everywhere zero, except for areas occupied by thin lifting surfaces and wakes. A Cartesian coordinate system is chosen fixed to the mean position of the body with the  $x$ -axis in the direction of the free-stream velocity vector  $V$ . The body can be rotated by the Angle of Attack and the Angle of side-slip A disturbance velocity potential is introduced which is split up into a steady part  $\phi$  and an exponentially varying unsteady part  $\phi e^{-sT}$ .  $s=g+ik$ ,  $g$  denotes the divergence rate,  $k$  is the reduced frequency of the motion,  $k = \omega L/V$ ,  $T$  the reduced time  $T=t V/L$ ,  $t$  is time and  $L$  a reference length.  $\omega$  denotes the frequency of oscillation.

All variables have been made dimensionless with the free stream velocity and/or the reference length  $L$ . The pressure coefficients have been made dimensionless with the dynamic pressure  $\frac{1}{2} \rho V^2$

### Flow equation

The steady velocity potential satisfies the Prandl-Glauert equation:

$$H\phi = \phi_{zz} + \phi_{yy} + (1 - M^2)\phi_{xx} = 0 \quad \text{E 1}$$

Which implies that the velocity disturbances are small compared to the speed of sound and that thickness, angle of attack and side slip angle should decrease asymptotically with  $|1-M| \Rightarrow 0$ .  $M$  is the Mach number. The unsteady velocity potential  $\phi e^{-sT}$  satisfies the equation:

$$H_s \phi = \phi_{zz} + \phi_{yy} + (1 - M^2)\phi_{xx} - 2sM^2\phi_x - s^2M^2\phi = 0 \quad \text{E 2}$$

where in addition the assumption is made that  $\phi$  and its derivatives are small compared to  $\phi$  and its derivatives. Both equations are valid in the fluid domain outside the wetted surfaces and wake areas.



It is required that disturbances propagate outwards from the body to infinity and in supersonic flow remain in the zone of dependence formed by the Mach cone with apex half-angle of  $\tan^{-1}(\frac{1}{1-M^2})$  which originates at the upstream origin of the disturbances.

### Boundary equations

At the boundaries of the bodies the conditions for tangential flow or for zero mass flux as described in references [14], [15] may be imposed for the steady flow:

$$\vec{V} \cdot \vec{N} = 0 \quad \text{E 3}$$

or

$$\vec{V} \cdot \vec{N} = M^2 \varphi_x N_x \text{ (mass flux [14] [15])} \quad \text{E 4}$$

For the unsteady flow the body boundary conditions are defined by one of the following formulas:

- The standard form for tangential flow:

$$\vec{q} \cdot \vec{N} + \vec{V} \cdot \vec{n} = s \vec{h} \cdot \vec{N} \quad \text{E 5}$$

- The linear formula for tangential flow:

$$\vec{q} \cdot \vec{N} + \vec{V}_f \cdot \vec{n} = s \vec{h} \cdot \vec{N} \quad \text{E 6}$$

- The unsteady mass flux formula:

$$\vec{q} \cdot \vec{N} + \vec{V} \cdot \vec{n} - M^2 \varphi_x (N_x - s N_x + n_x) = (1 - M^2 \varphi_x) s \vec{h} \cdot \vec{N} \quad \text{E 7}$$

$\vec{V}$  is the steady velocity vector defined by:  $\vec{V} = \vec{V}_f + \vec{\nabla} \phi$ ,  $\vec{q}$  is the unsteady part defined by  $\vec{q} = \vec{\nabla} \phi$ ,  $h$  denotes the displacement of the body from its mean position,  $\vec{N}$  is the mean steady out normal at the body boundaries and  $\vec{n}$  is the exponentially varying unsteady part of this direction.

$\vec{N}$  is defined by:

$$\vec{N} = \vec{S} \times \vec{T} \quad \text{E 8}$$

Where  $\vec{S}$  and  $\vec{T}$  are distinct in plane directions at the mean body surface.

$\vec{n}$  is defined as:

$$\vec{n} = \vec{S} \times \vec{t} + \vec{s} \times \vec{T} \quad \text{E 9}$$

Where  $\vec{t}$  and  $\vec{s}$  are distinct in plane directions caused by the motion or deformation.

At the trailing edge the Kutta condition is applied of a smooth potential continuation from the body surface to the wake surface. At sharp trailing edges of lifting components where the Mach number of the steady velocity normal to the edge is smaller than one (subsonic trailing edge) the Kutta condition is imposed in the form that the pressure difference between upper and lower side at such a trailing edge is zero. When the Mach number of this velocity component is larger than one (supersonic trailing edge) continuity of the potential difference between upper and lower side in free-stream direction is imposed. At trailing edges wake surfaces are emanating causing a jump in the potential. The jump in the potential adheres to the requirement of no pressure difference between the upper and lower surface of the wakes:

$$[[c_p]] = 0 \quad \text{E 10}$$

$$[[c_p^s]] = 0 \quad \text{E 11}$$

## Planar wakes

The direction and shedding velocity of the planar wake is defined by the  $x$ -axis and the free-stream velocity. The user is allowed to specify the direction in order to avoid the crossing of the wake with another thick surface, although the shedding velocity remains the free-stream velocity. The planar wakes should not intersect another configuration component.

## Flexible and rotating surfaces

The displacement  $h$  is modelled by one of the methods presented in section Downwash

## Gusts

The equivalent displacement  $h$  is modelled by one of the methods presented in section Downwash

## Solid Walls

The potential is assumed symmetric with respect to the wall.



## Symmetry & Anti-Symmetry

Semi models can be applied assuming the steady potential is symmetric and the unsteady potential is symmetric or anti-symmetric for symmetric and anti-symmetric modes, respectively.

## Runway

The ground effect during start/landing can be assessed using a solid wall.

## Transonic flow

A first order approximation of transonic effects is to introduce a shock patch and apply a shock condition [2]. The effect of transonic flow can be approximated by assuming a shock plane at a known position and speed jump  $[[\phi_x]]$ . At the shock surface the linearized shock condition of Landahl [16] is applied:

$$[[\phi_x]] = \frac{-2s}{\gamma + 1} \frac{[[\phi]]}{\langle \phi_x \rangle} \quad \text{E 12}$$

## Permeability

The permeability model for inlets/outlets & bluff body parts modelling is simply:

$$\vec{q} \cdot \vec{N} = P (\vec{q} \cdot \vec{N}) \quad \text{E 13}$$

$P$  is the permeability factor.

## Characteristics quantities

The steady pressure coefficient  $C_p$  is defined by one of the following formulae

$$\text{Isentropic } C_p = \frac{2}{\gamma M^2} \left[ \left( 1 - \frac{\gamma-1}{2} M^2 (V^2 - 1) \right)^{\frac{\gamma}{\gamma-1}} - 1 \right] \quad \text{E 14}$$

$$\text{Linear } C_p = -2 \vec{V}_f \cdot \vec{\nabla} \phi \quad \text{E 15}$$

$$\text{Quadratic } C_p = -2\phi_x - (1 - M^2)\phi_x^2 - \phi_y^2 - \phi_z^2 \quad \text{E 16}$$

The quadratic formula is compliant with the mas flux boundary condition.

At wakes the quasilinear formula is only applied:

$$C_p = -2 \vec{V}_* \cdot \vec{\nabla} \varphi \rho^0 \quad \text{E 17}$$

$\rho$  is the steady density defined by one of the following formulae:

$$\rho^0 = \left( 1 + \frac{\gamma - 1}{2} M^2 (1 - V^2) \right)^{\frac{1}{\gamma - 1}} \quad \text{E 18}$$

the linear formula:

$$\rho^0 = 1 - M^2 (\vec{V}_f \cdot \vec{\nabla} \varphi) \quad \text{E 19}$$

and  $\vec{V}_*$  denotes the part of the steady velocity vector which is tangential to the wake surface:

$$\vec{V}_* = \vec{V} - (\vec{V} \cdot \vec{N}) \vec{N} / (\vec{N} \cdot \vec{N}) \quad \text{E 20}$$

The unsteady pressure coefficient is defined by one of the following expressions:

i) the linear unsteady formula:

$$C_p^s = -2 \rho^0 (s \theta + \vec{V}_f \cdot \vec{\nabla} \theta) \quad \text{E 21}$$

11) the linear unsteady isentropic formula:

$$C_p^s = -2 \rho^0 (s \theta + \vec{V} \cdot \vec{\nabla} \theta) \quad \text{E 22}$$

the modified form which is consistent when the unsteady mass flux boundary conditions are applied:

$$C_p^s = -2 \rho^0 s \theta - 2 (\vec{V} \cdot \vec{\nabla} \theta - M^2 \varphi_x \theta_x) \quad \text{E 23}$$



The pressure coefficients have been made dimensionless with the free stream dynamic pressure  $0.5 \rho_f V_f^2$

### Mach number adaptation.

In supersonic (especially hypersonic flow) flow the local angle of attack at leading edges and bluff noses might be too high and needs to be reduced to avoid breaking down of the calculation or to obtain a better match with more sophisticated predictions. Therefore, two remedies can be applied which reduce the Mach number to a lower Mach number.

#### Local Mach number reduction

At an A/C fuselage nose one can reduce the Mach number locally compliant with the flow over a cone with the same local angle of attack based on the following formulae derived from an approximation of table 7 of [17].

$$M_{reduced} = \sum_{i=1}^3 \sum_{j=1}^2 c(i, j) e^{-0.225(i-1)(\sin \theta)^{0.66}} e^{-0.306(j-1)M_{\infty}^{0.33}} \quad \text{E 24}$$

$$c(1..3, 1..2) = /-5.30, 0.79, 5.75, 6.21, -0.48, -5.94/ \quad \text{E 25}$$

$\theta$  is the local angle of attack.

#### Global Mach number reduction

For a wing and even a complete configuration one can reduce the Mach number compliant with the flow over a wedge with an effective angle [18].  $\theta$  is the compliant equivalent wedge angle.

$$M_{reduced} = \sum_{i=1}^2 \sum_{j=1}^2 c(i, j) e^{-0.533(i-1)(\sin \theta)^{0.66}} e^{-2.78(j-1)M_{\infty}^{0.33}} \quad \text{E 26}$$

$$c(1..2, 1..2) = /-1.02, 2.11, 6.74, -7.28/ \quad \text{E 27}$$

## Quantities of Interest

Aerodynamic Forces are usually obtained by integration of the pressures over the wetted surface parts of the bodies. Moments are usually obtained by integration of the product pressures times distance to origin over the wetted surface parts of the bodies. An adequate discretization is needed to obtain accurate loads adhering to well-known properties (zero drag 2D) of potential flow associated with representing adequately the pressure gradients and the tangential flow conditions and in case of the lifting surface approximation it does not show the well-known property of no drag on a 2-D air foil in potential flow, due to the neglect of the suction force. Here we fortify the pressures with the additional term  $C_p = C_p - 2 \rho \vec{V} \cdot \vec{N}$  that is zero when the tangential flow is ideally satisfied and conserves the no drag properties implicitly no matter what discretization has been used. Its origin lies in formulas as derived by W.E. Cummings [19] in 1957 for the loads on a body in an arbitrary time-dependent incompressible potential flow including rotation. This permits the accurate determination of the suction force in case the lifting surface approximation is applied. Furthermore, an option is provided which rotates the steady and unsteady suction force normal to the wing (Polhamus suction analogy, [20]) in order to estimate global effects of leading-edge separation without modelling the wakes emanating from sharp

### Generalised forces

Generalised forces are obtained by integration of the product pressure times normal displacement  $C_p \vec{h} \cdot \vec{n}$  over the wetted surface parts of the bodies.

### Elementary solutions:

The source singularity of equation E 2 is:

$$E^s(x, y, z) = -\frac{e^{\frac{sM(Mx-R)}{1-M^2}}}{4\pi R}, M < 1 \quad \text{E 28}$$

$$E^s(x, y, z) = -u(x)u(x - \sqrt{(M^2 - 1)(y^2 + z^2)}) \frac{e^{\frac{sM^2x}{1-M^2}} Re(e^{\frac{-sMR}{1-M^2}})}{2\pi R}, M > 1 \quad \text{E 29}$$

$$R = \sqrt{x^2 - (M^2 - 1)(y^2 + z^2)} \quad \text{E 30}$$

$u$  denotes the Heaviside step function.





## Hydrodynamic model

Hydrodynamics are modelled about objects moving in the vicinity below of a free surface. The effect of the free surface is modelled with two methods:

- With Havelock [5] elementary solutions implicitly satisfying the free surface boundary condition or with
- The Rankine [4] approach requiring the discretization of the free surface and the discretization of the free surface condition

The hydrodynamics is modelled with the Laplace potential flow equations for incompressible flow. The potential flow is considered around an oscillating body, which is a superposition on a uniform flow with free-stream velocity or on the flow about the steady body. Alternatively the potential flow is considered around a steady body at a prescribed TRIM and Sinkage, which is a superposition on a uniform flow with free-stream velocity and incoming waves. The vorticity is everywhere zero, except for areas occupied by thin lifting surfaces and wakes. A Cartesian coordinate system is chosen fixed to the mean position of the free surface with the  $x$ -axis in the direction of the free-stream velocity vector  $V_f$ . A disturbance velocity potential is introduced which is split up into a steady part  $\varphi$  and an exponentially varying unsteady part  $\phi e^{-sT}$ .  $s=ik$ ,  $k$  is the reduced frequency,  $k = \omega L/V_f$ ,  $T$  the reduced time  $T=t V_f/L$ ,  $t$  is time and  $L$  a reference length.  $\omega$  is the frequency of the oscillation. The model is directed to slender or thin ship hull surfaces and its formulation is basically the same as the aerodynamic formulation for Mach=0 with the addition of the linear free surface condition and choosing the free surface at  $z=0$ .

## Flow equation

The steady velocity potential satisfies the Laplace equation:

$$H\varphi = \varphi_{zz} + \varphi_{yy} + \varphi_{xx} = 0 \quad \text{E 31}$$

Also, the unsteady velocity potential  $\phi e^{-sT}$  satisfies also the Laplace equation:

$$H_s\phi = \phi_{zz} + \phi_{yy} + \phi_{xx} = 0 \quad \text{E 32}$$

where in addition the assumption is made that  $\phi$  and its derivatives are small compared to  $\varphi$  and its derivatives. Both equations are valid in the fluid domain outside the wetted surfaces and wake areas.

## Boundary equations

At the free surface the boundary condition is:

$$V_f^2 \varphi_{xx} + g\varphi_z = 0 \quad \text{at } z=0 \quad \text{E 33}$$

for the steady flow and

$$s^2 \theta - 2V_f s \theta_x + V_f^2 \theta_{xx} + g\theta_z = 0 \quad \text{at } z=0 \quad \text{E 34}$$

for the unsteady flow

This implies relatively small deviations from the undisturbed situation,  $g$  is gravity.

At the boundaries of the bodies the conditions for tangential flow may be imposed for the steady flow:

$$\vec{V} \cdot \vec{N} = 0 \quad \text{E 35}$$

For the unsteady flow the body boundary conditions are defined by one of the following formulas:

- The standard form for tangential flow:

$$\vec{q} \cdot \vec{N} + \vec{V} \cdot \vec{n} = s \vec{h} \cdot \vec{N} \quad \text{E 36}$$

- The linear formula for tangential flow:

$$\vec{q} \cdot \vec{N} + \vec{V}_f \cdot \vec{n} = s \vec{h} \cdot \vec{N} \quad \text{E 37}$$

$\vec{V}$  is the steady velocity vector defined by:  $\vec{V} = \vec{V}_f + \nabla \phi$ ,  $\vec{q}$  is the unsteady part defined by  $\vec{q} = \nabla \phi$ ,  $h$  denotes the displacement of the body from its mean position,  $\vec{N}$  is the mean steady out normal at the body boundaries and  $\vec{n}$  is the exponentially varying unsteady part of this direction.

$\vec{N}$  is defined by:

$$\vec{N} = \vec{S} \times \vec{T} \quad \text{E 38}$$

Where  $\vec{S}$  and  $\vec{T}$  are distinct in plane directions at the mean body surface.

$\vec{n}$  is defined as:



$$\vec{n} = \vec{s} \times \vec{T} + \vec{S} \times \vec{t} \quad \text{E 39}$$

Where  $\vec{t}$  and  $\vec{s}$  are distinct in plane directions caused by the motion or deformation.

## Planar wakes

At sharp trailing edges wake surfaces are emanating causing a jump in the potential. At the trailing edge the Kutta condition is applied of a smooth potential continuation from the body surface to the wake surface. The jump in the potential adheres to the requirement of a zero pressure jump across the wake. Further it is required that no pressure difference exists between the upper and lower surface of the wakes:

$$[[C_p]] = 0 \quad \text{E 40}$$

$$[[C_p^s]] = 0 \quad \text{E 41}$$

## Flexible and rotating surfaces

The displacement  $h$  is modelled by one of the methods presented in section Downwash

## Waves

Incident wave modes can be applied, which satisfy the Laplace equation the free surface condition and the sea bed condition

## Solid Walls

Solid walls (seabed et cetera) are modelled with symmetry or zero tangential flow condition.

## Symmetry & Anti-Symmetry

Symmetric configurations can be modelled with the restriction to the starboard or portside side.

## Permeability

The permeability model for inlets/outlets & bluff body parts modelling is simple:

$$\vec{q} \cdot \vec{N} = P (\vec{q} \cdot \vec{N}) \quad \text{E 42}$$

$P$  is the permeability factor.

## Characteristics quantities

### *free surface elevation*

The free surface elevation is:

$$\eta = -\frac{V_f}{g} \varphi_x \quad \text{E 43}$$

$$\eta^s = -\frac{V_f}{g} \theta_x \quad \text{E 44}$$

### *Pressure coefficient*

The steady pressure coefficient  $C_p$  nondimensionalized with  $\rho V_f^2/2$  and without the hydrostatic part  $2 K_0 z$  where  $K_0 = \frac{g}{V^2}$  is defined by one of the following formulae:

$$\text{Isentropic: } C_p = 1 - V^2 \quad \text{E 45}$$

$$\text{Linear: } C_p = -2 \vec{V}_f \cdot \vec{\nabla} \varphi \quad \text{E 46}$$

$$\text{Quadratic: } C_p = -2\varphi_x - \varphi_x^2 - \varphi_y^2 - \varphi_z^2 \quad \text{E 47}$$

The hydrostatic part can be optionally applied in the pressure.

Quasilinear formula which is only applied at wakes:

$$C_p = -2 \vec{V}_* \cdot \vec{\nabla} \varphi \quad \text{E 48}$$

and  $\vec{V}_*$  denotes the part of the steady velocity vector which is tangential to the wake surface:

$$\vec{V}_* = \vec{V} - (\vec{V} \cdot \vec{N}) \vec{N} / (\vec{N} \cdot \vec{N}) \quad \text{E 49}$$



The unsteady pressure coefficient is defined as one of the following expressions:

1. the linear unsteady formula:

$$C_p^s = -2 (s \theta + \vec{V}_f \cdot \vec{\nabla} \theta) \quad \text{E 50}$$

2. the linear unsteady isentropic formula:

$$C_p^s = -2 (s \theta + \vec{V} \cdot \vec{\nabla} \theta) \quad \text{E 51}$$

At sharp trailing edges of lifting components the Kutta condition is imposed in the form that the pressure difference between upper and lower side at such a trailing edge is zero.

Finally, it is required that disturbances propagate outwards from the body to infinity. All variables have been made dimensionless with the free stream velocity and/or the reference length  $L$ . The frequency of the motion is defined as  $s = ik$  where  $k = \omega L/V_f$  and  $\omega$  denotes the frequency of oscillation. The pressure coefficients have been made dimensionless with the dynamic pressure  $\frac{1}{2} \rho V_f^2$ . The Froude number is defined as  $F_n = \frac{V_f}{\sqrt{gL}}$ .

## Quantities of Interest

Hydrodynamic forces are usually obtained by integration of the pressures over the wetted surface parts of the bodies. Moments are usually obtained by integration of the product pressures times distance to origin over the wetted surface parts of the bodies. An adequate discretization is needed to obtain accurate loads adhering to well-known properties (zero drag 2D) of potential flow associated with representing adequately the pressure gradients and the tangential flow conditions and in case of the lifting surface approximation it does not show the well-known property of no drag on a 2-D air foil in potential flow, due to the neglect of the suction force. Here we fortify the pressures with the additional term  $C_p = C_p - 2 \rho \vec{V} \cdot \vec{N}$  that is zero when the tangential flow is ideally satisfied and conserves the no drag properties implicitly no matter what discretization has been used. Its origin lies in formulas as derived by W.E. Cummings [19] in 1957 for the loads on a body in an arbitrary time-dependent incompressible potential flow including rotation. This permits the accurate determination of the suction force in case the lifting surface approximation is applied. Furthermore, an option is provided which rotates the steady and unsteady suction force normal to the wing (Polhamus suction analogy, [20]) in order to estimate global effects of leading-edge separation without modelling the wakes emanating from sharp leading edges.

### Generalised Hydrodynamic forces GHF (added damping/mass)

Generalised hydrodynamic forces are obtained by integration of the product pressure times normal displacement  $C_p \vec{h} \cdot \vec{n}$  over the wetted surface parts of the bodies. The added mass is defined as Real Part of GHF/k/k while the added damping is defined as the Imaginary part of GHF/ k.

### Elementary solutions:

The elementary solution of the Laplace equation  $\phi_{zz} + \phi_{yy} + \phi_{xx} = \delta(x, y, z)$ :

$$E^L(x, y, z) = \frac{1}{4\pi R} \quad \text{E 52}$$

$$R = \sqrt{(x)^2 + (y)^2 + (z)^2}$$

This singularity which doesn't satisfy the free surface condition is used in the so called Rankine approach, which requires also singularities on the free surface to take care of the latter.

The elementary solution of the Laplace equation that satisfies the free surface condition is chosen in the elegant form of Hoff [5] [6] using the complex exponential function.

$$E(x - u, y - v, z - w) = \frac{1}{4\pi R} - \frac{1}{4\pi R^m} + (I_{01} + I_{02} + I_{11} + \quad \text{E 53}$$

$$I_{12} - I_{21} - I_{22} + I_{33} + I_{34} - I_{43} - I_{44})/4\pi$$

$$R = \sqrt{(x - u)^2 + (y - v)^2 + (z - w)^2} \quad \text{E 54}$$

$$R^m = \sqrt{(x - u)^2 + (y - v)^2 + (z + w)^2} \quad \text{E 55}$$

The integrals are given by:

$$I_{01} = \frac{K_0}{\pi} \int_0^\gamma \frac{K_{1c} e^{K_{1c} \chi_1}}{i\sqrt{4\tau \cos \theta - 1}} E_p(K_{1c} \chi_1) d\theta - \frac{K_0}{\pi} \int_0^\gamma \frac{K_{2c} e^{K_{2c} \chi_1}}{i\sqrt{4\tau \cos \theta - 1}} E_q(K_{2c} \chi_1) d\theta \quad \text{E 56}$$

$$I_{02} = \frac{K_0}{\pi} \int_0^\gamma \frac{K_{1c} e^{K_{1c} \chi_2}}{i\sqrt{4\tau \cos \theta - 1}} E_p(K_{1c} \chi_2) d\theta - \frac{K_0}{\pi} \int_0^\gamma \frac{K_{2c} e^{K_{2c} \chi_2}}{i\sqrt{4\tau \cos \theta - 1}} E_q(K_{2c} \chi_2) d\theta \quad \text{E 57}$$

$$I_{11} = \frac{K_0}{\pi} \int_\gamma^{\frac{\pi}{2}} \frac{K_1 e^{K_1 \chi_1}}{\sqrt{1 - 4\tau \cos \theta}} E_{r1}(K_1 \chi_1) d\theta \quad \text{E 58}$$



$$I_{12} = \frac{K_0}{\pi} \int_{\gamma}^{\frac{\pi}{2}} \frac{K_1 e^{K_1 \chi_2}}{\sqrt{1 - 4\tau \cos \theta}} E_{r2}(K_1 \chi_2) d\theta \quad \text{E 59}$$

$$I_{21} = \frac{K_0}{\pi} \int_{\gamma}^{\frac{\pi}{2}} \frac{K_2 e^{K_2 \chi_1}}{\sqrt{1 - 4\tau \cos \theta}} E_{r2}(K_2 \chi_1) d\theta \quad \text{E 60}$$

$$I_{22} = \frac{K_0}{\pi} \int_{\gamma}^{\frac{\pi}{2}} \frac{K_2 e^{K_2 \chi_2}}{\sqrt{1 - 4\tau \cos \theta}} E_{r2}(K_2 \chi_2) d\theta \quad \text{E 61}$$

$$I_{33} = \frac{K_0}{\pi} \int_0^{\frac{\pi}{2}} \frac{K_3 e^{K_3 \chi_3}}{\sqrt{1 + 4\tau \cos \theta}} E_{r3}(K_3 \chi_3) d\theta \quad \text{E 62}$$

$$I_{34} = \frac{K_0}{\pi} \int_0^{\frac{\pi}{2}} \frac{K_3 e^{K_3 \chi_4}}{\sqrt{1 + 4\tau \cos \theta}} E_{r3}(K_3 \chi_4) d\theta \quad \text{E 63}$$

$$I_{43} = \frac{K_0}{\pi} \int_0^{\frac{\pi}{2}} \frac{K_4 e^{K_4 \chi_3}}{\sqrt{1 + 4\tau \cos \theta}} E_{r4}(K_4 \chi_3) d\theta \quad \text{E 64}$$

$$I_{44} = \frac{K_0}{\pi} \int_0^{\frac{\pi}{2}} \frac{K_4 e^{K_4 \chi_4}}{\sqrt{1 + 4\tau \cos \theta}} E_{r4}(K_4 \chi_4) d\theta \quad \text{E 65}$$

$$\gamma = 0 \quad \tau = \frac{\omega V}{g} < 1/4$$

$$\gamma = \cos^{-1} \frac{\tau}{4} \quad \tau > 1/4 \quad \text{E 66}$$

$$K_0 = \frac{g}{V_f^2} \quad \text{E 67}$$

$$E_p(Z) = E_1(Z) \quad \text{Re } Z \geq 0$$



$$E_p(Z) = E_1(Z) \quad \text{Re } Z < 0 \quad \text{Im } Z \geq 0 \quad \mathbf{E\ 68}$$

$$E_p(Z) = E_1(Z) - 2\pi i \quad \text{Re } Z < 0 \quad \text{Im } Z < 0$$

$$E_q(Z) = E_1(Z) \quad \text{Re } Z \geq 0$$

$$E_q(Z) = E_1(Z) \quad \text{Re } Z < 0 \quad \text{Im } Z < 0 \quad \mathbf{E\ 69}$$

$$E_q(Z) = E_1(Z) + 2\pi i \quad \text{Re } Z < 0 \quad \text{Im } Z \geq 0$$

$$E_{r1}(Z) = E_1(Z) \quad \text{Im } Z \geq 0$$

$$E_{r1}(Z) = E_1(Z) - 2\pi i \quad \text{Im } Z < 0 \quad \mathbf{E\ 70}$$

$$E_{r2}(Z) = E_1(Z) \quad \text{Im } Z < 0$$

$$E_{r2}(Z) = E_1(Z) + 2\pi i \quad \text{Im } Z \geq 0 \quad \mathbf{E\ 71}$$

$$E_{r3}(Z) = E_1(Z) \quad \text{Im } Z \geq 0$$

$$E_{r3}(Z) = E_1(Z) - 2\pi i \quad \text{Im } Z < 0 \quad \mathbf{E\ 72}$$

$$E_{r4}(Z) = E_1(Z) \quad \text{Im } Z \geq 0$$

$$E_{r4}(Z) = E_1(Z) - 2\pi i \quad \text{Im } Z < 0 \quad \mathbf{E\ 73}$$

Where  $E_1$  is the complex exponential function and further

$$\chi_1 = K_0((z + w) + i(-(x - u) \cos \theta + (y - v) \sin \theta))) \quad \mathbf{E\ 74}$$

$$\chi_2 = K_0((z + w) + i(-(x - u) \cos \theta - (y - v) \sin \theta))) \quad \mathbf{E\ 75}$$

$$\chi_3 = K_0((z + w) + i((x - u) \cos \theta + (y - v) \sin \theta))) \quad \mathbf{E\ 76}$$



$$\chi_4 = K_0((z + w) + i((x - u) \cos \theta + (y - v) \sin \theta))) \quad \mathbf{E\ 77}$$

And:

$$\sqrt{K_{1c}} = \tau \frac{1 - i\sqrt{4\tau \cos \theta - 1}}{2\tau \cos \theta} \quad \mathbf{E\ 78}$$

$$\sqrt{K_{2c}} = \tau \frac{1 + i\sqrt{4\tau \cos \theta - 1}}{2\tau \cos \theta} \quad \mathbf{E\ 79}$$

$$K_3 = \frac{1 + 2\tau \cos \theta - i\sqrt{1 + 4\tau \cos \theta}}{2(\cos \theta)^2} \quad \mathbf{E\ 80}$$

$$K_4 = \frac{1 + 2\tau \cos \theta + i\sqrt{1 + 4\tau \cos \theta}}{2(\cos \theta)^2} \quad \mathbf{E\ 81}$$

## Aeroacoustics model

This tool models acoustic scattering based on the well-known acoustic equation. It should be noted that for a zero Mach number the latter equation becomes the convective Helmholtz equation [13] provided that the reduced frequency is based on the speed of sound  $c$  and the potential is made dimensionless with  $Lc$  where  $L$  is the reference length. In addition to the aerodynamic model the code calculates 3-D aeroacoustics loads and pressure distributions for scattering and observer parts characterized by the divergence rate and the reduced frequency. The latter avoids using complex numbers. By means of analytical continuation results obtained for diverging rates can be used to obtain results for harmonic frequencies.

The unsteady aeroacoustics potential flow  $\phi e^{-s_a t}$  is considered around an oscillating body or in practise the unsteady acoustic potential flow is considered around a steady body, which is a superposition on an incident aeroacoustics potential  $\phi^i e^{-s_a t}$ . The effect of the mean aerodynamic flow might be added. A Cartesian coordinate system is chosen fixed to the mean position of the body. The body can be rotated by the Angle of Attack and the Angle of side-slip. A reduced acoustic frequency of the motion or the incident waves is defined as  $s_a = g_a + ik_a$ , where  $k_a = \omega L/c$  and  $\omega$  denotes the frequency of oscillation.  $g_a$  denotes the divergence rate,  $t$  is time and  $c$  is speed of sound.

### Flow equation

$$H_a \phi = \phi_{zz} + \phi_{yy} + (1 - M^2) \phi_{xx} - 2s_a M \phi_x - s_a^2 \phi = 0 \quad \text{E 82}$$

the incident acoustic potential  $\phi^i e^{-s_a T}$  satisfies also the same equation:

$$H_a \phi^i = \phi^i_{zz} + \phi^i_{yy} + (1 - M^2) \phi^i_{xx} - 2s_a M \phi^i_x - s_a^2 \phi^i = 0 \quad \text{E 83}$$

At Mach number zero the acoustic potential  $\phi e^{-s_a T}$  satisfies the convective Helmholtz equation:

$$H_a \phi = \phi_{zz} + \phi_{yy} + \phi_{xx} - s_a^2 \phi = 0 \quad \text{E 84}$$

Also, at Mach number zero the incident acoustic potential  $\phi^i e^{-s_a T}$  satisfies the convective Helmholtz equation:

$$H_a \phi^i = \phi^i_{zz} + \phi^i_{yy} + \phi^i_{xx} - s_a^2 \phi^i = 0 \quad \text{E 85}$$

where in addition the assumption is made that  $\phi, \phi^i$  and its derivatives are small compared to the undisturbed flow. Both equations are valid in the fluid domain outside the wetted surfaces.

It is required that disturbances propagate outwards from the body and remain bounded:

$$\lim_{R \rightarrow \infty} (R^2 |\phi_R - s_a \phi|) < \infty \quad \text{E 86}$$



Where  $R$  denotes the radial distance from the center.

## Boundary equations

At the boundaries of the bodies the normal velocity boundary conditions imposed for the oscillating body presented in equations E 5,E 6 are deployed using  $s_a$  instead of  $s$ :

Further writing the aforementioned boundary conditions in the short form:

$$\vec{q} \cdot \vec{N} = F \quad \text{E 87}$$

Equation E 87 is the hard surface condition and  $F$  denotes the other components of the equations E 5,E 6 .

The equation for a surface with a mixed boundary condition (finite surface impedance) is:

$$\vec{q} \cdot \vec{N} + a_z \phi = F \quad \text{E 88}$$

$a_z$  is the mixed boundary potential coefficient. In [13] for the convective Helmholtz equation it is defined as  $a_z = \frac{i}{Z}$ , with  $Z$  the acoustic impedance defined as  $Z = \frac{p}{q_n}$  the ratio of total surface pressure to total normal velocity.

At the boundaries of the bodies the normal velocity boundary conditions imposed for a body exposed to an incident sound field:

$$\vec{q} \cdot \vec{N} = F - \phi_n^i \quad \text{E 89}$$

or

$$\vec{q} \cdot \vec{N} + a \phi = F - \phi_n^i - a\phi^i \quad \text{E 90}$$

## Flexible and rotating surfaces

The displacement  $h$  is modelled by one of the methods presented in section Downwash

## Gusts

The equivalent displacement  $h$  is modelled by one of the methods presented in section Downwash

## Solid Walls

The potential is assumed symmetric with respect to the wall.

## Symmetry & Anti-Symmetry

Semi models can be applied assuming the steady potential is symmetric and the unsteady potential is symmetric or anti-symmetric for symmetric and anti-symmetric modes, respectively.

## Incident Waves

In the scattering case the incident wave can be described by:

- A planar wave

$$\phi^i = p^i e^{s_a(l_x x + l_y y + l_z z)}$$

**E 91**

**$p^i$  is the magnitude.**

$$(1 - M^2)l_x^2 - 2M l_x + l_y^2 + l_z^2 = 1$$

**E 92**

- or by a set of input sources

$$\phi^i = \sum I_i E^{s_a}(x_i, y_i, z_i)$$

**E 93**

**$I_i$  is the source strength**

**$(x_i, y_i, z_i)_i$  the source position.**

These model acoustic potentials which are supposed scaled with the speed of sound and the reference length.

## Characteristic quantities

The pressure coefficient is similar as the ones presented in equations E 21, E 22 & E 23, apart from using  $s_a$  instead of  $s$ . Further the pressure is often presented in SPL (Sound Pressure Level) of which the definition is given below.

$$p_{\text{SPL}} = 93.9794 + 20 \log_{10} p$$

$p$  is the pressure obtained by dimensionalizing the pressure coefficient with the dynamic pressure  $0.5 \rho c^2$

The acoustic impedance is:

$$z_i^* = \frac{C_{p_i}^s}{q_{n_i}} \quad \text{E 94}$$

## Quantities of Interest

### *Aeroacoustics loads*

Aeroacoustics forces are obtained the same way as the aerodynamic forces presented in Quantities of Interest .

### *Generalised acoustic forces*

Generalised aeroacoustics forces are obtained by integration of the product pressure times normal displacement  $C_p \vec{h} \cdot \vec{n}$  over the wetted surface parts of the bodies.

### Elementary solutions:

$$E^{S_a}(x, y, z) = -\frac{e^{\frac{s_a(Mx-R)}{1-M^2}}}{4\pi R}, M < 1 \quad \text{E 95}$$

$$R = \sqrt{x^2 + (1-M^2)(y^2 + z^2)}$$

$$E^{S_a}(x, y, z) \quad \text{E 96}$$

$$= -u(x)u(x - \sqrt{(M^2 - 1)(y^2 + z^2)}) \frac{e^{\frac{s_a M x}{1-M^2}} Re(e^{\frac{-s_a R}{1-M^2}})}{2\pi R}, M > 1$$

$$R = \sqrt{x^2 - (M^2 - 1)(y^2 + z^2)}$$

The source singularity of the convective Helmholtz equation is:

$$\phi_{zz} + \phi_{yy} + \phi_{xx} - s_a^2 \phi = \delta(x, y, z) \quad \text{E 97}$$

$$E^s(x, y, z) = \frac{e^{-s_a R}}{4\pi R}$$

**E 98**

$$R = \sqrt{x^2 + y^2 + z^2}$$





## Solution method

This chapter deals with the methods to obtain solutions of the mathematical models in the previous chapter. The basis of the solution is the integral equation method which presents the solution as a superposition of elementary solutions. The distribution is obtained with the gradient free boundary volume method.

### Integral equation method

The integral equation approach assumes that in the domain of interest a homogeneous equation is satisfied:

$$H = 0 \quad \text{E 99}$$

Further a solution can be expressed as:

$$\phi = I H \phi + f \quad \text{E 100}$$

With  $I$  the integral operator:

$$I m = \iiint m(u, v, w) E(x - u, y - v, z - w) du dv dw \quad \text{E 101}$$

Where  $E$  is the elementary solution of  $H$ :

$$H E(x, y, z) = \delta(x, y, z) \quad \text{E 102}$$

and

$$m = H \phi \quad \text{E 103}$$

$f$  is a solution of  $H=0$  and takes care that the applicable far field conditions are satisfied.  $m$  is the singularity distribution. **Note that  $I = H^{-1}$ !**

In the aerodynamic method the singular distribution is restricted to the wetted surfaces or the camber surface of the bodies under consideration and the wakes<sup>5</sup>.

In the hydrodynamic method the singular distribution is restricted to the wetted surfaces or the camber surface of the bodies under consideration, to the free surfaces<sup>6</sup>, walls, sea bottom and the wakes.

In the aeroacoustics method the singular distribution is similar to the ones of the aerodynamic method.

To account for symmetry (walls) and/or ground(bottom) singularities can be mirrored.

The integral equation formulation reduces the problem for the complete  $xyz$  to the space in the immediate neighbourhood of the bodies, wakes and other surfaces. The integral formulation that is applied here for the unsteady flow is<sup>7</sup>:

$$\begin{aligned} \phi(x, y, z, s) &= \iint_S \sigma(u, v, w, s) E(x - u, y - v, z - w, s) du dv dw \\ &+ \iint_{S+W} \mu(u, v, w, s) \vec{N} \cdot \vec{\nabla} E(x - u, y - v, z - w, s) du dv dw \end{aligned} \quad \text{E 104}$$

Where  $S$  and  $W$ , denote the body surface (bi-panel or camber surface, shock, free surface, sea bottom etc) and wake surface, respectively.  $\sigma$  is a surface source distribution and  $\mu$  is a surface doublet distribution which are to be determined by the computational method which is described in section Solution method.  $\vec{N}$  is the normal vector from the surfaces into the field.

$E$  is the unsteady elementary solution satisfying

$$H(x, y, z, s) = \delta(x, y, z) \quad \text{E 105}$$

and the radiation conditions.

In this expression  $\delta(x, y, z)$  denotes the Dirac delta function. The solution of  $E$  is given in the previous sections.

<sup>5</sup> The approximate transonic model assumes singularities on the patch representing the shock surface.

<sup>6</sup> Only in the Rankine approach singularities are placed on the free surface and optionally the singularities at the bodies are mirrored with respect to the free surface.

<sup>7</sup> The formulation for steady flow is the same applying  $s=0$



## Gradient free boundary volume method

The method comprises the calculation of the potential due to source and/or doublet panels at the boundaries of the configuration while satisfying the boundary conditions by means of a finite volume discretization on an external one-layer mesh. Therefore, the potential has to be calculated not only on collocation points at the panels but also at exterior points on the one-layer mesh. The BVM method is a strict potential integral equation method applying source and/or doublet singularity layers at the wetted surfaces (or free surface) or at the camber surface and consist of a discretization method, imposing boundary conditions with a flux-balance model in subsonic flow and characteristic differentiation for supersonic flow. It uses the evaluation of the potential at the wetted surfaces and at (dummy) surfaces (ghost points) located a characteristic distance from it. Flow velocities and quantities of interest are derived by numerical differentiation. The wakes which start at the sharp trailing edges of the lifting components can be modelled in a fairly arbitrary way, extending towards downstream infinity as planar wakes in the direction of the  $x$ -axis.

The BVM modelling has strong advantages:

- The efficient evaluation of influence coefficients. The calculation of surface singularity integrals is straightforward and less cumbersome even for complicated elementary solutions. Especially this applies for the Havelock free surface elementary solution. No evaluation and storage of velocity influence coefficients.
- The field equation is fulfilled at least in the immediate neighbourhoods of the surfaces. The boundary conditions and other conditions are uncoupled which allows realization of a better balance between them (reduction of work).
- The suction force<sup>8</sup> (required for induced drag prediction on lifting surface models) is calculated up to machine zero!
- More flexibility with respect to the grid system (panel shapes). Reduction of computational work by evaluating the potential instead of 3 velocity components.

The boundary conditions at the body surfaces, represented by equations 3, 4, 5, 6, 7, 12, 13, 33, 34, 35, 40, 41, 86, 87, 88 & 89 are discretized as explained below (see [21] [22] and [1]). For this technique dummy grid points are constructed on a secondary surface normal to the body surface. The distance between the dummy points and the corresponding panel midpoint depends on the dimensions of the panel and the local curvature. The discretization of the normal velocity at the surface by an obvious one-sided difference along the normal direction is hampered by insufficient accuracy and stability. Therefore, the flow equation at the boundary is discretized as follows. The discretization is performed on the set of collocation points at the boundary and on the set of exterior points which are constructed for subsonic flow in normal direction and for supersonic flow along the characteristic direction, respectively at about one half of the mesh spacing measured along the boundary.

---

<sup>8</sup> An accurate determination of the suction force on cambered lifting surfaces (Zero drag on 2-D lifting surfaces at angle of attack), according to D'Alembert's paradox).

**Finite volume discretization.** When the component of the Mach number normal to a panel leading edge is subsonic (subsonic edge) the flux balance discretization as introduced and described in reference [23] [21] is used. This technique discretizes mass-conservatively the equation by using local geometric and fluid relations between neighbouring panel midpoints, and is second-order accurate on smooth grids. It reduces mainly to a surface integral of (mass-)fluxes along the cell surfaces of and the surface integral of (mass-)fluxes at the body cancels partially or completely against the cell surface integrals depending on the boundary equation which is used. By this the downwash (normal velocity or mass-flux) at the boundary surface is expressed approximately in tangential velocities (mass-fluxes) along its surface and a normal velocity or mass-flux at a finite distance from the body surface. This approach works very well when the flow has an elliptical character (subsonic flow, supersonic flow with subsonic edges).

The volume integration of the governing equation takes place over the number of volumes  $V_{ij}$  which are formed by the collocation points and ghost points:

$$\iiint_{V_{ij}} H(u, v, w) du dv dw = \sum_m C_m \phi_{ijk(m)} - B_{ij} = 0 \quad \text{E 106}$$

$C_m$  denote the coefficients of the potential  $\phi_{ijk(m)}$  at the neighbouring points  $ijk(m)$ .  $B_{ij}$  is the prescribed boundary part. For the Laplace equation and the steady Prandl-Glauert equation the discretization which is compliant with the discretization applied in [1] results in 6 fluxes through the surfaces of which one is prescribed by the boundary condition. In addition for the acoustic equation additional  $s$  related fluxes and a  $s^2$  volume term discretization results. In the discretization of the free surface condition downwinding is applied in free stream direction to eliminate unphysical waves.

**Characteristic discretization.** Furthermore in supersonic flow upwinding is applied in free stream direction or characteristic differentiation. When the flow has a hyperbolic character, the aforementioned approach may give problems with respect to stability and accuracy of the discretization. Then the characteristic direction is applied. If the component of the Mach number normal to the panel leading edge is supersonic (supersonic edge) the boundary equations are discretized by finite differences. Therefore, dummy grid points are constructed on a secondary surface in the "characteristic" direction formed by the intersection of the "characteristic" cone with apex half-angle  $\tan^{-1}(\sqrt{M^2 - 1} \cdot \tan(\Lambda))$  at the panel midpoint and the plane through the apex and parallel to the  $x$ -axis and the normal to the panel.  $\Lambda$  is the sweep angle of the panel edge. Along the characteristic direction the potential gradient is zero and the downwash is again expressed in tangential velocities.

Lifting components<sup>9</sup> with small thickness can be modelled by a thin lifting surface approximation applying the BVM method on the upper or lowerside.

The load integration scheme allows the exact determination of the suction force in case of a lifting surface approximation and improves the drag prediction in case of a full body

---

<sup>9</sup> Lifting surfaces (zero thickness) can be handled without any modification and without extra cost because the potential (jump) at the lifting surface is known a priori.



approximation. In addition, it is possible to rotate the suction force in a direction normal to the wing (Polhamus suction analogy, [20]) in order to estimate global effects of leading-edge separation without modelling the wakes emanating from sharp wing leading and tip edges.

On substitution of the potential due to the singularities a linear system results for the strength of the source or doublet distributions which is solved by direct solution. After that the potential can be calculated and pressures and velocities can be derived by similar finite differences expressions.

### Kutta condition

At a trailing edge the continuation of the the potential is imposed by the following discretization:

$$\kappa C_p^{\text{upwind edge}} + (1-\kappa)C_p^{\text{downwind edge}} = 0$$

which is applied at the wing panel at the trailing edge.  $\kappa=0.25$  proved to give good results and actually means that the pressure jump is zero at a quarter mesh width downstream of the trailing edge. The square root behaviour of the pressure jump can then be properly simulated already with a very coarse grid. At a supersonic trailing edge of a lifting body continuity of the potential jump is required or the velocity boundary condition is imposed.

### Rankine approach

In the Rankine approach at the free surface the finite volume discretization involves the fluid equation together with the free surface boundary equations. Down winding is applied to eliminate problems with respect to stability and accuracy of the discretization.

## Potential Influence Coefficients

This chapter presents the evaluation of the influence coefficients for the aerodynamic, the hydrodynamic and the aeroacoustic model, respectively. The influence coefficients require the double integration over a panel containing a constant, a linear and an exponential singularity distribution. The latter occurs at the wakes.

The potential influence coefficients are obtained by integrating the elementary solutions over the surface panels and/or wakes:

$$\Phi_{jk,i}^{\sigma}(s) = \quad \text{E 107}$$

$$\iint_{S_i} \sigma_i(p_1, p_2, s) E(x_{jk} - u(p_1, p_2), y_{jk} - v(p_1, p_2), z_{jk} - w(p_1, p_2), s) dp_1 dp_2$$

$$\Phi_{jk,i}^{\mu}(s) = \quad \text{E 108}$$

$$\iint_{S_i} \mu_i(p_1, p_2, s) \vec{N}_i \cdot \vec{\nabla} E(x_{jk} - u(p_1, p_2), y_{jk} - v(p_1, p_2), z_{jk} - w(p_1, p_2), s) dp_1 dp_2$$

The potential influence coefficients represent the potential at mesh centroid points  $j,k=0$  and its ghost point ( $j, k=1$ ) obtained by integrating unity elementary solutions (constant or linear tentlike<sup>10</sup> or sinusoidal (exponential)<sup>11</sup>) over the surface panel with index ( $i$ ). The panel surface is constructed bilinearly,  $(p_1, p_2)$  are the local coordinates. The integration over the oscillatory singularity distribution over the wakes is performed with a doublet lattice like method. To avoid problems in supersonic flow about thick bodies due to internal reflections of artificial waves two alternatives can be used. The first one places the singularities at a mean streamwise(camber) surface of the bodies while the second one introduces for each body panel a secondary panel inside the body with opposite strength which cancels the internal disturbance field due to the body panels.

Denoting the discretization [24] of the equations [L], the discretization of the downwash equation [D] the discretization of the pressure equation [P] the discretization of the velocity components [U],[V],[W], the free surface elevation [Z] and the singularities  $(m) = \begin{pmatrix} \sigma \\ \mu \end{pmatrix}$  we obtain the equations:

$[L][\Phi](m) = [D](d)$	<b>E 109</b>
$(C_p) = [P][\Phi](m)$	<b>E 110</b>
$(u) = [U][\Phi](m)$	<b>E 111</b>

<sup>10</sup> Supersonic

<sup>11</sup> Wakes



$(v) = [V][\Phi](m)$	E 112
$(w) = [W][\Phi](m)$	E 113
$(\eta) = [Z][\Phi](m)$	E 114

## Aerodynamic influence coefficients

### *Wings and bodies*

Source and doublet integrals are evaluated by a summation of weight factors (influence coefficients) times the doublet or source strength at the panel midpoints on the bodies and wakes or camber surfaces. Single midpoint rule is often sufficient. Receiving points in the immediate neighbourhood of the boundary of the zone of influence formed by the downwind Mach cones from the panel edges require an extended numerical integration by analytical expressions. Also this applies for the higher frequencies and the Mach number close to 1. Analytical expressions are applied for the first two terms in a series expansion of the elementary solution in  $s$  based on a constant doublet distribution.

Analytical expressions are applied for the first term in a series expansion of the elementary solution in  $s$  based on a constant source distribution.

Analytical expressions are applied for the first two terms in a series expansion of the elementary solution in  $s$  based on a linear doublet distribution distribution in  $x$ -direction in supersonic flow.

The remaining parts are calculated with an extended two-dimensional midpoint rule. A semi-analytical option has been included for the remaining parts using the approximation D24.2 of reference [25], thus reducing the two-dimensional integration to a one-dimensional one.

### *Bi-panel*

The calculation of supersonic flow about thick bodies with singularities on the surface might be hampered by the occurrence of purely artificial numerical oscillations due to internal reflections. These internal reflections might be reduced by adding to each body panel a bi-panel along an inward characteristic direction with opposite singularity distribution. The bi-panel is meant to damp spurious oscillations due to internal reflections ( $M > 1$ ) for thick bodies. It is constructed along the Mach lines emanating from the vertices of the body panel and contains the same singularities. The integration is performed the same way.

### *Planar wakes*

The planar wake integrals are evaluated with a technique related to the Doublet-Lattice method [26] using the approximation D24.2 [25]. The planar wakes should not intersect another configuration component

The direction and shedding velocity of the planar wake is defined by the  $x$ -axis and the free-stream velocity. If  $M = 0$ , the user is allowed to specify the direction in order to avoid the crossing of the wake with another thick surface, although the shedding velocity remains the free-stream velocity.

### **Hydrodynamic influence coefficients**

#### *Wings, bodies, free surface, seabed*

In the Rankine approach all influence coefficients are obtained analytically. In the Havelock approach the first two terms (Rankine) are dealt with analytically, the other terms are dealt with a special designed numerical quadrature method, consisting of Telles [12] transformation and Filon quadrature fortified with asymptotics [27] to deal with the singular and highly oscillatory behaviour.

#### *Planar wakes*

In the Rankine approach the influence coefficients are obtained analytically. In the Havelock approach the first two terms (Rankine) are dealt with analytically, the other terms are dealt with a special designed numerical quadrature method, consisting of Telles transformation [12] and Filon quadrature fortified with asymptotics [27] to deal with the singular and highly oscillatory behaviour.

### **Aeroacoustics influence coefficients**

The aeroacoustics influence coefficients are obtained the same way as used for the aerodynamic influence coefficients in section [Aerodynamic influence coefficients](#)

### **Solution method**

The resulting linear system E 109 is solved by the well-known Crout method. Thereafter the quantities of interest are obtained by means of E 110, E 111, E 112, E 113 and E 114.





## Downwash

The body boundary conditions require the description of the downwash by which we mean external velocities induced by the moving/oscillating structure or incident waves/gusts in the fluid.

The following types of downwash are modelled:

- A: Rigid translation and rotation of the whole configuration.
- B: Sub Rigid translation and rotation of individual patches (effectors).
- C: Regular vibration modes (obtained from FEM or arbitrary), which are warped to the configuration surface.
- D: Polynomial modes, for each individual patch.
- E: Special modes, for individual patches.
- F: Sinusoidal gust modes defined by the reduced frequency and sinusoidal variation in  $x$  (invariant in  $y, z$ ), Amplitude is linear varying in  $|y|$  and  $|z|$ .
- G: Patches with zero downwash
- H: Incident wave modes defined by the reduced frequency which satisfy the Laplace equation the free surface condition and the sea bed condition.
- I: Incident plane and source wave modes. These model acoustic potentials.

Furthermore, a special type of downwash is the trim vector which accounts for geometry corrections or settings.

It should be noted that the steady velocity field can be applied to the unsteady boundary condition and the unsteady pressure coefficient.

The unsteady route may be run with a steady velocity flow field obtained from a previous steady run of the AES=O= system, with data from other sources or straightforward with the undisturbed steady flow field. The mean velocity field can be defined at arbitrary  $(x, y, z, \text{Alpha} \ \& \ M)$  points. The data is interpolated in space and in Alpha and Mach with a 5 dimensional biharmonic volume spline.

Application of geometry corrections by means of adding Boundary Layer Thickness allows a corrected prediction of pressures in zones where the prediction is known to be way off reality (effectors et cetera). The correction can be applied by specifying positive thickness in normal direction at arbitrary  $(x, y, z, \text{Alpha}, M \ \& \ Re)$  points. The data is interpolated in space and in Alpha, Mach and Reynolds with a 6 dimensional volume spline .

## The outputs

The output consists mainly of the pressure coefficient distribution on the wetted surfaces and on the observer surfaces and the velocity distribution. In addition, the height of the free surface in the hydrodynamic mode and the SPL level in the aeroacoustics mode are calculated.

Loads are obtained by integration of the calculated pressures over the surface of the bodies. This gives satisfactory results as long as the applied discretization is good enough to represent adequately the pressure gradients and the tangential flow condition. Otherwise the discretization will fail for some of the components. This way the drag force in case of the lifting surface approximation does not show the well-known property of no drag on a 2-D airfoil in potential flow, due to the neglect of the suction force. To conserve the global no drag property the integration is fortified and conserves the no drag properties implicitly. Its origin lies in formulas as derived by W.E. Cummings [19] in 1957 for the loads on a body in an arbitrary time-dependent incompressible potential flow including rotation. The suction force is calculated, allowing accurate induced drag calculation or the suction force analogy to estimate globally effects of leading edge separation.

To correct the prediction of pressures in zones where the prediction is known to be way off reality (eg effectors) gain factors can be applied with respect to the pressure coefficients applied in the generalised forces and loads (only unsteady!). A gain factor distribution is defined by specifying the Real and Imaginary parts of the gains at arbitrary (x,y,z,k & M) points. The data is interpolated in space and in frequency & Mach with a 5 dimensional biharmonic volume spline.

3-D loads are calculated including sectional forces & moments coefficients ( $C_l$  &  $C_d$  and  $K$ ,  $M$  (AGARD manual on aeroelasticity notation [28])) and generalised force coefficients for rigid & flexible displacement modes.

The generalized forces are defined by  $G_{ij} = \iint_S C_p^j h_i dS$  where  $j$  denotes the vibration mode for which the pressure distribution has been calculated and  $i$  denotes the downwash mode on which the pressure distribution is acting.  $h$  is the displacement function normal to the lifting surface.



## Warping

Efficient methods are included in AES=O= with respect to the warping of the (un)structured support data to the receiving geometry patches. This information transfer at the fluid/structure interface is performed by:

- Volume spline interpolation introduced/originated in [29] and
- Planar surface spline interpolation [30]
- Least Squares Polynomial approximation [9].

The first two approximations A&B can be applied in a combined hybrid way with the last enabling a noise-free interpolation with respect to algebraic type of motions (rigids). [10] Nearest neighbours strategies are embedded to reduce computational work.

Various nearest neighbors (NNB) strategies are available to reduce computational work. The *smoothed* global and patch NNB are advised. These take care of local and global trends of the support data.

Also computational work can be reduced by coarsening the number of support points. The Warping matrices are stored for reuse, accommodating follow on stages of a design cycle ( Mach/Froude number and/or frequency changes).

Warping is the technique of interpolation or extrapolation of discrete data (mode shapes) defined at a set of arbitrary support points (mostly FEM structure related) to a set of arbitrary receiver points (wetted surfaces of configuration). An evaluation of warping techniques has been presented in 1995 [9] with the conclusion that the volume spline method introduced by Hounjet in 1994 [29] is the absolute best method to consider. Basically it assumes that the distribution near the set of receiving points satisfies the biharmonic or the Laplace equation. In 2003 [10] further enhancements of the method have been presented. Besides warping the volume spline method has come since its introduction into purpose in many other cases: multidimensional interpolation for a measurement balance, visualization of pressures on unstructured meshes (CFD and experimental [31]), multidimensional inverse interpolation for rotor blade [32], smooth intersection generation of geometries (wing pylon, wing/fuselage, ship/ free surface (sinkage/hydrostatic force)) [33], mesh deformation/morphing and enhanced visualization of experimental data [34], the H flutter analysis method which automatically extents harmonic data to damped and diverging data by means of fitting free harmonic interpolation [8], Mass Warping [35] et cetera.

It has also been further developed into the mollifying technique which is part of the AES=V= method [36] [33]. The mollifying technique takes the warping technique a step further by continuation a trusted set of data (A) defined at arbitrary support points to a baseline set of data (B) defined at arbitrary supports points in such a way that the result is cardinal with respect to the trusted data and adheres to the trends(/conformity) of the baseline dataset. The mollifying technique is developed for occasions in which a trusted set of data (A) describing

systems are scarce/coarse (reduced in order) due to economic reasons. Often a correction method or surrogate model is developed to continue/interpolate the data. The mollifier can be regarded as intruding the valuable (accurate) scarce data in an already existing dataset in a black box manner. The approach is suitable for impact assessment of design (market) changes, starting data for optimization, reverse engineering and many more.

We refer to the next section for the explanation of the volume spline and the mollifying method.

### **Volume spline/Mollifying method or VSIC (Volume Spline Injection Continuation) method**

This section describes the volume spline and mollifying method. the volume spline is introduced in 1994 [29]. To obtain data in regions where the support data is not specified the data needs to be continued according to a realistic model. Therefore, an interpolation is needed that provides a realistic continuation. Methods based on the volume spline class technique are used that are robust, automatic and cardinal. For a theoretical background on the volume spline method Refs. [9] [10] should be consulted. Ref. [9] introduces the volume spline and various core functions and discusses their behaviour and implementation aspects extensively. Ref. [10] deals with further developments. Here as a bonus we present also the mollifying (alias VSIC) method which is available in the AES=V= method and embeds the volume spline method.

There are many occasions in which characteristic data describing A/C systems are scarce/coarse (reduced in order) due to economic reasons (wind tunnel testing, flight testing and Hi-Fi CFD simulations). Examples are tabular data for engines, lift & drag aerodynamic forces, high-fidelity generalised forces needed in flutter certification, Hi-Fi CFD data in optimization processes. Often a correction method or surrogate model is developed to continue/interpolate the data in the unknown zones. In flutter certification so called Mach correction tables are implemented on top of the Doublet Lattice method to account for transonic effects.

The mollifier can be regarded as injecting the valuable approach is suitable for impact assessment of design changes, starting data for optimization and reverse engineering. The model is described in details in the next sections.



## The volume spline method

Supposing a basic data set  $D_b(1..N_b)$  is available in a multidimensional space  $[x, y, z, u, v, w, \dots]$  we interpolate the data by:

$$V_b(x, y, z, u, v, w, \dots) = C^0 + \sum_{i=1}^{N_b} C^i E(x, y, z, u, v, w, \dots; x_i^b, y_i^b, z_i^b, u_i^b, v_i^b, w_i^b, \dots) \quad \text{E 115}$$

Where  $V_b$  is the interpolation function,  $C$  are its coefficients which are determined by satisfying the afore mentioned equation at the  $N^b$  support points  $(x_i^b, y_i^b, z_i^b, u_i^b, v_i^b, w_i^b, \dots)$  and an additional closure relation:

$$\sum_{i=1}^{N_b} C^i = 0 \quad \text{E 116}$$

Further we select the interpolation to be harmonic or bi-harmonic meaning that the kernel function  $E$  satisfies the Laplace equation or bi-harmonic equation, respectively:

$$\Delta E = \delta \quad \text{E 117}$$

or

$$\Delta^2 E = \delta$$

Examples of bi-harmonic core functions are:

- **1-D kernel** The bi-harmonic kernel in 1D:

$$E(x: x_i) = r^3 \quad \text{E 118}$$

Where  $r$  is the absolute distance  $r = |x - x_i|$

- **2-D kernel** The bi-harmonic kernel in 2D:

$$E(x, y: x_i, y_i) = r^2 \ln r \quad \text{E 119}$$

Where  $r$  is the distance  $r = \sqrt{(x - x_i)^2 + (y - y_i)^2}$

- **3-D kernel** The bi-harmonic kernel in 3D is:

$$E(x, y, z: x_i, y_i, z_i) = r \quad \text{E 120}$$

Where  $r$  is the distance  $r = \sqrt{(x - x_i)^2 + (y - y_i)^2 + (z - z_i)^2}$

- **4-D kernel** The bi-harmonic kernel in 4D is:

$$E(x, y, z, u: x_i, y_i, z_i, u_i) = \ln r \quad \text{E 121}$$

Where  $r$  is the distance  $r = \sqrt{(x - x_i)^2 + (y - y_i)^2 + (z - z_i)^2 + (u - u_i)^2}$

- **5-D kernel** The bi-harmonic kernel in 5D is:

$$E(x, y, z, u, v: x_i, y_i, z_i, u_i, v_i) = 1/r \quad \text{E 122}$$

Where  $r$  is the distance

$$r = \sqrt{(x - x_i)^2 + (y - y_i)^2 + (z - z_i)^2 + (u - u_i)^2 + (v - v_i)^2}$$

- **Et cetera**

Examples of harmonic core functions are:

- **1-D kernel** The harmonic kernel in 1D:

$E(x: x_i) = r$	<b>E 123</b>
-----------------	--------------

Where  $r$  is the absolute distance  $r = |x - x_i|$

- **2-D kernel** The harmonic kernel in 2D:

$E(x, y: x_i, y_i) = \ln r$	<b>E 124</b>
-----------------------------	--------------



Where  $r$  is the distance  $r = \sqrt{(x - x_i)^2 + (y - y_i)^2}$

- **3-D kernel** The harmonic kernel in 3D is:

$$E(x, y, z: x_i, y_i, z_i) = 1/r \quad \text{E 125}$$

Where  $r$  is the distance  $r = \sqrt{(x - x_i)^2 + (y - y_i)^2 + (z - z_i)^2}$

- **4-D kernel** The harmonic kernel in 4D is:

$$E(x, y, z, u: x_i, y_i, z_i, u_i) = \ln r / \mathbf{r} \quad \text{E 126}$$

Where  $r$  is the distance  $r = \sqrt{(x - x_i)^2 + (y - y_i)^2 + (z - z_i)^2 + (u - u_i)^2}$

- **5-D kernel** The harmonic kernel in 5D is:

$$E(x, y, z, u, v: x_i, y_i, z_i, u_i, v_i) = 1/r / \mathbf{r} \quad \text{E 127}$$

Where  $r$  is the distance

$$r = \sqrt{(x - x_i)^2 + (y - y_i)^2 + (z - z_i)^2 + (u - u_i)^2 + (v - v_i)^2}$$

- **Et cetera**

Note  $E$  bi-harmonic in ND is  $E$  harmonic (N-2)D! When applying the singular kernels, a regularization is needed for which one can consult [10]

### The mollifier or the VSIC method

In this section the VSIC or mollifier is described that can be regarded as injecting the valuable (accurate) scarce data in an already existing dataset in a black box manner. The black box model is based on an interpolation model of a baseline system where the scarce data available from the new system is injected. Thereto an injection model based on the volume spline method is adapted to allow for injection of the scarce data points.

This Volume Spline Injection Continuation model adheres to the following:

- The assumption is made that in between the support points the harmonic or bi-harmonic equation governs the distributions;
- This leads to two sets of sources at the support points of the original set and the new set;
- The sources at the support point of the original set closest to each of the support points of the new set are (blanked) deleted;
- The resulting sets are combined in one set of sources;
- When no injection is done this model is the original model;
- When the new set is large enough the model is the new model;
- The resulting model will generate the true data close to the new data at the support points and smoothly drift away according to the original trends.

Next we assume that a data set  $D_{\$}(1..N_{\$})$  with respect to a new development is available for a limited set of  $N_{\$}$  numbers. We can also interpolate/extrapolate the data by the volume spline:

$$V_{\$}(x, y, z, u, v, w, \dots) = C_{\$}^0 + \sum_{i=1}^{N_{\$}} C_{\$}^i E(x, y, z, u, v, w, \dots; x_i, y_i, z_i, u_i, v_i, w_i, \dots) \quad \text{E 128}$$

where  $C_{\$}^i$  are the coefficients which are determined by satisfying the afore mentioned equation at the  $N_{\$}$  injection points  $(x_i, y_i, z_i, u_i, v_i, w_i, \dots)$  and the additional closure relation.

This data will be fairly good near the injected points but at some distance away the likeliness of the data will be questionable. Therefore we interpolate the data such that close to the injected points the data is fairly good represented by the last equation and at some distance away it should follow the trend of the baseline data. It should be regarded as the generalization of the transfinite interpolation method [37].





The resulting equation is:

$$M(x, y, z, u, v, w, \dots) = C^0 + \sum_{i=1}^{N^b} C_z^i E(x, y, z, u, v, w, \dots; x_i, y_i, z_i, u_i, v_i, w, \dots) + C_{\$m}^0 + \sum_{i=1}^{N^\$} C_{\$m}^i E(x, y, z, u, v, w, \dots; x_i, y_i, z_i, u_i, v_i, w, \dots) \quad \text{E 129}$$

where  $C_z^i$  are the modified volume spline coefficients of the baseline interpolator which are blanked afterwards to zero in regions close to the injection points:

$$C_z^i = C^i, \min_i |r_i^b - r_i| > core \quad \text{E 130}$$

$$C_z^i = 0, \min_i |r_i^b - r_i| \leq core$$

*Core* is a characteristic minimal (blanking) distance between the support points.

$$V_b^z(x, y, z, u, v, w, \dots) = C^0 + \sum_{i=1}^{N^b} C_z^i E(x, y, z, u, v, w, \dots; x_i, y_i, z_i, u_i, v_i, w, \dots) \quad \text{E 131}$$

The  $C_{\$m}^0$  coefficients are obtained by satisfying the volume spline equation for the differences between the injected data  $D_{\$}$  and the interpolated  $V_b^z(x, y, z, u, v, w, \dots)$ . By this the resulting interpolation is cardinal and adheres to the trend of the baseline data.

## Mollifier demo

The procedure is applied for a structured set of baseline data and a structured/unstructured set of injected data and presented in

Figure 1, Figure 2,

Figure 3 and Figure 4. The first figure present all datasets. The upper left data is injected in the baseline data (lower left) resulting in the upper right data. Note that the injected data is invariant for the mollifying and the result is cardinal with respect to the injected data and adheres to the trends of the baseline dataset. The second figure depicts the baseline and the mollified data. The third one shows the the injected after the data is visualized by means of triangularization and finally the fourth one show contours of the baseline and the mollified data.

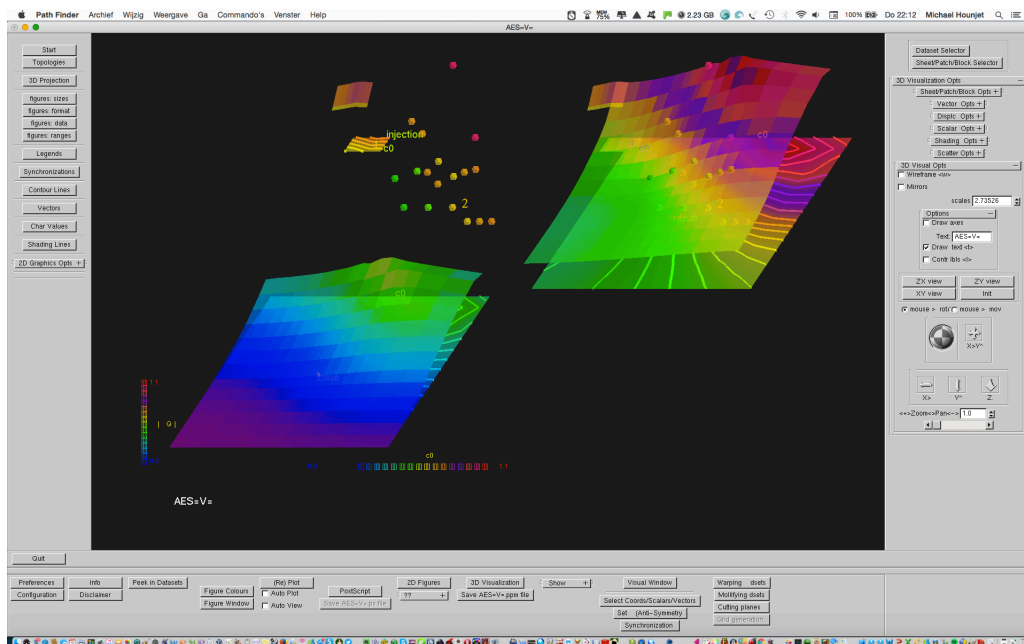


Figure 1 The datasets of the mollifier procedure. Left top the data to be injected. Left bottom the baseline data. Right top the resulting composed data.

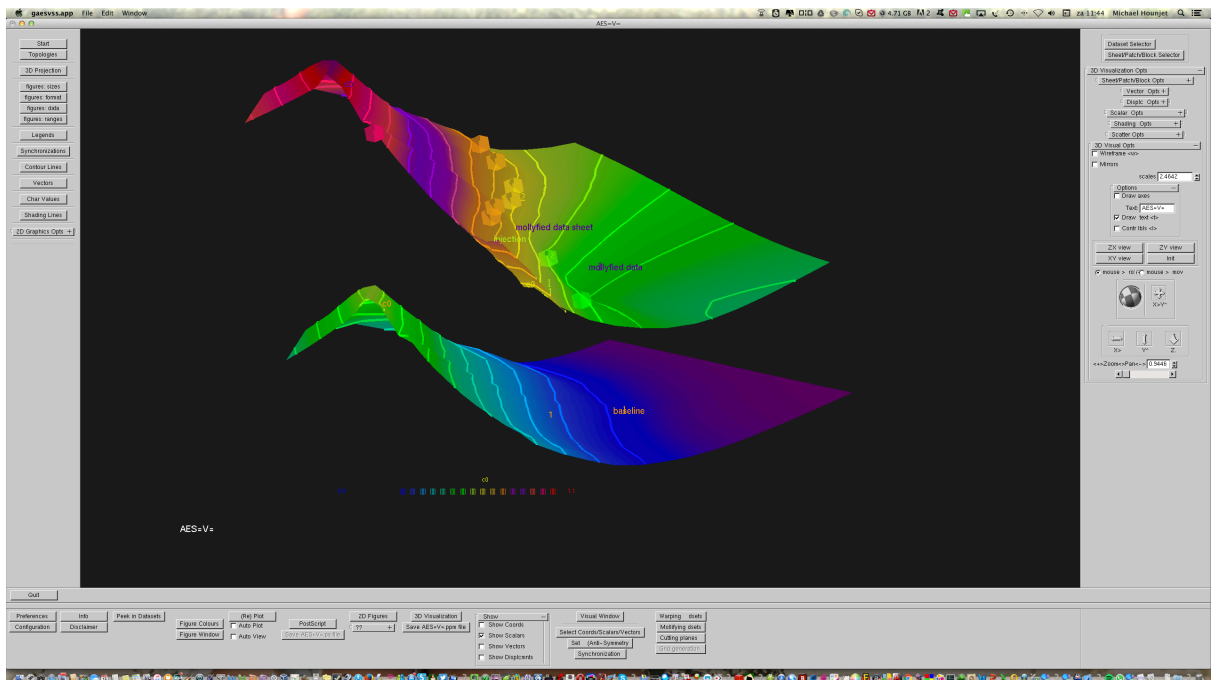


Figure 2 The datasets of the mollifier procedure. Bottom the baseline data. Top the resulting composed data

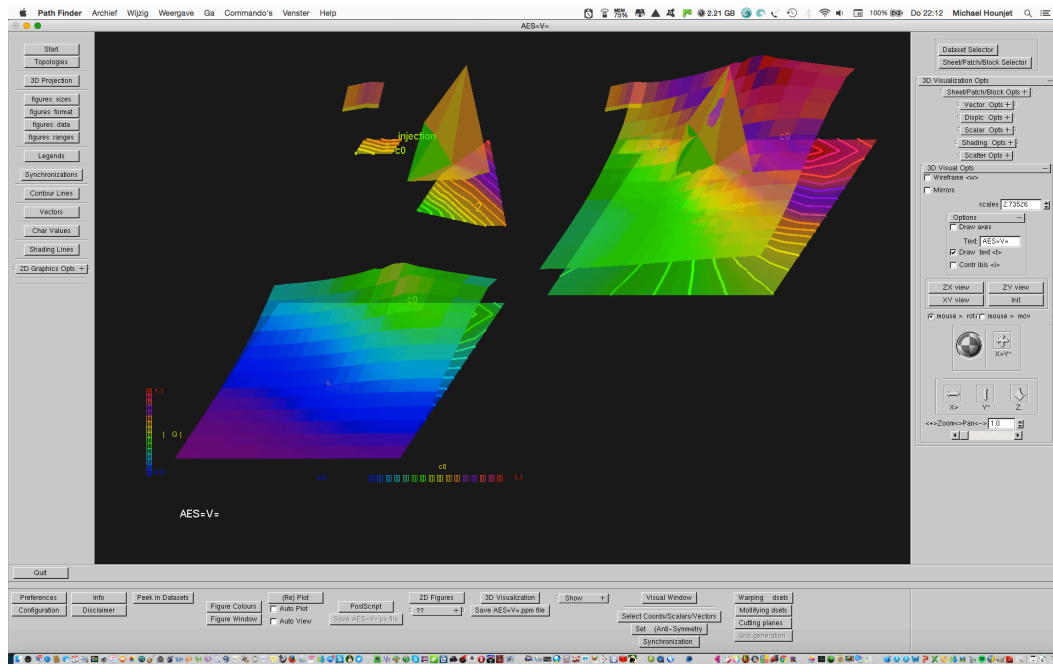


Figure 3 The datasets of the mollifier procedure. Left top the injected scattered data to be injected visualised after triangularization. Left bottom the baseline data. Right top the resulting composed data.

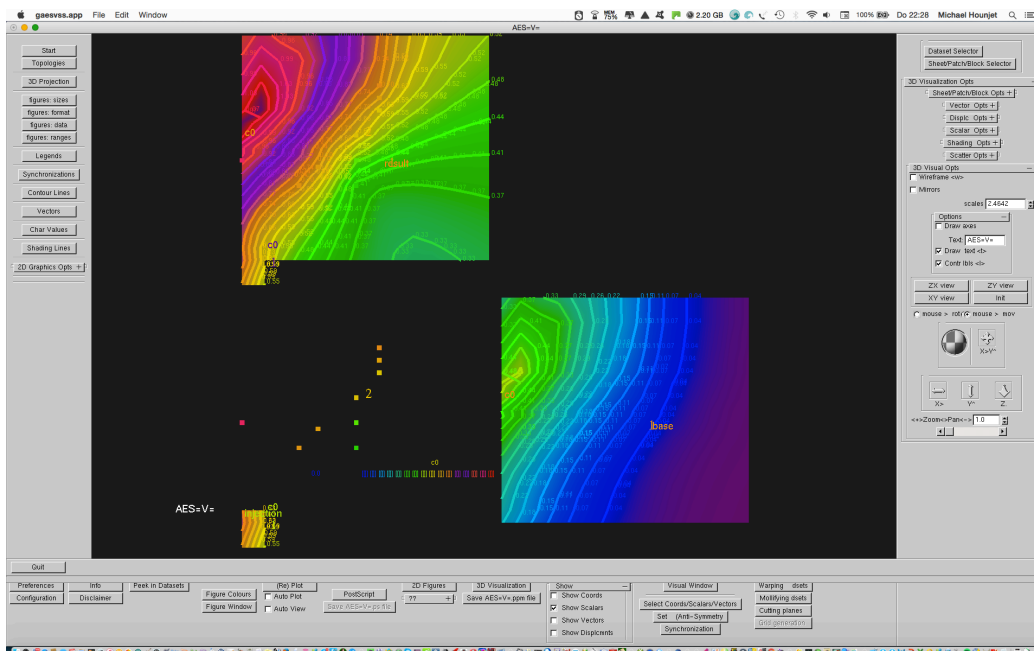


Figure 4 Contour plots of the datasets of the mollifier procedure. Left bottom the data to be injected. Left bottom the baseline data. left top the resulting composed data.

## Digital model description

To carry out the calculations a digital model has to be provided or generated on the fly together with case parameters. The model describes the geometry and/or the motions/vibrations of the bodies and/or the gusts/ waves/ incident sound fields. The digital model consist of bulk data (geometry, geometry and flow disturbances) and case data. Both can be stored in a single .cnf file.

### Geometry

The wetted surfaces of the configuration are divided into components (patches). Each component is divided into quadrilaterals (panels).

The surfaces of the configuration under consideration is described by a number of patches. It is advised to use a minimum of patches for which  $AES=V= [33]$  can be used. Each patch is defined by a quadrilateral mesh defined by a number of subsequent chordwise lines, which start at the leading edge (thin-airfoil approximation) or trailing edge lower side , continue clockwise and end at a assumed uniform wake position and by a number of subsequent span lines which start at the portside of the patch and end at the starboard side of it. The normal direction of each segment is assumed to be in the direction of the out product of the directions formed by the chordwise and spanwise lines. The sequence of the spanwise lines should be chosen such that the normal is pointing outward. When the thin airfoil approximation is applied the chordwise line should start at the leading edge else the chordwise line start at the lower side trailing edge and continues clockwise to end at the upper side trailing edge.

### Geometric Input file

Besides interactive generation/change of the paneling one might specify the geometric data on the first file on  $aes=o=.cnf$ . In general, the patches will be described on the geometry file with default name  $aes=o=.geo$ . The geometry file contains the geometry in the format presented in Table 1.



recs 1	int	npatch (number of patches)
recs 1	Char*	patchid(p=1) (name patch 1)
recs 1	Int*3	npj(1), npi(1), xoption (number of vertices on patch p=1 along span and chord, respectively , input option)
if(xoption==1) {		
recs 1	Float*3	xa(1,1),ya(1,1),za(1,1) (x,y,z vertices of panels)
.....		
recs npi(1)*npj(1)	Float*3	xa(npi(1),npj(1)),ya(npi(1),npj(1)),za(npi(1),npj(1)) (x,y,z vertices of panels)
else {		
recs 1	Float*3	xa(1,1,1),ya(1,1,1),za(1,1,1) (x,y,z vertices of LE-PE patch corner)
recs 1	Float*3	xa(npi(1),1,1),ya(npi(1),1,1),za(npi(1),1,1) (x,y, z vertex of TE-PE patch corner)
recs 1	Float*3	xa(1,npj(1),1),ya(1,npj(1),1),za(1,npj(1),1) (x,y,z vertices of LE-SE patch corner)
recs 1	Float*3	xa(npi(1),npj(1),1),ya(npi(1),npj(1),1),za(npi(1),npj(1),1) (x,y,z vertex of TE-SE patch corner)
}		
recs 1	Char*	patchid(2) (name patch2)
et cetera		

Table 1 Geometry file

Additional patches can be generated ab initio on the fly by entering the corner coordinates at the portside and starboard edges. The panelling inside the corners are carried out with the specified numbers and according to a hyperbolic distribution. Also existing patches might be changed, cloned or mirrored in interactive mode.

### Patch types

The following patch types can be selected:

- A body patch
- A wake patch
- Free surface patch
- Observer patch
- A shock patch
- Lift Carry Over patch(strip)

## Lift Carry Over strips

The so-called LCO (Lift Carry Over) extension strips are embedded to avoid unphysical velocities at wake edges and need to be defined by the user.

The singularity distribution on the LCO planes is extrapolated from the neighbouring planes

## Wakes

Parts of a patch can be set to wake parts. A positive value indicates the trailing(shedding) edge. A negative values indicates shedding before the trailing edge. The option GP\_K (see Table 2) should be used for the geometric autoconnection at the sharp trailing edge of a wing (airfoils).

## Static Geometry

The static (mean) geometry of the model is described by a composition of patches:

- Tabular data of patches on input file
- Patch creation ab initio
- Patch editing of geometry (including sweep, taper, dihedral, thickness & twist).

Further the geometry can be corrected according to:

- Trim vector to model static deformation and effector settings.
- Artificial geometry corrections to accommodate boundary layer and edge effects specified for a set of xyz co-ordinates and parameters.
  - Mach (Froude) number
  - Angle of Attack, TRIM(SINKAGE)
  - Reynolds number

The set is interpolated with a 6-dimensional bi-harmonic volume spline.



## Connection of Patches

When a configuration is modelled with multiple patches the BVM method require potential data at the edges of patches to carry out the discrete evaluation of potential gradients. In general, this can be performed by natural connection with other patches or by extrapolation.

Extrapolation can reduce cost (less influence coefficient evaluations), increases accuracy and increase robustness with evaluation of velocity components. At edges of patches, it is possible to prescribe the geometric and the potential continuation as follows:

	Geometry	Potential
GL_PL	linear	linear
GL_PC	linear	constant
GN	linear,	Natural (tip edge)
GP_PC	periodic	constant
GP_PL	periodic	linear
GP	periodic	Natural (fuselage)
GP_K!	periodic,	Kutta condition at LE/TE (airfoil/wing)
TE_p	continuously connected at TE to LE other patch	continuously connected at TE to LE other patch
LE_p	continuously connected at LE to TE other patch	continuously connected at LE to TE other patch
PE_p	continuously connected at PE to SE previous patch indice	continuously connected at PE to SE previous patch indices
SE_p	continuously connected at SE to PE next patch indice	continuously connected at SE to PE next patch indices

Table 2 Connections

In general segments will have natural (FREE) boundaries which are not connected to other segments. Examples are leading ,trailing and tip edges of lifting surfaces and apices of bodies. Use the natural nonconnection option (GN) for these cases. In case of an abrupt end of a thick body without a trailing wake use the linear extrapolation nonconnection option GP\_PL. Incase of troubles with apex flow use this option.

Another 'natural' boundary is an edge in the symmetry planes. When the natural nonconnection option GN is specified a special treatment is given to these edges.

This special treatment is not completely embedded for the calculation of the pressure on lifting surfaces with the non-linear pressure formula. In that case use linear extrapolation GP\_PL for anti-symmetric modes and constant extrapolation GP\_PC for steady flow and symmetric modes. Better is to use the linear pressure option.

In general patches will share boundaries with other segments with the following properties:

- Geometry (panelling) and solution smooth across segment boundaries. The cross connection options LE\_p, TE\_p, PE\_p, SE\_p or the autoconnection option GP are the obvious best choices. Choosing another option always results in extrapolation of the geometry at the boundary and will affect the results.  
Choosing the natural connection option GN will result in an increase of computational cost because additional AICs will be calculated and might lead to wrongly calculated pressures at lifting surfaces because the program then might make the wrong assumption that the potential jump which is needed for the pressure calculations across the boundaries is zero. In such a case use the nonconnection linear extrapolation option GL\_PL although in most cases it is less accurate than the natural one it will keep you always out of trouble especially in supersonic flow because only data is used generated at the segment itself and therefore it is less sensitive to changes in panelling's at the boundary. Moreover, the fact that supersonic flow potential solutions basically behave linearly contributes to the preference.
- Geometry (panelling) non-smooth (non-aligned panelling) and solution smooth across boundaries. For the same reasons as mentioned in the previous section prefer the GL\_PL options over the GP options.
- Solution non-smooth across the boundaries (abrupt geometry change, wing fuselage junction). For all segment longitudinal strip edges the program checks if there are any neighbouring non-smooth connections with longitudinal strip! edges of other! segments (There is no hunt for auto non-smooth strip! connections). In which case the program automatically applies the GL\_PL option for the relevant connected points (not the whole strip!). For a segment longitudinal edge this is only done when the natural nonconnection option GP is specified otherwise the prescribed option is applied. This procedure will deal with most wing-body junction cases and LCO connections. When the geometry is non-smooth along the boundary apply the GL\_PL linear extrapolation option. This is also true for LCO connections or wing fuselage connections which for some reason have been missed by the program checks. The automated procedure deals with most wing (wake) (LCO) body junction problems as long as the longitudinal segment border of the wing (wake)(LCO) can be connected by that procedure to a longitudinal strip edge of a body segment. So there is no need for a body segment to have a segment border at the junction! When this fails you should always use the nonconnection GL\_PL, GP\_PL options. Beware the longitudinal edge of the wing (wake) (LCO) should never cross a longitudinal strip edge of a body.
- When the geometry (panelling) auto connects (tip store at a wing tip) use the GP\_PL option.

The constant solution extrapolation options GP\_PC are preliminary ment for the cases where the cross velocities are known to be zero. (Wing fuselage junction in steady flow). This option can also be recommended when due to very nonsmooth panellings the linear extrapolation will fail. However in supersonic flow options GL\_PC, GP\_PC are not recommended.





The VB 1 and VB 2 are alternatives to the BVM methods:

VB1	apply the normal boundary condition by a one-sided difference in normal direction
VB2	apply the normal boundary condition by a one-sided difference in normal direction in addition cross derivatives are neglected when VB 2 is selected in evaluation of pressure et cetera.

Table 3 Alternatives to BVM method

At edges of the free surfaces radiation conditions can be imposed:

D	Dirichlet condition free surface
N	Neuman condition free surface
A	Absorbing condition free surface

Table 4 Radiation Condition at free surface

The so-called LCO (Lift-Carry Over) extension strips are embedded to avoid unphysical velocities at wake edges and need to be defined by the user.

The singularity distribution on the LCO planes is extrapolated from the neighbouring planes

Parts of a patch can be set to wake parts. A positive value indicates the trailing(shedding) edge. A negative values indicates shedding before the trailing edge. The option GP\_K should be used for the geometric autoconnection at the sharp trailing edge of a wing (airfoils)

## Dynamics Geometry

The geometry dynamics of the model is described by:

1. Structural data (geometry & mode shapes) on input file (see Table 5) which are warped with efficient volume spline class methods
2. Polynomial data on input file (see Table 6)
3. Rigid motions (rotations and translations)
4. Sub-rigid (effectors) motions
5. Arbitrary motions/deformations which are warped with efficient volume spline class methods

The information transfer at the fluid/structure interface is performed by the following interpolation methods:

- A) Volume spline interpolation
- B) Planar surface spline interpolation
- C) Least Squares Polynomial approximation.
- D) =A+C
- E) =B+C

The combined hybrid D) and E) methods enabling a noise-free interpolation with respect to algebraic type of motions.

## General modes file format

### Regular Vibration Input file

The second file on aes=0=.cnf containing regular vibration modes should be specified on a input file with discrete format described in Table 5:

recl 1	Int*3	npart, nv, ndis (number of structural parts, vertices, modes, respectively)
recl 1	Char*	partid(1) (name part 1)
.....		
recl Npart	Char*	partid(1) (name last part )
recl 1	int	nas(1) (number of vertices on part 1
.....		
recl Npart	int	nas(npart) (number of vertices on last part
recl nv	Float*3	(xs(i),ys(i),zs(i);i=1,nv) (vertices)
recl 1	Char*	modeid(1) (name mode 1)
recl nv	Float*3	(dx(i,1),dy(i,1),dz(i,1);i=1,nv) (vertices)
.....		
recl 1	Char*	modeid(nd) (name last mode )
recl nv	Float*3	(dx(i,nd),dy(i,nd),dz(i,nd);i=1,nv) (displacement at vertices)

Table 5 General Displacement File



## Polynomial modes file

The second file on aes=0=.cnf containing polynomial vibration modes should be specified on a input file with discrete format described in Table 6:

recs 1	(int)	ndis	number of polynomial displacements (modes)	
recs 1	(char*)	modeid	name mode 1	
recs 1	(int)*8	(ipp(l);l=1,8)	patch ids of affected patches, npp is number of different entries)	
recs 1	(float)*6*6*npp	(xpcs(i,j,l);i=1,6,j=1,6,l=1,npp)	x-direction polynomial coefficients along chord, span	
recs 1	(float)*6*6*npp	(ypcs(i,j,l);i=1,6,j=1,6,l=1,npp)	y-direction polynomial coefficients along chord, span	
recs 1	(float)*6*6*npp	(zpcs(i,j,l);i=1,6,j=1,6,l=1,npp)	z-direction polynomial coefficients along chord, span	
line 6	(char*)	modeid	(name mode 2)	
et cetera	(int)*8			
			s=x-x_LP and t=arclenght((y,z)- (y,z)_LP).	Note the polynomials are defined along local patch coordinates (s,t).
	(int)			lines starting with % or # are treated as comments. ;

Table 6 Polynomial file

## Flow Dynamics

The dynamics of the incoming fluid can be described by:

1. Gusts (Aerodynamics)
2. Waves (Hydrodynamics)
3. Incident sound fields and waves (Aeroacoustics)

## Outputs

- Pressure Coefficients
- Flow velocities
- Forces and moment's coefficients on strips of patch (according to AGARD manual on aero elasticity notation [28]), on patches and on the whole configuration and generalized force coefficients for rigid and flexible displacement modes<sup>12</sup>
- Free surface height
- Data, xls and graphical output

The outputs are available on the files described in the next section.

## File outputs

AES=O= can create the output files presented in Table 7:

.aes=o=.prfs	contains preferences data
aes=o=.cnf	contains all input, control data and .aes=o=.prfs
aes=o=.cps	A text file containing unsteady pressure data
aes=o=.zcps	A text file containing steady pressure data
aes=o=.frcs	A text file containing unsteady aero forces data
aes=o=.zfrcs	A text file containing steady aero forces data
aes=o=.gafs	A text file containing the GAFs (generalized aero forces).
aes=o=.gafsV	A text file containing the GAFs in AES=V= format.
aes=o=.Hgafs	A text file containing GAFs extended to the

---

<sup>12</sup> The calculated pressure distribution can be factored with a correction (Mach (Froude) number, frequency and position dependent!) to accommodate transonic, boundary layer and edge effects.



	diverging rate domain
aes=o=.HgafsV	A text file containing GAFs extended to the diverging rate domain GAFs in AES=V= format.
aes=o=.ppm	A graphics file
aes=o=.ps	A postscript file
aes=o=.cpsV	A text file containing pressure data in AES=V= format
aes=o=.xls	An excel file containing many data of interest
=o=.hot	Matrice data for the unsteady restart case
=o=.zhot	Matrice data for the steady restart case
=o=.dvs_in_use	Warped regular modes on the surface paneling

Table 7 File outputs

The files are supposed to be self-explaining and are not further documented.

### Efficiency

The CPU time depends on the total number of panels(NP):  $NP^2$  for dealing with the determination of the influence coefficients and :  $NP^3$  for dealing with the solution of the linear system.

The requires memory is equivalent to the largest number of panels on a single patch.

The solution matrices can be reused after storage accommodating follow on stages of a design cycle (mode shape changes). With a one button click it is possible to coarsen the panelling to reduce computational time.

The warping matrices can be reused after storage accommodating follow on stages of a design cycle ( Mach number and/or frequency changes).

The calculations can also be performed in batch.

## Examples of applications

Applications of the general lifting surface AES=3= panel method (<http://www.aes4ac.com/app3/apps3.html>) have been described earlier in the report [38]. This chapter shows some examples of applications demonstrating the versatility of the AES=0= calculation and visualization method. These are the following:

### 1. Aerodynamic

- The calculated steady flow about a set of 4 donuts demonstrating the ability to deal with thick and interfering bodies at high angle of attack and side slip at a low subsonic Mach number.
- The calculated steady flow about a set of 8 payloads demonstrating the ability to deal with thick and interfering bodies at high angle of attack and side slip at a transonic Mach number.
- The warping of four FEM vibration modes to a wing body configuration.
- The calculated unsteady harmonic pressure distribution on a rectangular wing at a transonic Mach number demonstrating the ability to deal with approximate transonic flow by introducing a shock plane.
- Calculations of the AGARD wing w445.6 pressures, loads et cetera. Thickness increases real part of pressures and loads, lowers frequency response and probably more prone to flutter.

### 2. Hydrodynamic

- the Wigley hull model [39]
- The steady solutions due to a submerged sphere with the radius  $R = l$
- The submerged Delta wing of Rene Coene [40]
- Steady calculations of a 1.6m submerged spheroid [4]

### 3. Aeroacoustics

- An acoustic demonstration at Mach number zero has been performed for one of the cases proposed by Hess [13].

## Aerodynamic examples

### A set of donuts

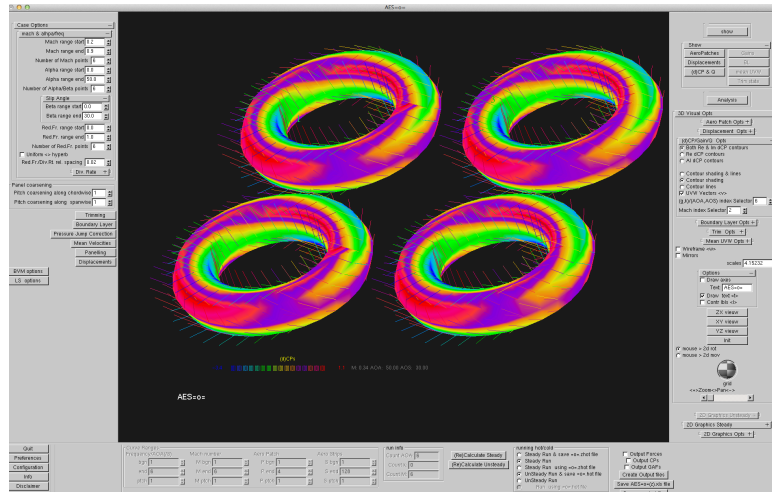


**Figure 5** Calculated steady pressure coefficient and velocity distributions on a set of donuts at a subsonic Mach number and relatively high angles of attack and sideslip

Figure 5 shows is a visualization of the calculated (steady flow) steady pressure coefficient distribution and the velocity vector distribution about a set of 4 donuts at a relatively low subsonic Mach number 0.34 , Angle of Attack 50° and Angle of Sideslip 30°.

### A set of payloads

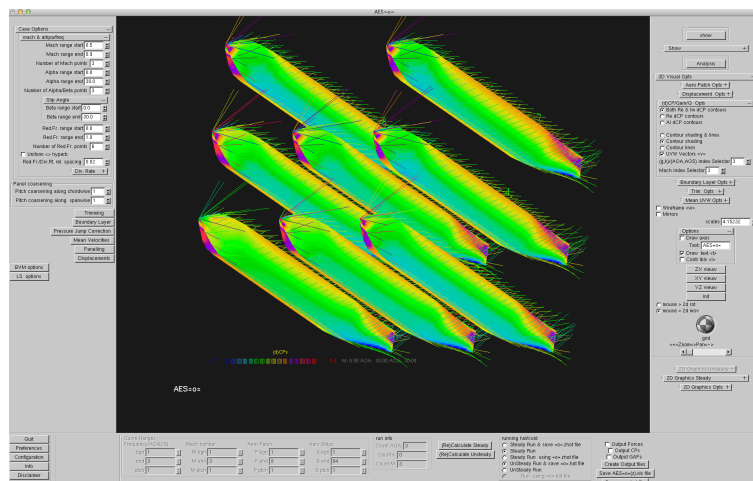


**Figure 6** Calculated steady pressure coefficients and velocity distribution on a set of payloads at a relatively high subsonic Mach number. Mach is 0.9, Angle of Attack 30° and Angle of Sideslip 30° for a set of 8 payloads.

Figure 6 shows a visualization of the calculated steady pressure distribution and the velocity vector distribution at a relatively high subsonic Mach number. Mach is 0.9, Angle of Attack 30° and Angle of Sideslip 30° for a set of 8 payloads.

## Change of geometry

Shown in Figure 7 is the workbench when changing the dihedral and thickness of a thick

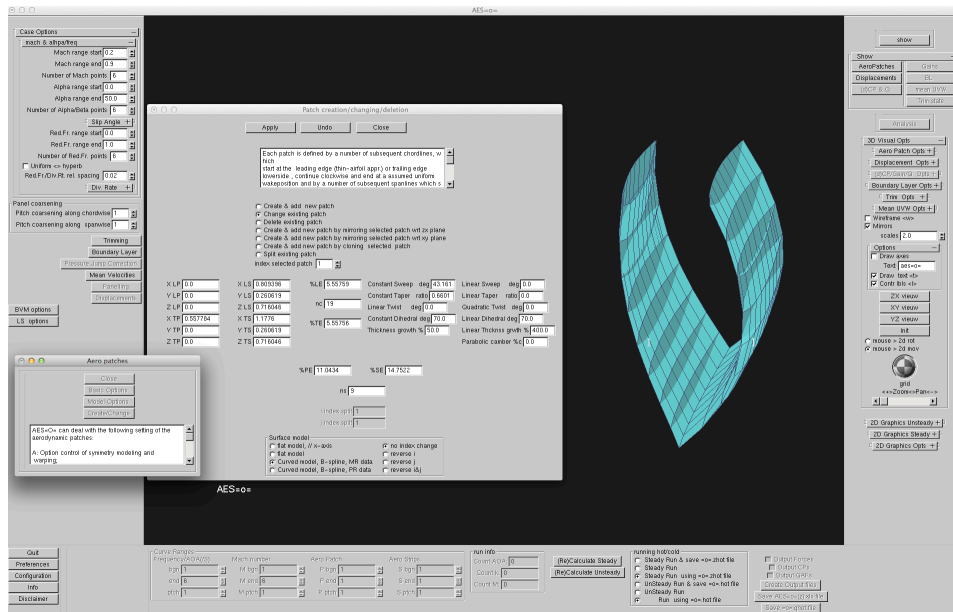


Figure 7 Inspection/generation panelling (changing dihedral & thickness of a thick wing)

wing [41]. Originally wing 445.6 was selected by the AGARD Structures and Materials Panel as the first three-dimensional standard lifting surface configuration to provide a common basis for comparison of pressures and forces. [28] [41].

## Warping on a wing fuselage

Figure 8 shows a visualization by AES=O= of 4 vibration modes of AGARD wing 445.6 warped to a F4 wing fuselage combination.

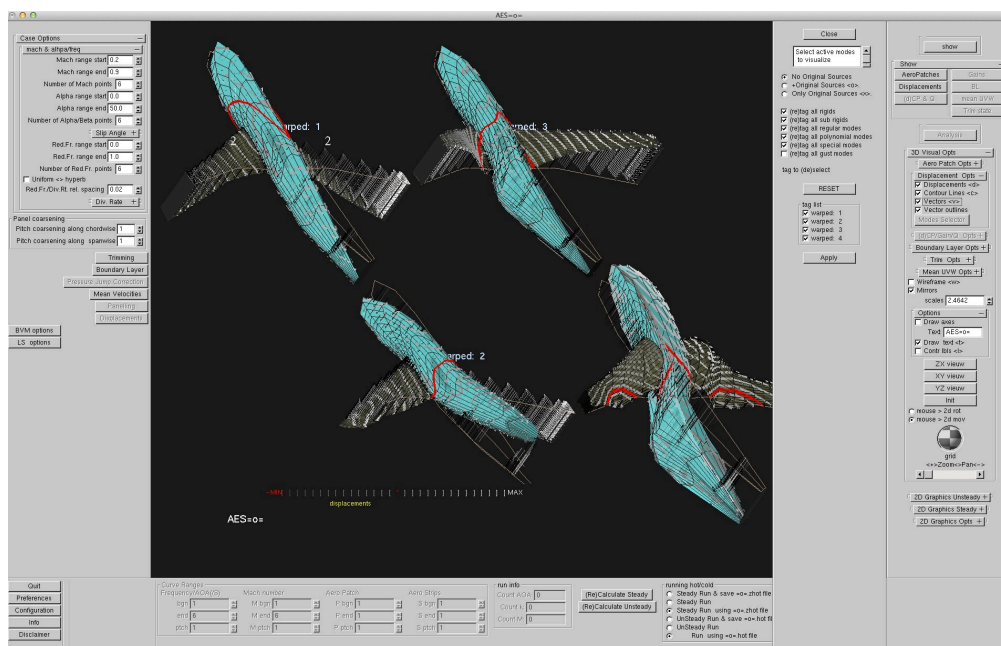
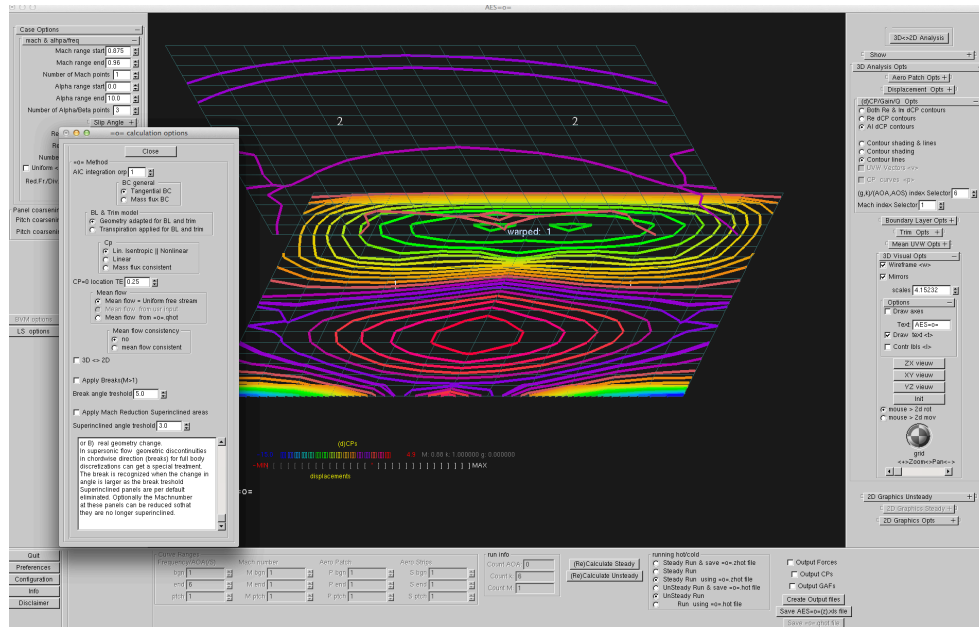


Figure 8 Warping on a F4 wing body





## Approximate transonic modelling



This figure presents a visualisation of the calculated imaginary part of the unsteady  $C_p$  jump distribution at a rectangular lifting surface with a shock patch at 70% chord at Mach 0.875 and reduced frequency=1.0.

**Figure 9** Unsteady pressure distributions on an oscillating rectangular wing in a transonic flow condition Mach number 0.875 and reduced frequency 1.0.

## Wing 445.6 Steady

The calculated steady pressure distribution for a thick 445.6 wing at a relatively high Mach number 0.9 and angle of attack  $20^\circ$  is presented in Figure 10.

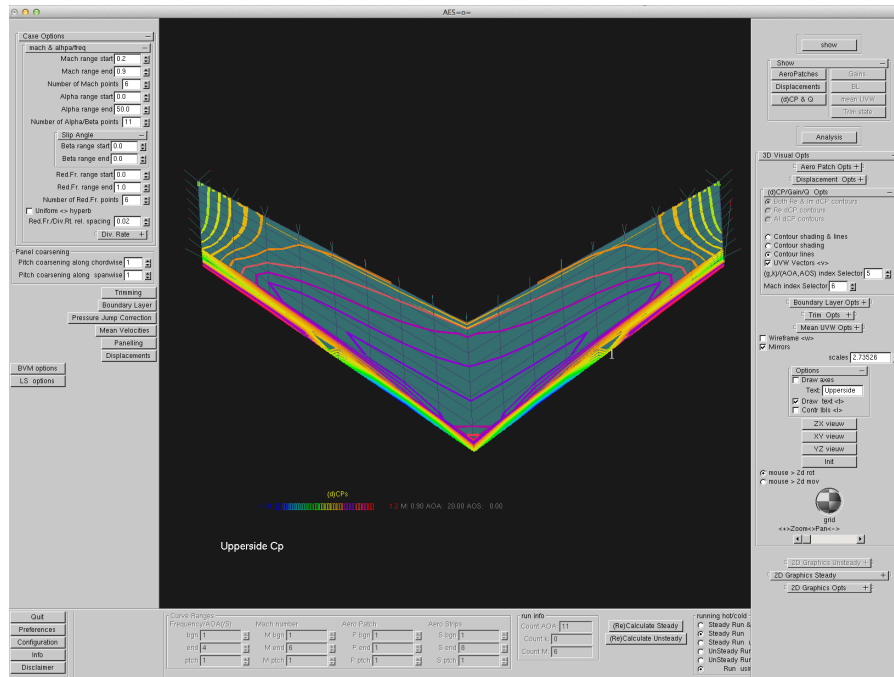


Figure 10 Inspection of calculated steady Cp distribution at upper side of a thick wing at Mach = 0.9 and AOA= $20^\circ$

The calculated steady Cp distributions at spanwise sections of a thick wing at Mach = 0.9 and AOA= $0.83^\circ$  is presented in Figure 11.

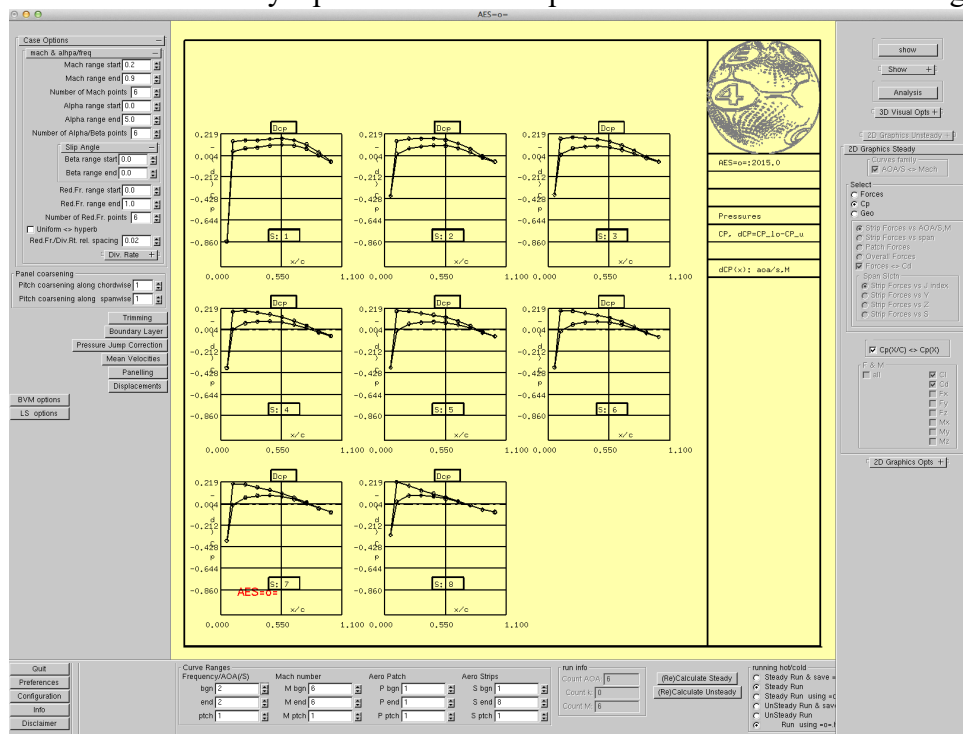


Figure 11 Inspection of calculated steady Cp distributions at spanwise sections of a thick wing at Mach = 0.9 and AOA= $0.83^\circ$ .



Figure 12 depicts the calculated Cl-Cd curves at Mach number =0.2 .. 0.9 of a thick 445.6 AGARD wing are presented.

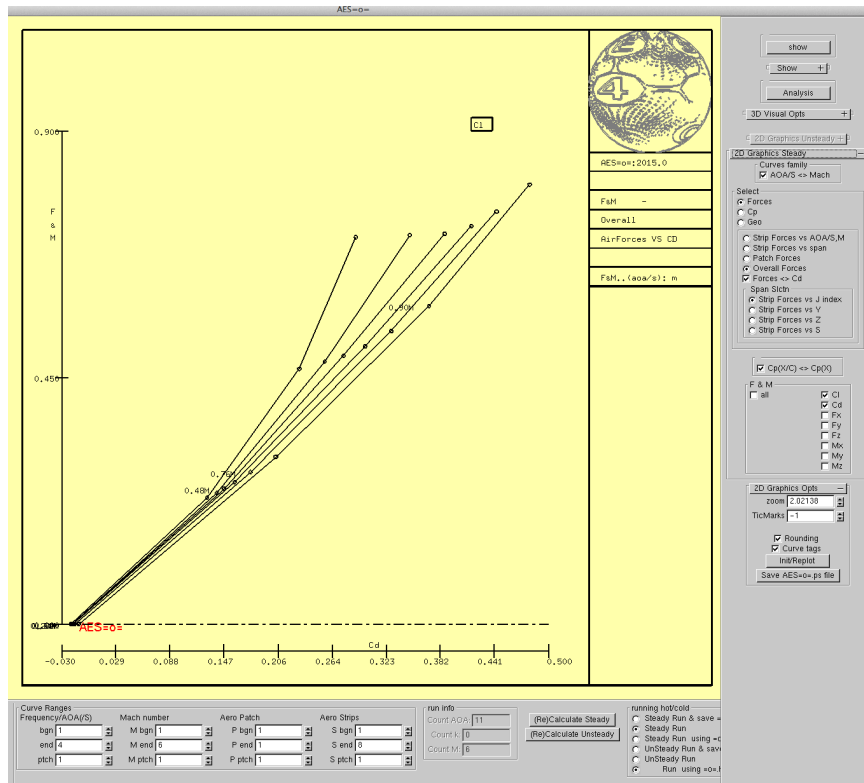
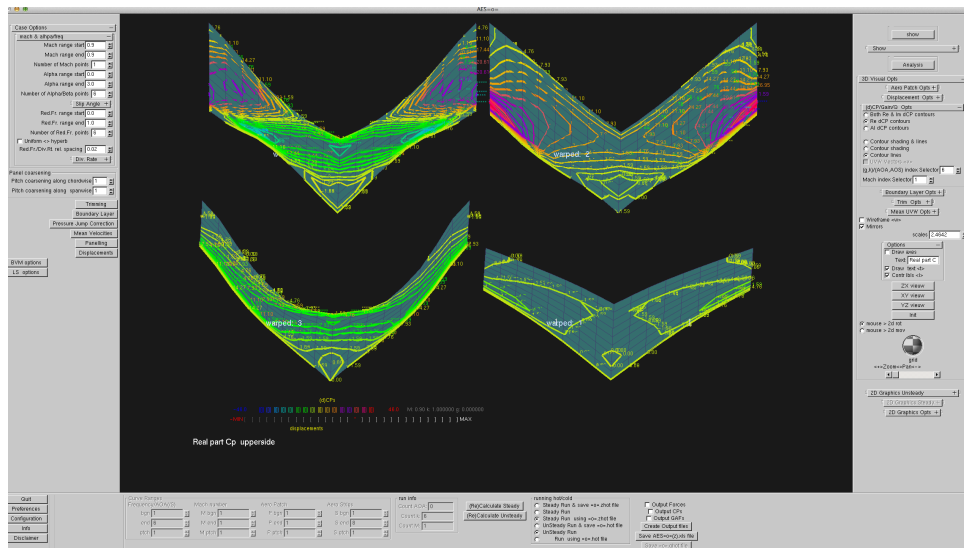


Figure 12 Inspection of calculated Cl-Cd curves at Mach number =0.2 .. 0.9 of a thick 445.6 AGARD wing

## Wing 445.6 unsteady

The calculated real part of unsteady  $C_p$  distribution at the upperside of a thick 445.6 AGARD wing at

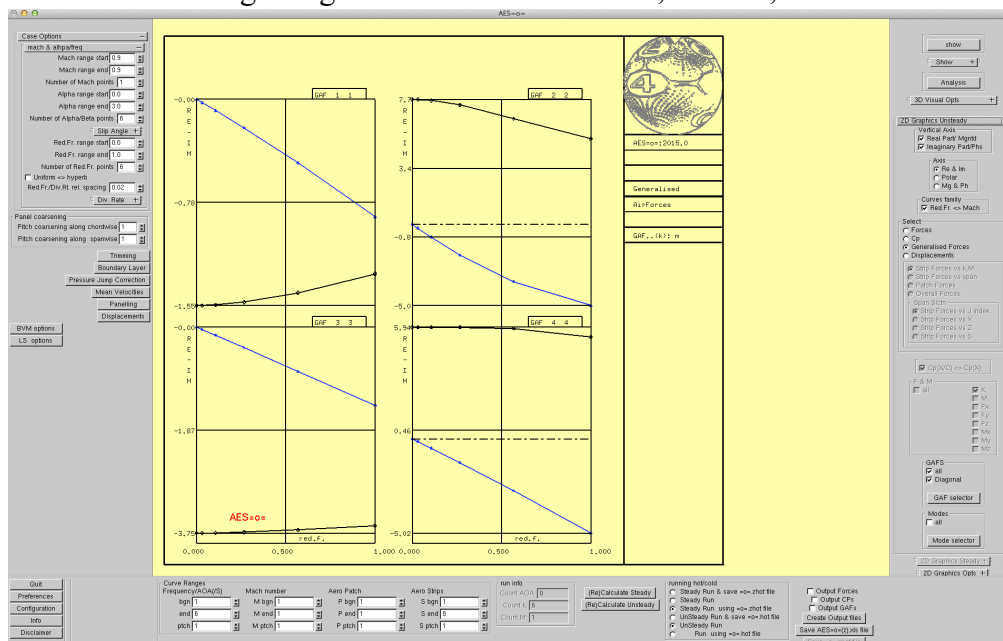


wing at extreme position of the modeshape, at Mach number 0.9 and reduced frequency 1. Is presented in

Figure 13.

Figure 13 Inspection of calculated real part of unsteady  $C_p$  distribution at upper side of a thick wing at extreme position of the mode shapes at Mach 0.9 and reduced frequency=1.

The calculated diagonal generalized forces GAF11, GAF22, GAF33 and GAF 44 on thick



AGARD wing 445.6 at Mach number 0.9 are presented in Figure 14 versus reduced frequency.

Figure 14 Inspection of calculated generalized forces GAF11, GAF22, GAF33 and GAF 44 on thick wing 445.6 at Mach=0.9



The calculated real and imaginary parts of the unsteady pressure distributions along sections of wing 445.6 are presented for the first mode and 6 frequencies (0.0 .. 1.0) in Figure 15

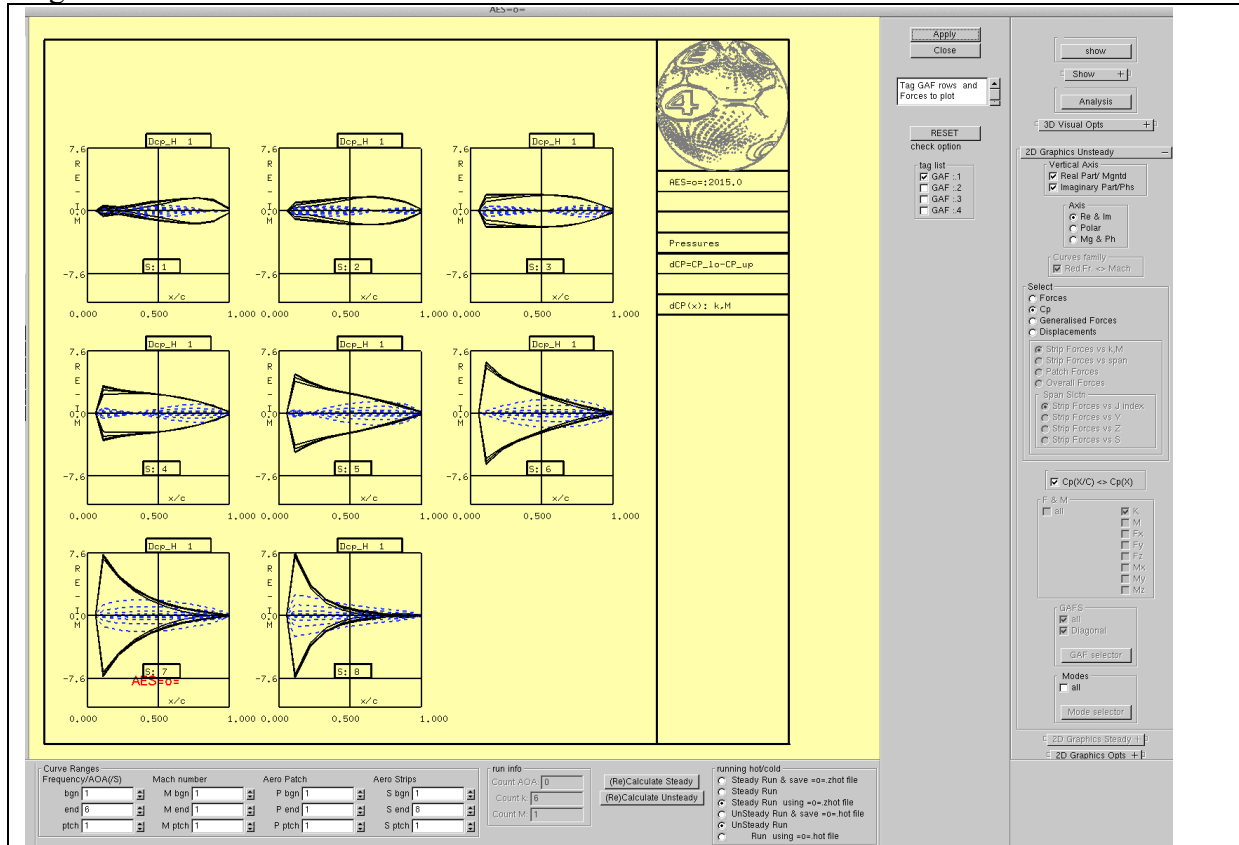


**Figure 15 Unsteady pressure distributions due to the first mode on the thick 445.6 wing**

## Hydrodynamic examples

The hydrodynamic examples presented here are all made using the Havelock elementary function, avoiding to need to model the free surface explicitly. An observer surface is used for the free surface to show the elevation.

### The Wigley Hull

For further investigation, numerical calculations have been made for the Wigley hull model Wigley III [39] using a mesh of 19x20 points at the port side of the hull considering geometric symmetry and presented in Figure 16. The figures show the elevation on the free surface and the pressure coefficient distribution on the free surface.

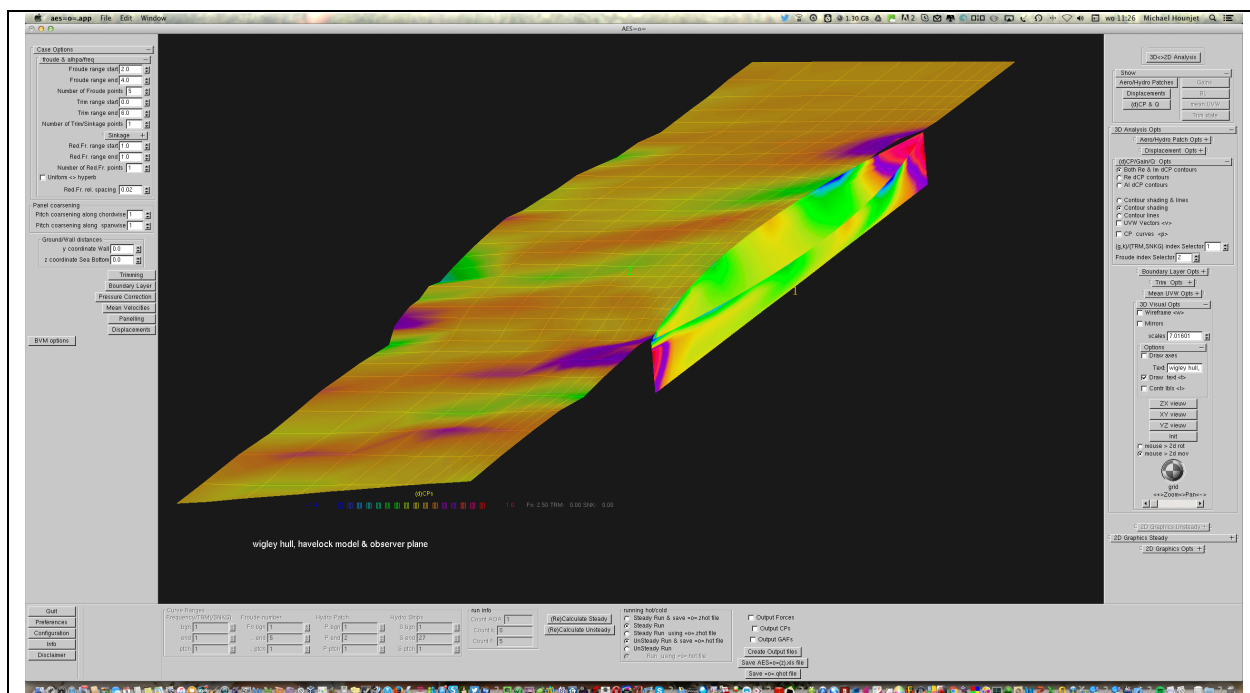


Figure 16 Inspection of calculated Cp and wave elevation due to a Wigley hull moving at various Froude numbers



## The submerged sphere

Figure 17 presents the steady solutions due to a submerged sphere with the radius  $R = 1$  are considered. Computations are made on a  $13 \times 13$  mesh on the port side, considering lateral symmetry about the  $xz$  plane. Five Froude numbers in the range 0.0 to 1.25 are considered together with 5 sinkage numbers in the range 0.0 to 3.0

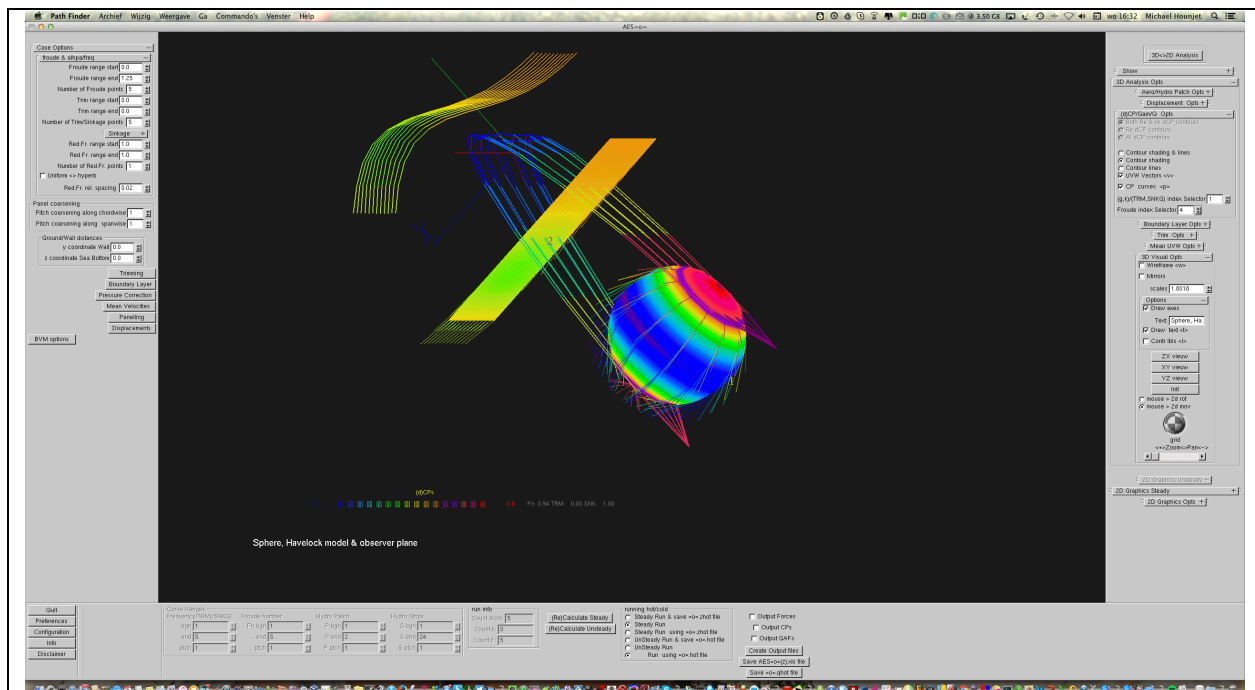
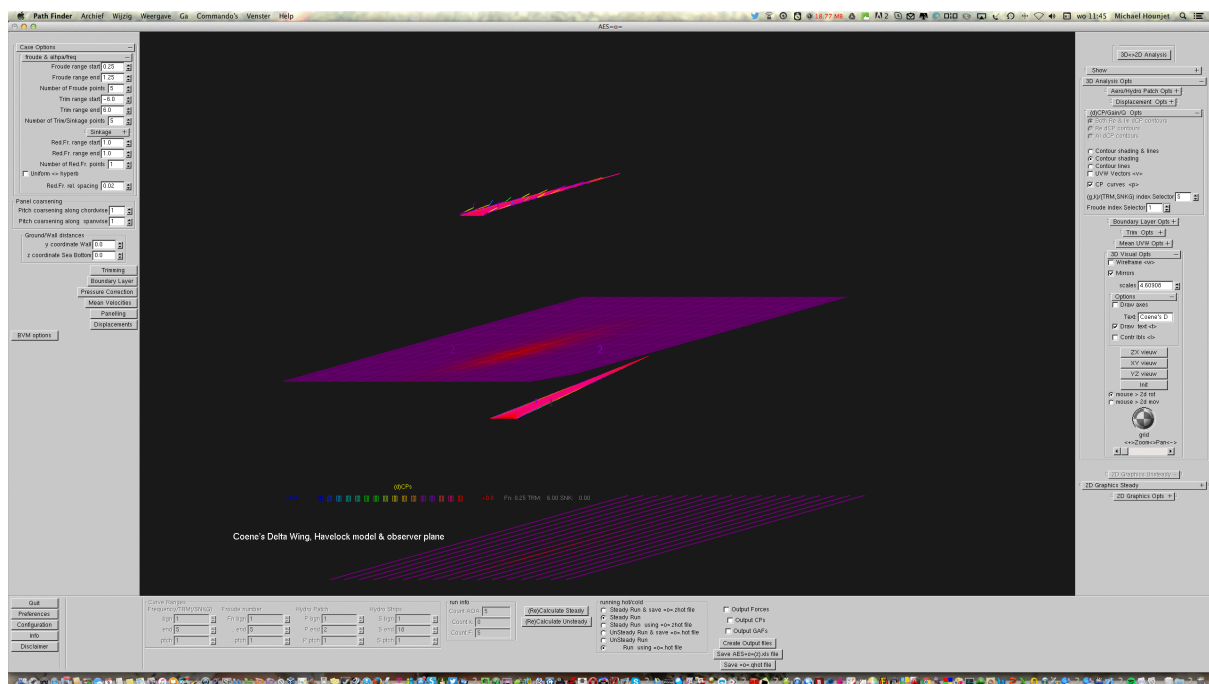


Figure 17 Inspection of calculated  $C_p$  and wave elevation due to a sphere moving at various Froude numbers and at various depths. Inspection of calculated  $C_p$  and wave elevation due to a sphere moving at various Froude numbers and at various depths.

## The submerged Delta wing of Rene Coene

In [40] an experimental experimental and theoretical investigation of cases of unsteady propulsion in non-uniform flow conditions have been discussed at the hand of a not-so deeply submerged rigid slender delta wing-like body in heaving and pitching oscillatory motion moving horizontally through a regular train of surface waves at at the frequency of encounter. The wave resistance has been calculated by the author in [42] as part of obtaining the master degree at the Technical University of Delft in 1975.

For this configuration we performed several simulations and Figure 18 shows a visualization of the calculated Cp and wave elevation due to Coene's delta wing moving at various Froude numbers (0.0 to 1.25) and angle of attack (TRM) (-6 deg to 6 deg) and zero heave (Sinkage) in order to analyse the free surface effects of not-so-deeply submerged wings which can be associated with swimming slender bodies in surface waves and contribute to better understanding of the resistance characteristics of surface ships in a wavy sea.



**Figure 18 Inspection of calculated Cp and wave elevation due to Coene's delta wing moving at various Froude numbers and angle of attack [40]**





## A submerged spheroid

Steady calculations of a 1.6 m submerged spheroid with length 10 m and thickness 2 m have been performed for various Froude numbers (0.0 to 2.41). This is a well-known testcase (see pp 27-32 of [4]). The spheroid is approximated with a mesh consisting of  $9 \times 10$  points and an observer plane at the free surface with a mesh of  $9 \times 10$  points. A visualization of the calculated pressure and wave elevation data is presented in Figure 19.

The main calculated forces  $F_x$ ,  $F_y$  and  $M_y$  are presented in Figure 20. They are compliant with the results presented in [4] (using a reference length 10 m) which are embedded with the red, blue and green open circles in Figure 21. Note that our applied Froude number is a factor 3.003 higher due to the fact that we have applied implicitly a reference length of 1m. Also, we have applied a factor 50 to the forces and a factor 500 to the moment presented in [4] to account again for the different reference length.

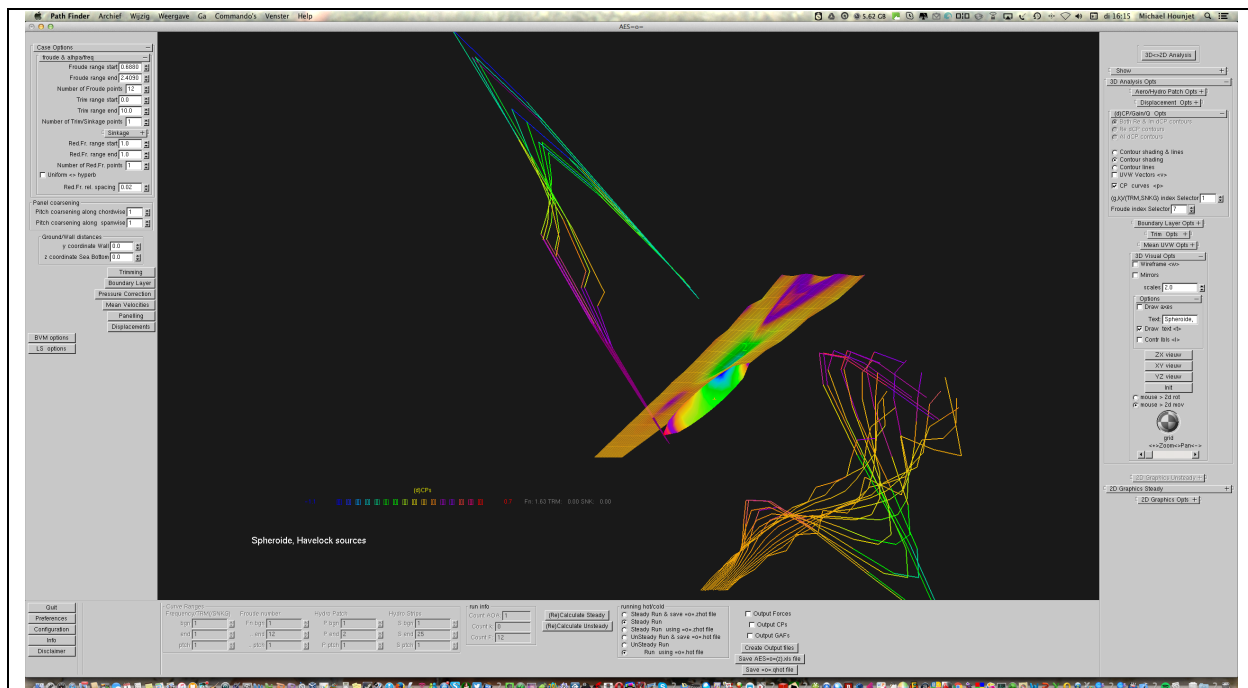


Figure 19 Inspection of calculated  $C_p$  and wave elevation due to a spheroid moving at various Froude numbers

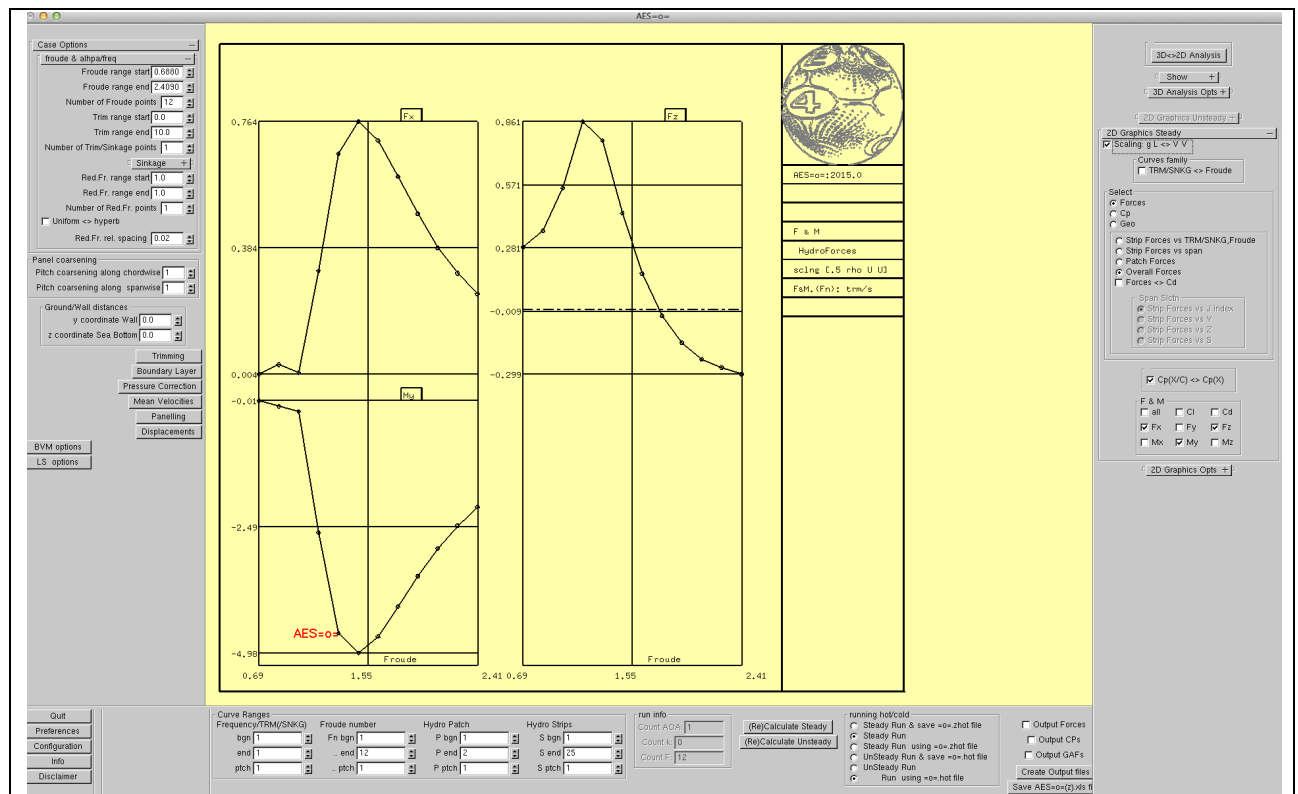


Figure 20 Inspection of calculated forces (Drag, Lift and Moment) on a submerged ellipsoid

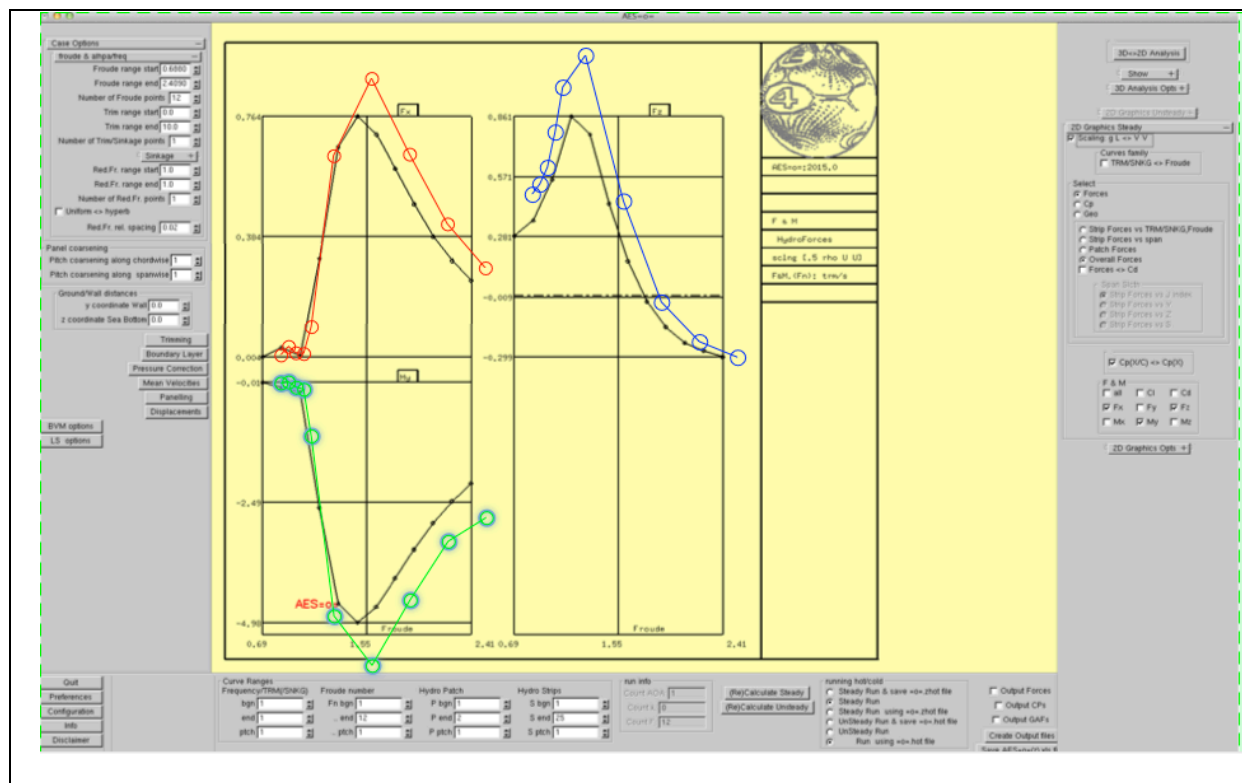
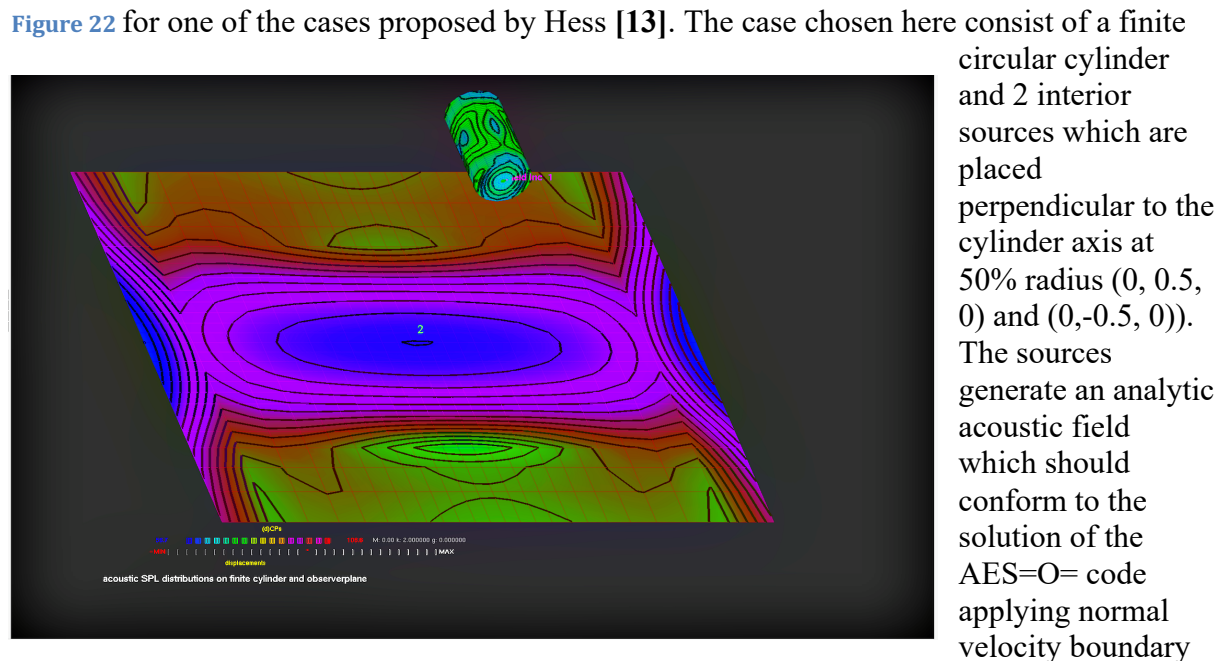


Figure 21 Comparison of calculated forces (Drag, Lift and Moment) on a submerged ellipsoid with results presented in [4]. The symbols are from [4].

## Aeroacoustics example

An acoustic demonstration has been performed and presented in



conditions derived from the analytic acoustic field. The radius of the cylinder is 1, its length is 4, the wave number is 2. The latter yields a sound wave length of about 75% of the cylinder length. An observer plane is located at the bottom.

**Figure 22** SPL levels on finite cylinder and observer plane

## Summary of the AES=O= method

- Running of AES=O= requires basically ONE file the aes=o=.cnf file.
- Output is provided in text, Excel and Postscript format.
- The AES=O= system may be run along two main routes:
  - steady and
  - unsteady. The unsteady route may be run with steady flow field data obtained from a previous steady run of the AES=O= system, with steady data from other sources or with the undisturbed steady flow field.
- AES=O= uses the GLUI user interface library (Version 2.36). Control h is backspace in the input boxes.

The AES=O= method supports 3 disciplines:

- I. Steady and Unsteady Aerodynamics,
- II. Steady and Unsteady Hydrodynamics and
- III. Aeroacoustics

### I: Steady and Unsteady Aerodynamics

The AES=O= is a general steady and unsteady method with an almost unlimited application range with respect to Mach number, angle of attack, angle of sideslip, frequency and configuration. The code calculates 3-D airloads and pressure distributions for oscillating parts with general unsteady motions characterized by the divergence rate and the reduced frequency. Sinusoidal motions or gusts characterized by the reduced frequency and exponential growing motions characterized by the diverging rate are modeled. The method calculates pressure coefficients, overall forces, sectional forces&moments coefficients ( $C_l$  &  $C_d$  and  $K, M$  (AGARD manual on aeroelasticity notation [28])) and generalised force coefficients for rigid & flexible displacement modes. The pressure is calculated at the centroid of panel leading and trailing edges and applied in the calculation of generalized forces. At subsonic edges of lifting surfaces care has been taken to deal with the singular behaviors of the pressure and to integrate the pressures consistent with the evaluation of forces by global methods. AES=O= calculates the suction force, allowing accurate induced drag calculation or the suction force analogy to estimate globally effects of leading edge separation|

### II: Steady and Unsteady Hydrodynamics

AES=O= solves the Laplace equation for incompressible flow conditions about thick and thin structures composed of wetted surfaces or by thin lifting surfaces which are parallel to the free stream. The free surface is modelled as a wetted surface with the appropriate free surface condition. The tool is a general steady and unsteady method with an almost unlimited application range with respect to Froude number, Trim, Sinkage, frequency and configuration.

The code calculates 3-D hydrodynamic loads and pressure distributions for oscillating structural parts with general unsteady motions characterised by the reduced frequency. Waves characterized by the reduced frequency and the distance to sea bottom are allowed. The method calculates sectional forces&moments coefficients ( $C_l$  &  $C_d$  and  $K, M$  (AGARD



manual on aeroelasticity notation [28]) and generalised force (or added mass, damping)-coefficients for rigid & flexible displacement and wave modes.

The pressure are calculated at cgs of panel leading and trailing edges and applied in the calculation of forces. At leading edges of lifting surfaces care has been taken to deal with the singular behaviour of the pressure and to integrate the pressures consistent with the evaluation of forces by global methods, allowing accurate induced drag calculation or the suction force analogy to estimate globally effects of leading edge separation.

### III: aeroacoustics

AES=O= models acoustic scattering based on the acoustic equation which is the same as the one applied in unsteady aerodynamics. It is basically the same compared to the unsteady aerodynamics model apart from the nondimensionalization with the speed of sound and the modelling of incident acoustic fields.

## Installation

The installation is performed as follows:

1. Installation should be performed for OSX Sonoma 14.2.1
2. Unzip the aes=o=.zip file
3. Move the files in the aes=o=/bin directory to your preferred bin location and/or set the path.
4. Move the file in the aes=o=/home directory to your HOME.
5. Move the files in the aes=o=/run directory to your preferred run location.
6. Install a GLUT and an OPENGL framework when they are not already installed
7. Install gfortran libraries when AES=O= complaints about missing libraries.

The runs/445.6 directory contains:

- the preferences file .prefs\_aes=o=(Table 33) and
- the configuration file: aes=o=.cnf.



## How to Run and Use information

This chapter covers usage issues.

After executing the command `bin/aes=o=` the **AES=O=** workbench will show up in aerodynamic (Figure 23), hydrodynamic (Figure 24) or aeroacoustics (Figure 25) mode, respectively.

The workbench consist of a sidebar at the left, a sidebar at the right and a horizontal bar at the bottom.

### Left sidebar

The left top panel allows the setting of the case parameters.

The left mid panel allows the setting of the cconfiguration parameters.

The left bottom panel deals with general info and licensing parameters which will be discussed in the next section

### Bottombar

The mid bottom controls 2D graphics.

The right bottom panel deals with the execution.

### Right sidebar

The top right panel controls 3D graphics

The mid right panel controls 2D graphics

Apart from the geometric and modes shape settings and many other aspects for which one could also consult the documents [38] [3] this section explains the main aerodynamic and structural (warping)control settings.

In the following sections we will primarily describe the aerodynamic usage while the **hydrodynamic** and **aeroacoustics** usage will be only be described and highlighted in **blue** and **green**, respectively when different.

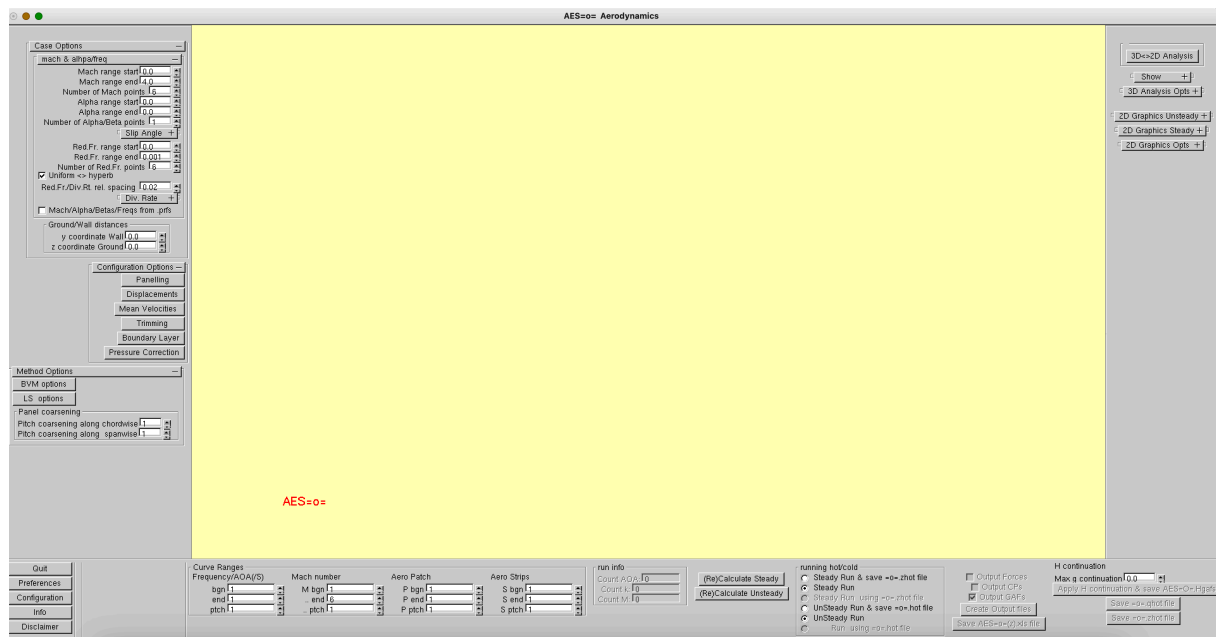


Figure 23 The start-up screen of AES=0= in aerodynamic mode

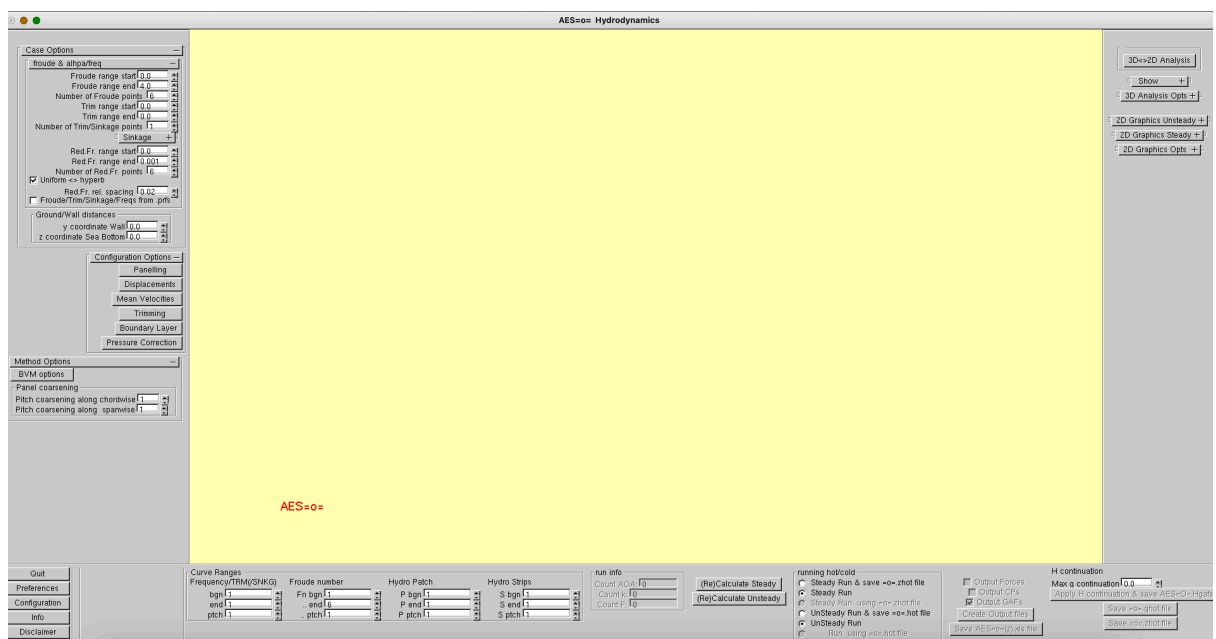


Figure 24 The start-up screen of AES=0= in hydrodynamic mode



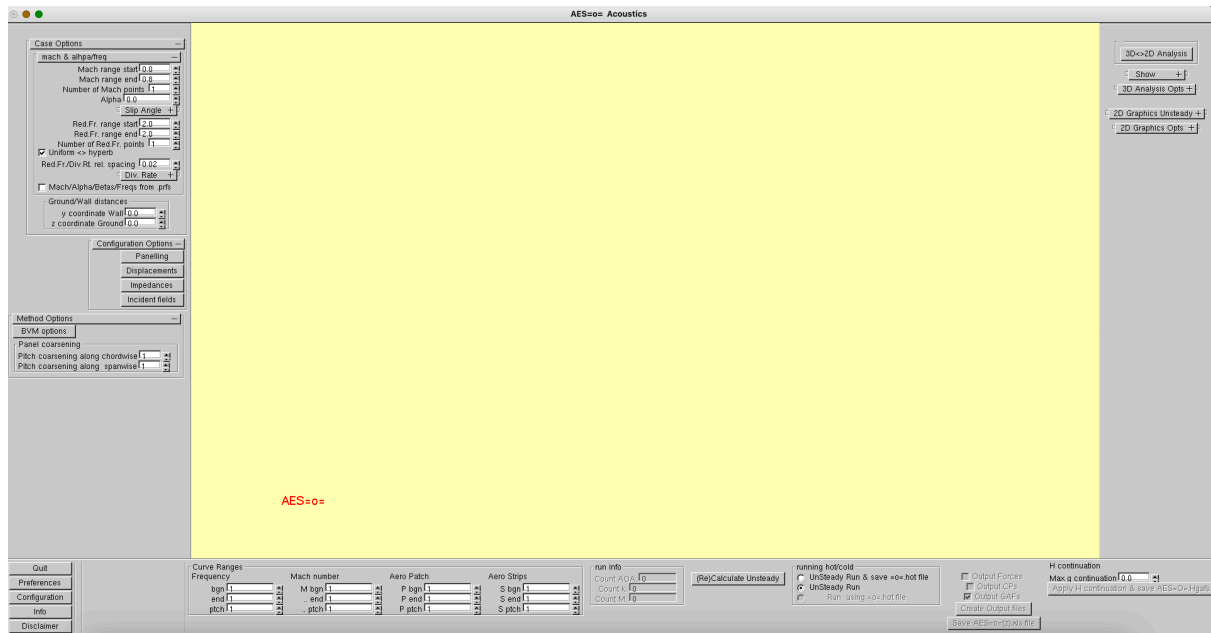


Figure 25 The start-up screen of AES=0= in aeroacoustics mode

Activation is not needed for the evaluation version during the trial period. The trial period is set to X days starting from first run.

1. Open a terminal.
2. Go to your run directory.
3. Run AES=O= (see Figure 26)
4. Press info button. The info window opens.
5. Press activation in the info windows.
6. KEY in your validation license code.
7. Press activates.
8. Quit AES=O=





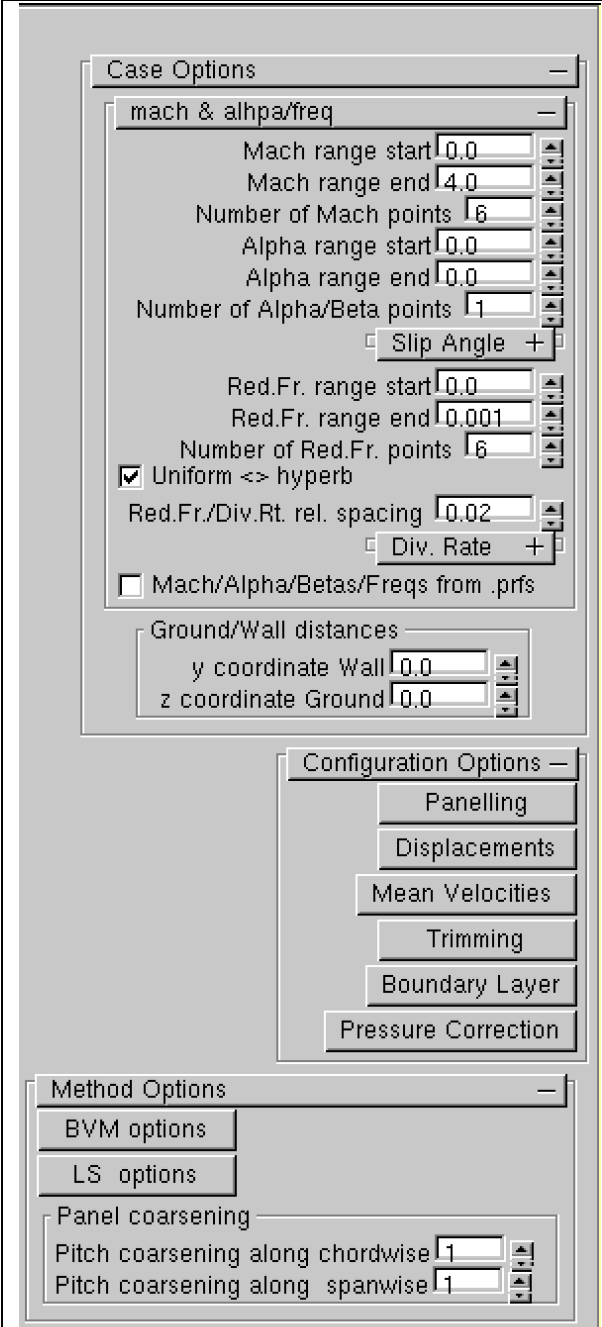
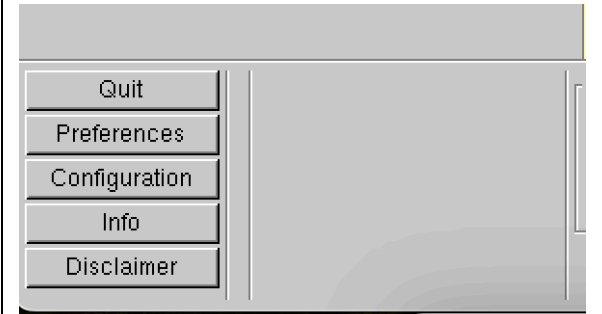
## Left Sidebar

After starting up the workbench in aerodynamic mode the left sidebar deals with the case, the configuration and general info depicted in Table 8 . The case parameters (Mach number, angle of attack, angle of slip, reduced frequencies/ diverging rates and ground/wall distances) can be prescribed in the top part and are explained in Table 11. In the middle part the rollouts can be opened to prescribe configuration data: Geometry, Downwash and Pressure corrections and the parameters of the calculation method can be set. One can reduce the number of panels/meshpoints in the main directions of the patches to reduce computer time. At the bottom one can stop the program, save the configuration file et cetera.

After starting up the workbench in **hydrodynamic** mode the left border window deals with the case, the configuration and general info depicted in Table 9 . The case parameters (Froude number, the TRIM and Sinkage, reduced frequencies and seabed/wall distances) can be prescribed in the top part and are explained in Table 12. In the middle part the rollouts can be opened to prescribe configuration data: Geometry, Downwash and Pressure corrections and the parameters of the calculation method can be set. One can reduce the number of panels/meshpoints in the main directions of the patches to reduce computer time. At the bottom one can stop the program, save the configuration file et cetera.

After starting up the workbench in **aeroacoustics** mode the left border window deals with the case, the configuration and general info depicted in Table 10. The case parameters (Mach number, Angle of attack, angle of slip, reduced frequencies/ diverging rates and ground/wall distances) can be prescribed in the top part and are explained in Table 11. In the middle part the rollouts can be opened to prescribe configuration data: Geometry, Downwash and Pressure corrections and the parameters of the calculation method can be set. one can reduce the number of panels/meshpoints in the main directions of the patches to reduce computer time. At the bottom one can stop the program, save the configuration file et cetera.

**It is advised to close rollouts after use to prevent their window growing beyond the screen bottom border resulting in losing control.**

 <p>The sidebar contains three main panels:</p> <ul style="list-style-type: none"> <li><b>Case Options:</b> Includes input fields for Mach range (start: 0.0, end: 4.0, points: 6), Alpha range (start: 0.0, end: 0.0, points: 1), Red.Fr. range (start: 0.0, end: 0.001, points: 6), and checkboxes for Slip Angle, Uniform &lt;-&gt; hyperb, Div. Rate, and Mach/Alpha/Betas/Freqs from .prfs. It also has Ground/Wall distances for y coordinate Wall (0.0) and z coordinate Ground (0.0).</li> <li><b>Configuration Options:</b> A vertical stack of buttons: Panelling, Displacements, Mean Velocities, Trimming, Boundary Layer, and Pressure Correction.</li> <li><b>Method Options:</b> Includes buttons for BVM options and LS options, and a Panel coarsening section with Pitch coarsening along chordwise (1) and spanwise (1).</li> </ul> <p>At the bottom of the sidebar is a menu with buttons: Quit, Preferences, Configuration, Info, and Disclaimer.</p>	<p>Main case panel</p> <p>See table Table 11 Main Case Parameters</p> <p><i>Configuration Rollout</i>  Set/change patches and types  Set downwash  Set explicit velocities  Set static state of geometry  Set a boundary Layer change to geometry</p> <p>Set a Pressure correction  <i>Set method options</i>  Set Boundary Volume options.  Set Lifting Surface options</p> <p>Reduction of number of panels in the calculation.</p>
 <p>The bottom sidebar contains a vertical stack of buttons: Quit, Preferences, Configuration, Info, and Disclaimer.</p>	<p>Stop  Read preferences  Read and save configuration</p>

**Table 8 Left sidebar in aerodynamic mode**

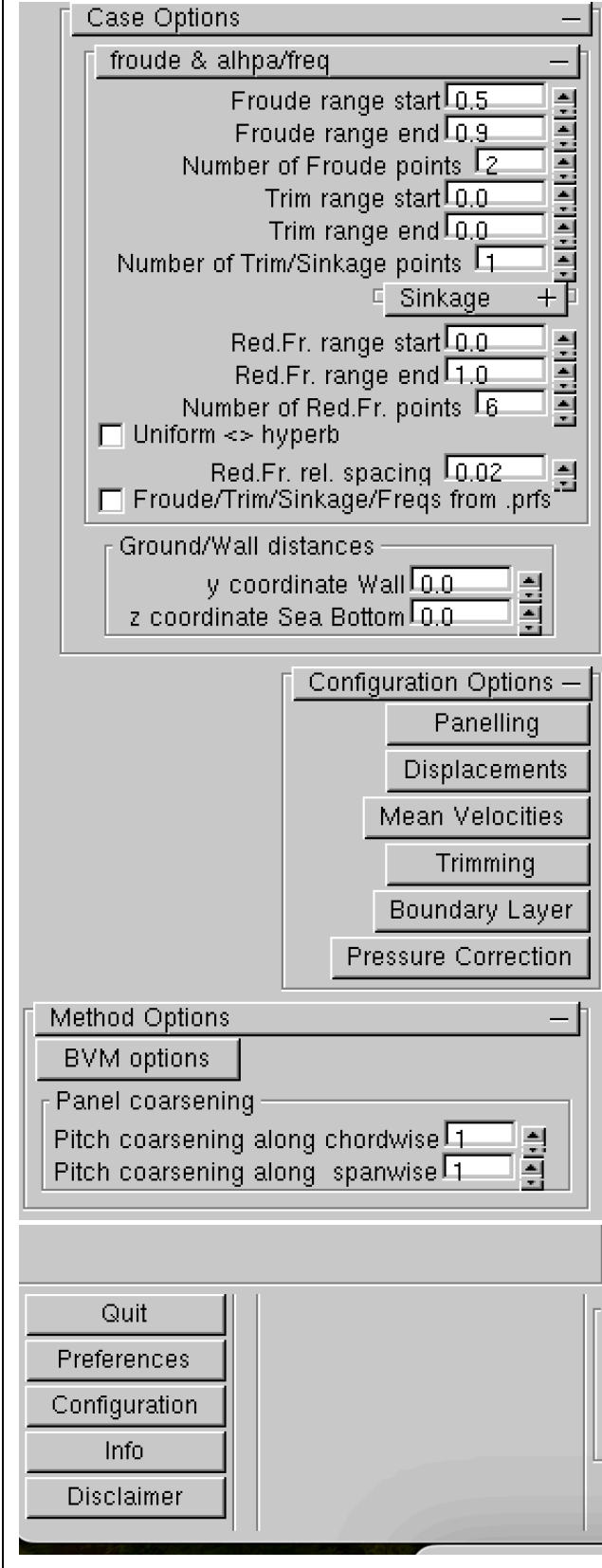
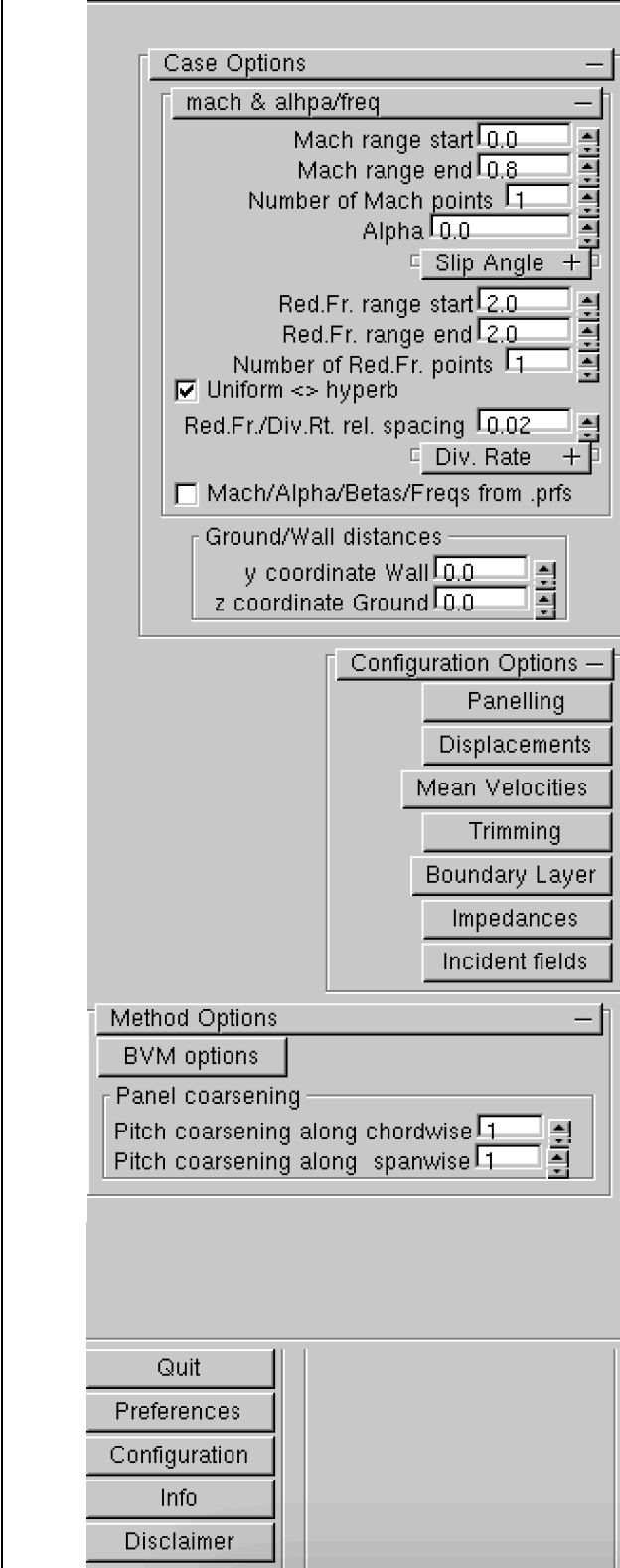
 <p>The screenshot shows the AES4AC software interface. The 'Case Options' panel is active, showing settings for Froude range (0.5 to 0.9), Number of Froude points (2), Trim range (0.0 to 0.0), Number of Trim/Sinkage points (1), Sinkage (+), Red.Fr. range (0.0 to 1.0), Number of Red.Fr. points (6), Uniform &lt;-&gt; hyperb (unchecked), Red.Fr. rel. spacing (0.02), and Froude/Trim/Sinkage/Freqs from .prfs (unchecked). The 'Ground/Wall distances' panel shows y coordinate Wall (0.0) and z coordinate Sea Bottom (0.0). The 'Configuration Options' panel shows buttons for Panelling, Displacements, Mean Velocities, Trimming, Boundary Layer, and Pressure Correction. The 'Method Options' panel shows BVM options, Panel coarsening, Pitch coarsening along chordwise (1), and Pitch coarsening along spanwise (1). At the bottom, there are buttons for Quit, Preferences, Configuration, Info, and Disclaimer.</p>	<p>Main case panel</p>
	<p>See Table 12</p>
	<p><i>Configuration Rollout</i> Set/change patches and types</p>
	<p>Set downwash Set explicit velocities Set static state of geometry Set a boundary Layer change to geometry Set a Pressure correction</p>
	<p><i>Set method options</i> Set Boundary Volume options.</p>
	<p>Reduction of number of panels in the calculation.</p>
	<p>Stop Read preferences Read and save configuration</p>

Table 9 Left Sidebar in hydrodynamic mode

	<p>Main case panel</p> <p>See table Table 11 Main Case Parameters</p> <p><i>Configuration Rollout</i></p> <p>Set/change patches and types Set downwash</p> <p>Set explicit mean velocities Set static state of geometry</p> <p>Set a boundary Layer change to geometry Set impedances</p> <p>Set Incident fields</p> <p>Set Boundary Volume options.</p> <p>Reduction of number of panels in the calculation.</p> <p>The setting of trimming, Boundary layer, Angle of Attack, Slip are meant for the steady calculations which can be useful for the effect on the boundary conditions and the pressure, similar as a setting of the mean velocities</p> <p>Stop</p> <p>Read preferences Read and save configuration</p>
--	---

**Table 10 Left Sidebar in Aeroacoustics mode**



## Case Parameters

	<p>Set Mach number range Set number of Mach runs. Set Angle of Attack range Set number of Alpha/Beta runs.</p> <p>Angle of Slip range Set reduced frequency range Set number of frequency runs</p> <p>Set diverging rate range.</p> <p>Override data with data on .aes=o=.prfs</p> <p>Set y coordinate of side wall or symmetry plane. Set z coordinate of symmetry plane or runway</p>	<p>The distribution of the Mach numbers is uniform.</p> <p>The distribution of the Angle numbers is uniform</p> <p>The distribution of the frequencies can be uniform or hyperbolic with an initial step.</p>
--	---	---

**Table 11 Main Case Parameters Rollout in aerodynamic/aeroacoustics mode**

	<p>Set Froude number range</p> <p>Set number of Froude runs.</p> <p>Set Trim range</p> <p>Set number of Trim/Sinkage.</p> <p>Sinkage range</p> <p>Set reduced frequency range</p> <p>Set number of frequency runs</p> <p>Override data with data on .aes=o=.prfs</p> <p>Set y coordinate of side wall or symmetry plane.</p> <p>Set z coordinate of Sea bed</p>	<p>The distribution of the Froude numbers is uniform.</p> <p>The distribution of the Trim/Sinkage numbers is uniform</p> <p>The distribution of the frequencies can be uniform or hyperbolic with an initial step.</p>
--	---	--

**Table 12 Main Case Parameters Rollout in hydrodynamic mode**



## Configuration Parameters

The configuration rollout allows to set several modelling options et cetera:

- Panelling: set/change patches and types
- Displacements: set downwash
- Mean velocities: set explicit velocities
- Trim: set static state of geometry
- Boundary layer: add boundary layer thickness to geometry
- Pressure correction: set a correction gain on the pressures

In addition, in aeroacoustics mode one can set:

- incident sound field potentials and
- impedance distributions

Pressing the button will open associated windows which are detailed in the following sections.

### *Panelling* *button*

The first is the panelling button which opens the Aero Patches window depicted in Figure 27. There are 3 buttons: the Basic options, the Model options and the Create/Change button, respectively which will open associated windows described in the following sections.

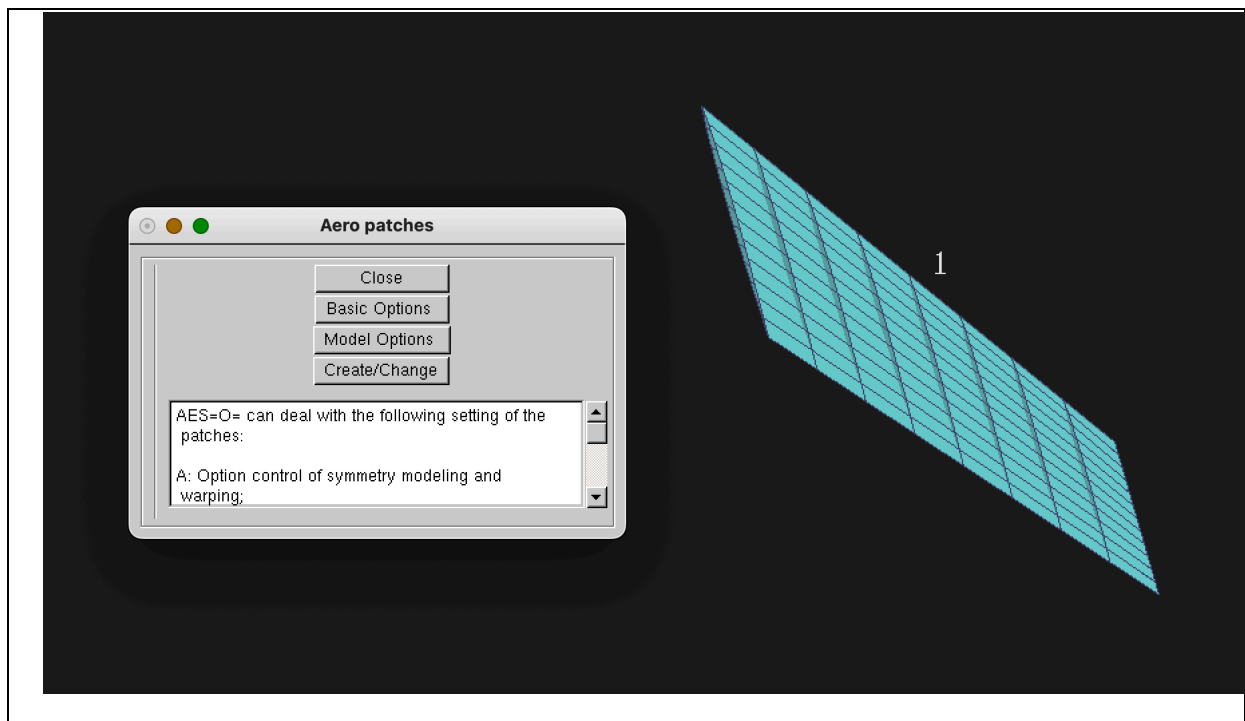


Figure 27 Panelling Window

Basic

Basic Options

options button

The basic options button opens the aero patch basic control window depicted in Figure 28.

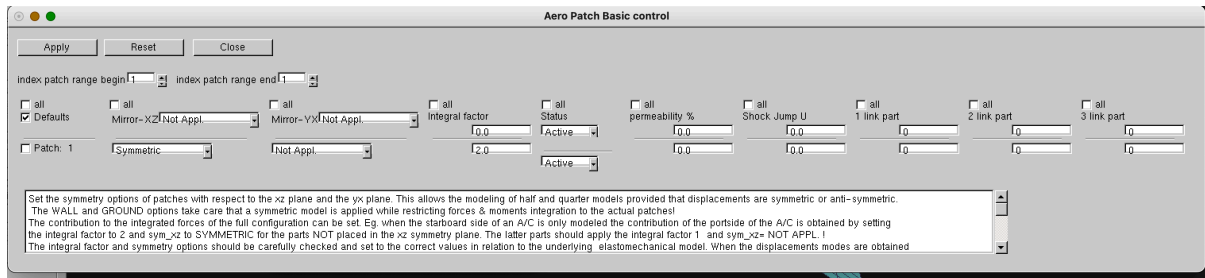


Figure 28 Aero patch control

The Listbox options are presented in Table 13.

The window allows to set the symmetry options of patches with respect to the  $xz$  plane and the  $yx$  plane. This allows the modeling of half and quarter models provided that

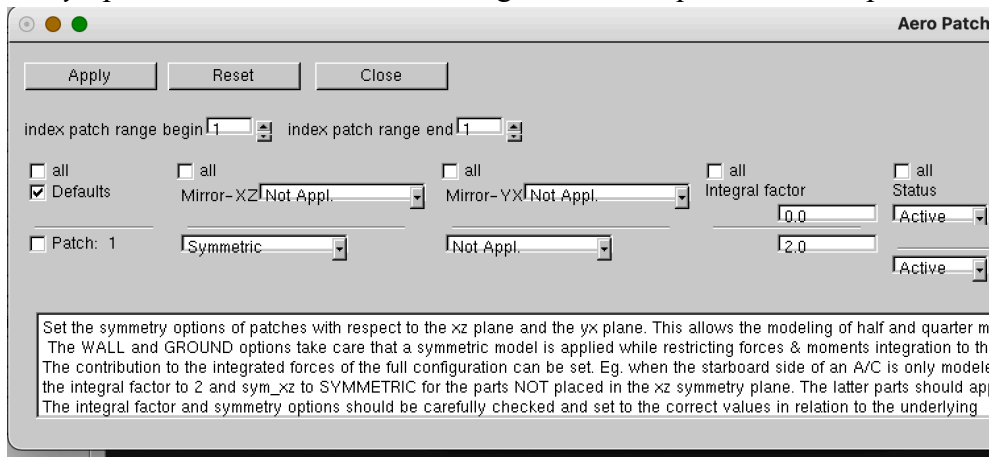


Figure 29 Left part aero/hydro patch control

displacements are symmetric or anti-symmetric with respect to these planes

Special symmetry options are provided to deal with ground/runway/sea bottom and wall effects. These options take care that a symmetric model is applied while restricting forces & moments integration to the actual patches! The

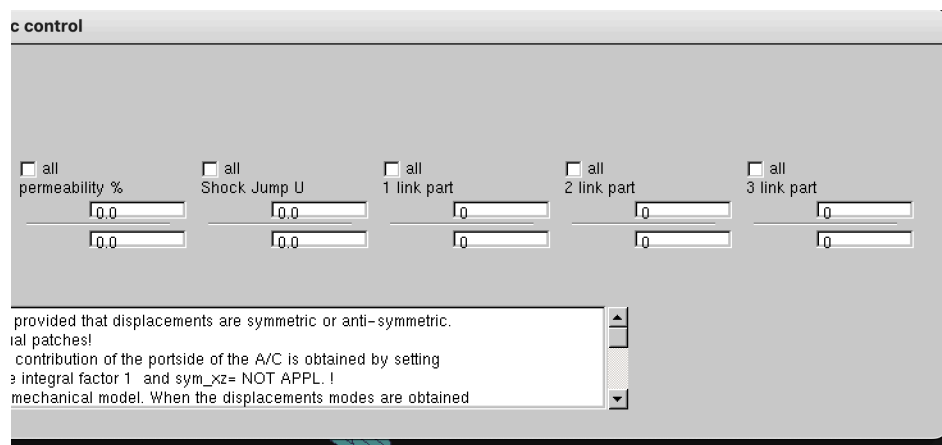


Figure 30 Right part aero/hydro patch control

forces of the full configuration can be set. For example when the starboard side of an A/C is only modeled the contribution of the portside of the A/C is obtained by setting the integral factor to 2 and sym\_xz to SYMMETRIC for the parts NOT placed in the  $xz$  symmetry plane. The latter parts should apply the integral factor 1 and sym\_xz= NOT APPL. ! The integral

contribution to the integrated

factor and symmetry options should be carefully checked and set to the correct values in relation to the underlying elastomechanical model.

The status of a patch can be set to active, observer or inactive. When the displacements modes are obtained from an external dataset (eg FEM) the warping can be restricted to selected parts (maximum 3) of the dataset (for example a winglet or effector). Entering zero selects the full set. The permeability should be set to a nonzero value when modelling inlets ,outlets or blunt afterbodies. The shockjump parameter resembles the normal velocity jump and applies to shock plane patches;

Mirror XZ	Mirror XY	Status						
Not Appl. Symmetric Anti-Symm. modes Symmetric/Wall	Not Appl. Symmetric Anti-Symm. modes Symmetric/Ground	Active Deactive Observer						
Not Appl. Symmetric Anti-Symm. modes Symmetric/Wall	Not Appl. Symmetric Anti-Symm. modes Symmetric/Sea Bottom							

Table 13 Listbox options basic patch control

Model options



button

The model options button opens the aero patch model control window depicted in Figure 31.

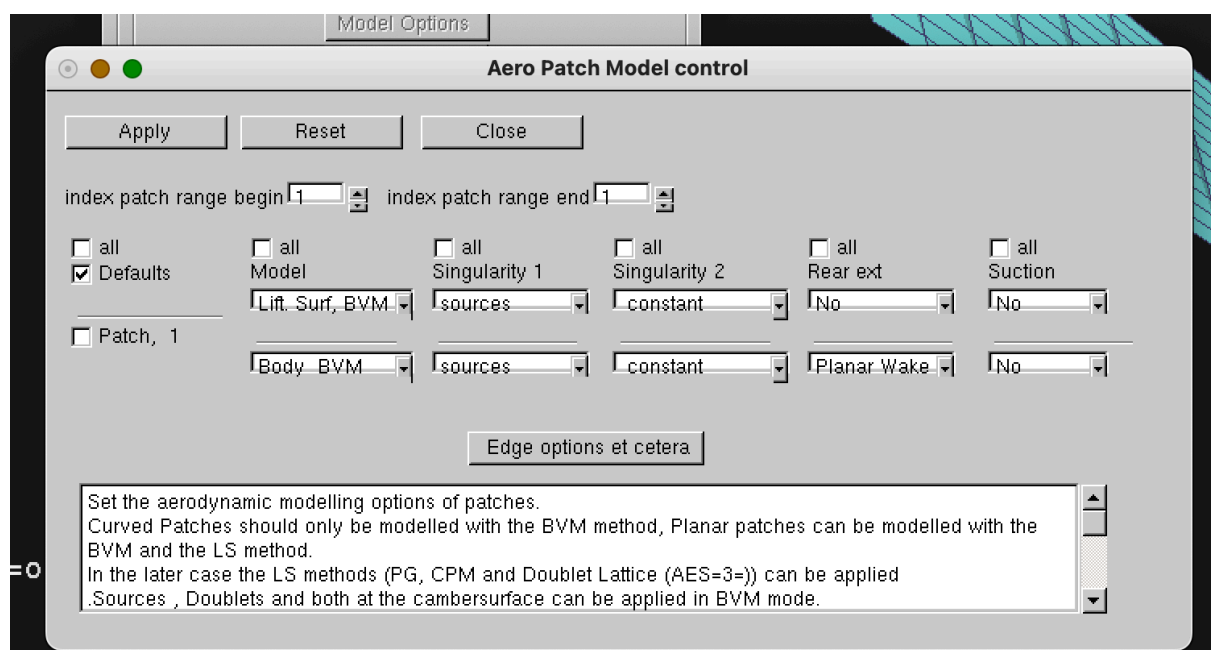


Figure 31 Model Options

The Listbox options are presented in Table 14. The window sets the aerodynamic modelling options of patches. Planar patches can be modelled with the BVM and the LS method. Non planar Patches should only be modelled with the BVM method, Planar patches can be modelled with the BVM especially when the suction force is required and with the LS (Lifting Surface) method (PG, CPM and Doublet Lattice [1]) although it is recommended to apply the AES=3= method in such a case. Apply sources for non-lifting parts, doublets for lifting parts and the camber option in case of thin parts. In the later case the LS methods (PG, CPM and Doublet Lattice (AES=3= like)) can be applied. The BVM method requires data at the edges of patches by A) natural connections with other patches and B) extrapolation which can be set in the edge options window which opens after pressing the Edge options button.. Type of modeling: A) LS: Lifting Surface and B) BVM Body modeling, Type of loads integration: A) no calculation of suction forces, B) including suction forces & including suction forces according to Polhamus suction force analogy [20]. Patches might have a planar wake extension at their rear end. A constant source and constant doublet distribution is applicable. In supersonic flow a linear distribution is applicable for the lifting surface BVM and recommended which applies a linear distribution in chordwise direction with special treatment of leading and trailing edges to approximate closest the potential gradient method; In supersonic flow a linear distribution is applicable for the lifting surface BVM and recommended which applies a linear distribution in chordwise direction with special treatment of leading and trailing edges to approximate closest the potential gradient method. The calculation of suction forces and their adaption to the Polhamus suction force analogy [20] can be set. Patches might have a planar wake extension at their rear end.

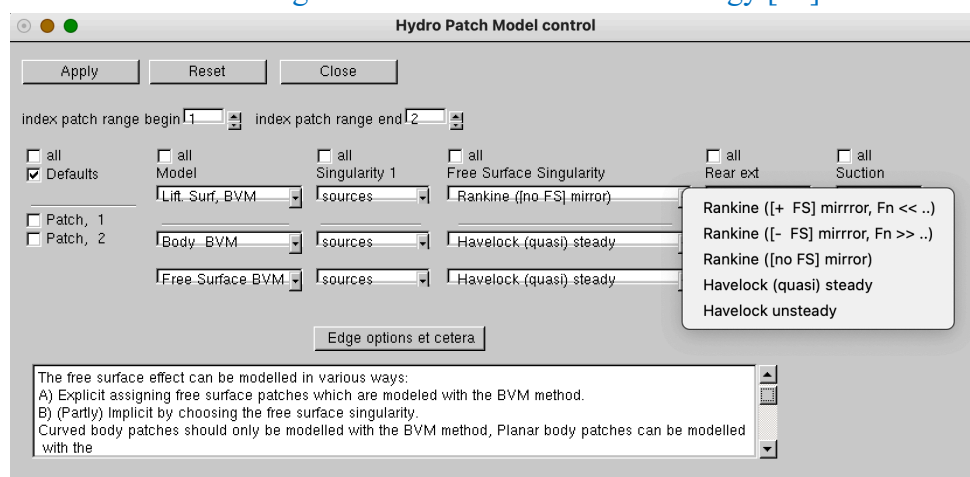
The model options button opens the hydro patch model control window depicted in Figure 32 which allows to set the hydrodynamic modelling options of patches. The Listbox options are presented in Table 1.

The free surface effect can be modelled in various ways:

- A) Explicit assigning free surface patches which are modeled with the BVM method.
- B) (Partly) Implicit by choosing the free surface singularity.

Constant Sources and Doublets and both at the cambersurface can be applied. Apply sources for non-lifting parts, doublets for lifting parts and the camber option in case of thin parts. The calculation of suction forces and their adaption to the Polhamus suction force analogy [20] can be set. Patches might have a planar wake extension at their rear end.

Type of modeling: A) Lifting Surface BVM and B) BVM Body modeling, Type of loads integration: A) no calculation of suction forces, B) including suction forces & including suction forces according to Polhamus suction force analogy [20].



The modeling of the free surface can be performed implicitly (Havelock) or explicitly (Rankine approach). The latter places singularities at the free

Figure 32 Model Options



surface and at the body. The singularities at the body can be optionally mirrored with respect to the free surface. The BVM method requires data at the edges of patches by A) natural connections with other patches and B) extrapolation which can be set in the window that opens after pressing the Edge options et cetera button.

	model	Singulativity 1	Singularity 2	Rear end	Suction
Aero/aco ustics mode	Lift. Surf, BVM Body BVM Lift. Surf, BEM Shock BVM	sources doublets both (camb	constant T-linear M C-linear M	No Planar Wa	No On Polham
			Free surface		
Hydrody namic mode	Lift. Surf, BVM Body BVM Free Surface		Rankine ([+ FS] mirro Rankine ([- FS] mirro Rankine ([no FS] mirro Havelock (quasi) stead Havelock unsteady		

Table 14 Model listbox options

Edge options et cetera



button

The edge options button et cetera button opens the aero(hydro) patch model control B window depicted in Figure 33.

The BVM method requires data at the edges of patches by natural connections with other patches and or extrapolation explained in this section. The Listbox options are presented in

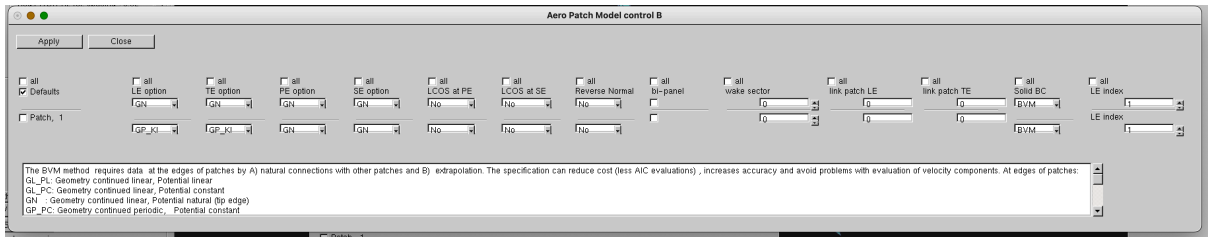


Figure 33 Edge Options

Table 15. The specification can reduce cost (less AIC evaluations), increases accuracy and avoid sometimes problems with evaluation of velocity components. In general patches will have natural (FREE) boundaries which are not connected to other segments. Examples are leading, trailing and tip edges of lifting surfaces and apices of bodies. Use the natural connection option for these cases.

Further the geometry at edges of patches can be set to a linear continuation, a periodic continuation (autoconnection) with our without Kutta condition (airfoil/wing), a continuation to the edges of another patch of the geometry, respectively. The potential can be set to a constant, a linear, a periodic and natural continuation, respectively. The options are explained in Table 2. The connected patches at leading and trailing edge should be specified by the user. The connected patches at the port and starboard site are automatically searched for.

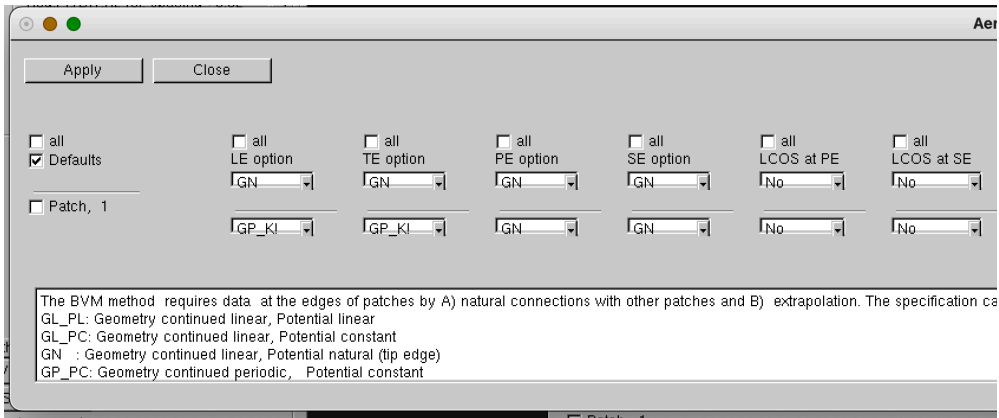


Figure 34 Left part edge options window

The so-called LCO (Lift-Carry Over) extension strips are embedded to avoid unphysical velocities at wake edges and need to be defined by the user. The

singularity distribution on the LCO strips is extrapolated from the neighbouring planes. The normal on a patch can be reversed for the case the patch normal definition leads to an inward normal. The bi panel is meant to damp spurious oscillations due to internal reflections ( $M > 1$ ). Parts of a patch can be set to wake parts. A positive value indicates the trailing(shedding) edge. A negative values indicates shedding before the trailing edge.

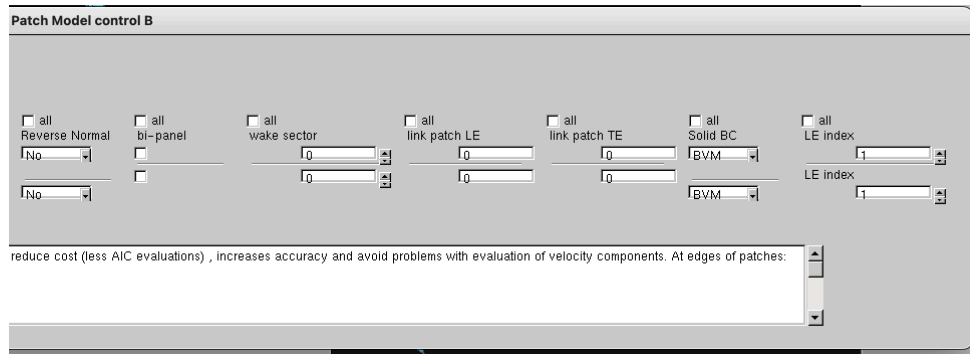


Figure 35 Right part edge options Window

In case of an abrupt end of a thick body without a trailing wake use the linear extrapolation connection option. In case of troubles with apices use also the

aforementioned option. The connected patches at leading and trailing edge can be specified by the user. The VB 1 and VB 2 are alternatives to the BVM methods and apply the normal boundary condition by a simple difference in normal direction. In addition, cross derivatives are neglected when VB 2 is selected in evaluation of pressures et cetera. The LE index is used to determine the leading edge chordwise position.

In general segments will share boundaries with other segments to which the following recommendations apply:

#### *Geometry (panelling) and solution smooth across segment boundaries.*

The cross connection options LE\_p, TE\_p, PE\_p, SE\_p or the autoconnection option GP are the obvious best choices. Choosing another option always results in extrapolation of the geometry at the boundary and will affect the results. Choosing the natural connection option GN will result in an increase of computational cost because additional AICs will be calculated and will lead to wrongly calculated pressures at lifting surfaces because the program then makes the wrong assumption that the potential jump which is needed for the pressure calculations across the boundaries is zero. In such a case use the nonconnection linear extrapolation option GL\_PL although in most cases it is less accurate than the natural one it will keep you always out of trouble especially in supersonic flow because only data is used generated at the segment itself and therefore it is less sensitive to changes in panellings at the boundary. Moreover the fact that supersonic flow potential solutions basically behave linearly contributes to the preference.

#### *Geometry (panelling) non-smooth (non-aligned panelling) and solution smooth across boundaries.*

For the same reasons as mentioned in the previous section prefer the GL\_PL options over the GP options

#### *Solution non-smooth across the boundaries (abrupt geometry change, wing fuselage junction).*

For all segment longitudinal strip edges the program checks if there are any neighbouring non-smooth connections with longitudinal strip edges of other segments (There is no hunt for auto non-smooth strip connections). In which case the program automatically applies the GL\_PL option for the relevant connected points (not the whole strip). For a segment longitudinal edge this is only done when the natural nonconnection option GP is specified otherwise the prescribed option is applied. This procedure will deal with most wing-body junction cases and LCO connections. In case the geometry is non-smooth along the boundary apply the GL\_PL linear extrapolation option. This is also true for LCO connections or wing fuselage connections which for some reason have been missed by the program checks. The automated procedure deals with most wing (wake) (LCO) body junction problems as long as the

longitudinal segment border of the wing (wake)(LCO) can be connected by that procedure to a longitudinal strip edge of a body segment. So there is no need for a body segment to have a segment border at the junction!. In case this fails you should always use the nonconnection GL\_PL, GP\_PL options. Beware the longitudinal edge of the wing (wake) (LCO) should never cross a longitudinal strip edge of a body .

*In case the geometry (panelling) autoconnects (tipstore at a wing tip)*

use the GP\_PL option.

*The constant solution extrapolation options GP\_PC*

are preliminary meant for the cases where the cross velocities are known to be zero. (Wing fuselage junction in steady flow). This option can also be recommended when due to very nonsmooth panellings the linear extrapolation will fail. However in supersonic flow options GL\_PC, GP\_PC are not recommended.

*Another 'natural' boundary is an edge in the symmetry planes.*

When the natural nonconnection option GN is specified a special treatment is given to these edges. This special treatment is not completely embedded for the calculation of the pressure on lifting surfaces with the non-linear pressure formula. In that case use linear extrapolation GP\_PL for anti-symmetric modes and constant extrapolation GP\_PC for steady flow and symmetric modes. Advice is to use the linear pressure option.

[In hydrodynamic mode one can set Dirichlet, Neumann and Absorbing radiation conditions with respect to the free surface. The Listbox options are presented in Table 15.](#)





	LE	TE	PE	SE	LCO PE	LCO SE	REv erse Nor mal	Bi pa nel	Wa ke sec tor	Li nk L E	Li nk T E	Boun dary Condi tion	
	GP_K! GL_PL GL_PC GN GP_PC GP_PL GP TE_p LE_p	GP_K! GL_PL GL_PC GN GP_PC GP_PL GP LE_p	GL_PL GL_PC GN GP_PC GP_PL GP SE_p	GL_P GL_P GN GP_P GP_P GP PE_p	No 50% str 1e strip	No 50% stri Last strip	No Yes					BVM VB 1 VB 2	
Hydrodynamic mode													
	GP_K! GL_PL GL_PC GN GP_PC GP_PL GP TE_p LE_p D N A	GP_K! GL_PL GL_PC GN GP_PC GP_PL GP LE_p D N A											

Table 15 Selectable edge options

Create/Change

Create/Change

Button

The create/change button opens the Patch creation/change/deletion window depicted in Figure 36.

There you can inspect and/or change the geometry of patches. You can easily change the

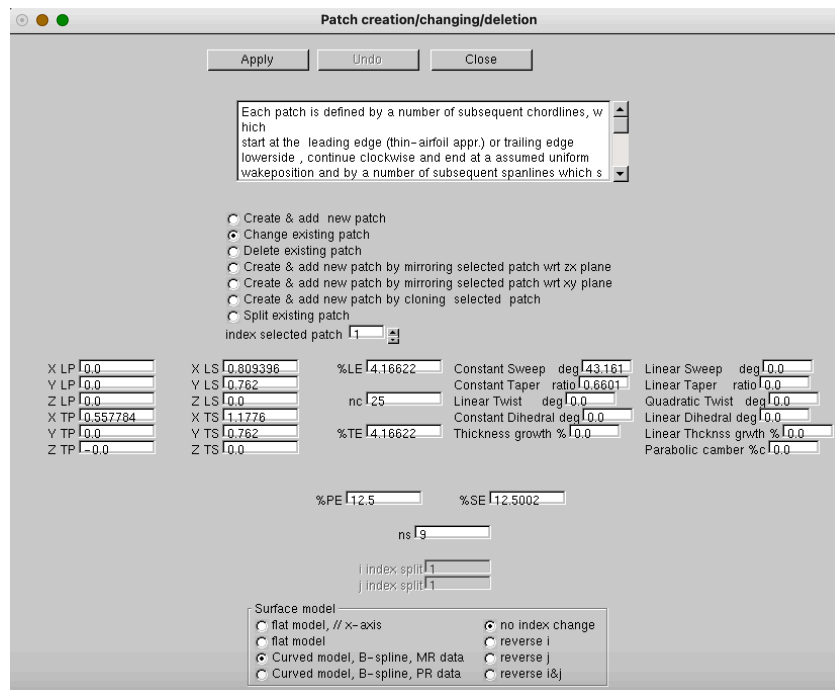


Figure 36 The patch edit window

sweep, the taper and/or dihedral, thickness, twist et cetera of selected aero patches. Also you can clone and split patches. You can set various symmetry options et cetera. Additional patches can be generated ab initio by entering the corner coordinates at the portside and starboard edges. Note these should be parallel to the x-axis when the LS like modelling is chosen. The normal direction of each segment is assumed to be in the direction of the out product of the directions formed by the chord and span lines. The sequence

of the chord and span lines should be chosen such that the normal is pointing outward. It is possible to reverse the chord line (i) and span line (j) indices. When the thin aerofoil approximation is applied the chord line should start at the leading edge else the chord line start at the lower side trailing edge and continues clockwise to end at the upper side trailing edge ( a assumed uniform wake position ) and by a number of subsequent span lines which start at the portside of the patch and end at the starboard side of it. The panelling inside the corners are carried out with the specified numbers and according to a hyperbolic distribution. Also existing patches might be changed, cloned or mirrored. A change of curved patch is performed with a B-spline using the latest patch data (MR) or the pristine patch data. After changing the geometry, the original structural data is applied to model the vibration modes with respect to the modified and/or new parts.



## Downwash

The boundary conditions (downwash) due to oscillations or deformation of the configuration or the flow are accessible/(de)activated by four windows:

- The displacements window (see [Figure 37](#)). Deals with the setting of:
  - Rigid translation and rotation of the whole configuration (Figure 39)
  - Sub Rigid translation and rotation of individual patches (effectors) (Figure 40)
  - Regular modes, which are warped to the aerodynamic surface (Figure 41)
  - Polynomial modes, for each aero patch (Figure 43, Figure 44)
  - Special modes, which involve warping for individual aero patches (Figure 45)
  - Sinusoidal gust modes in aerodynamic mode (Figure 46) [or waves in hydrodynamic mode](#) (Figure 47) [or sound waves in aeroacoustics mode](#).
  - Patches with zero downwash (Figure 48)

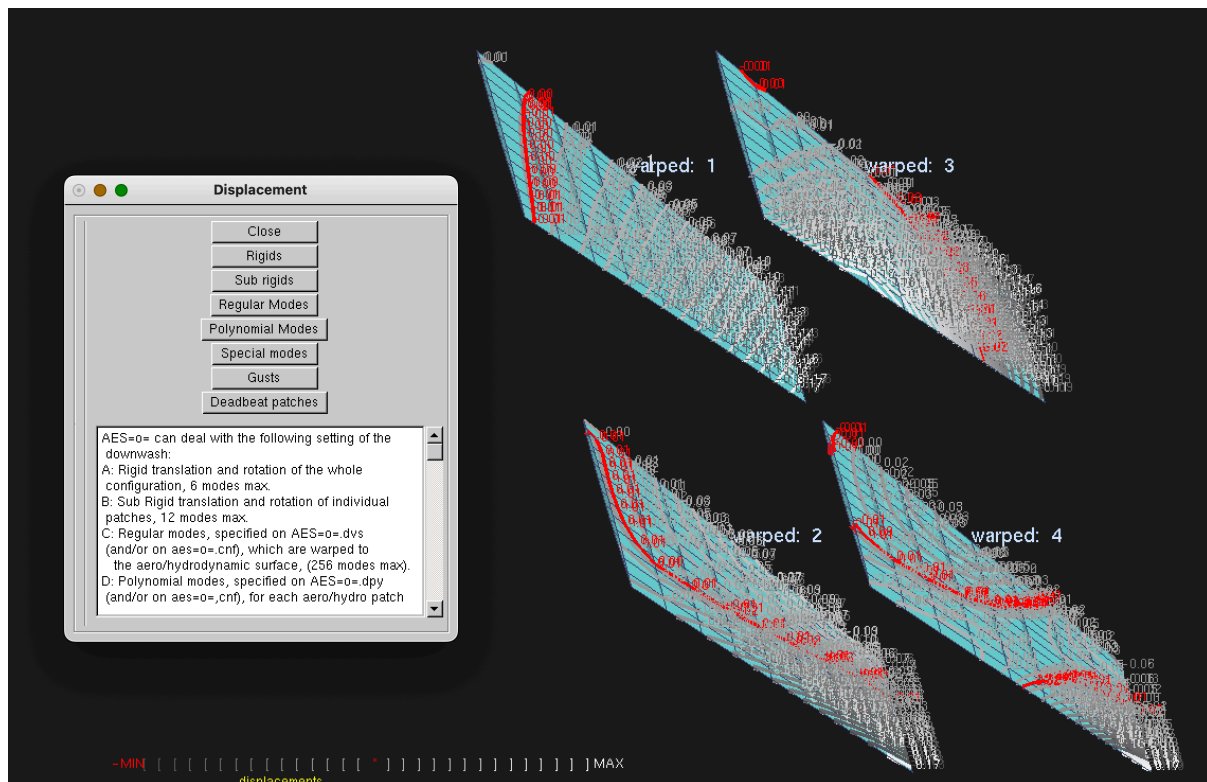
All the aforementioned modes can be inspected separately/by group/simultaneously and moreover the regular and special modes can be simply compared to the original support data. Various warping options for the regular and special modes can be selected to accommodate accuracy and/or efficiency. A trim state can be set by prescribing amplitudes of the modes to define a trimmed state.

- The trim window (Figure 51). Activates the modified geometry of the configuration.
- The BL windows (Figure 53, Figure 52). Sets and activates a modified geometry of the configuration due to boundary layer effects.
- The mean flow windows (Figure 50, Figure 49). Sets and activates a steady velocity field which can be part of the boundary condition and the pressure evaluation.
- [The impedances](#) (Figure 56)
- [The incident fields](#) (Figure 57)

The windows are described in the next sections.

## Displacement button > The displacement window

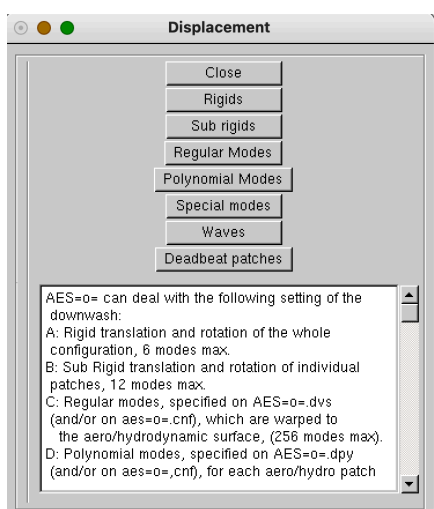
After pressing the displacement button you can inspect and/or change the displacement modes (Figure 37). You can activate/create/deactivate rigid, sub-rigid (effectors), regular



(warped), polynomial, special (warped) and gust (waves) modes (see sections below).

Figure 37 Main Displacement Window (Downwash and Inspection)

The embedded example uses 4 regular modes, which are warped with the default volume spline to the patches. All the modes can be inspected separately/by group/simultaneously and moreover the regular and special modes can be simply compared to the original support data (FEM). Various warping options for the regular and special modes can be selected to accommodate accuracy and/or efficiency. Warping's can be stored for [reuse](#) accommodating follow on stages of your design cycle (Mach number and/or frequency changes). Most of the modes can be used in steady calculations with a prescribed amplitude.



In hydrodynamic mode the displacement window is slightly different by showing the waves button instead of the gusts button.

Figure 38 The Downwash Window

### Rigid button > Rigids Window

The user can apply 6 modes consisting of rotations and translations of the whole configuration (Figure 39). Also, the mean amplitude setting  $q$  activated in steady trimmed calculations can be set.

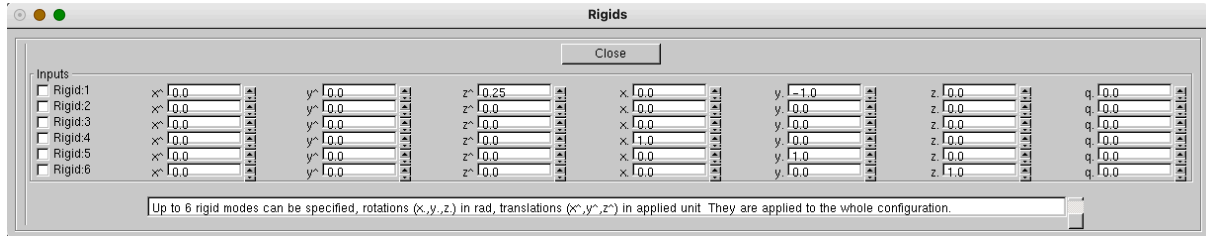


Figure 39 The rigids

### Sub Rigid button > Sub Rigids Window

Sub Rigid modes (a maximum of 12) can be applied by selecting the patch and specifying the displacements at the 4 corners of the selected aero patch. LP,TP,LS and TS denote the

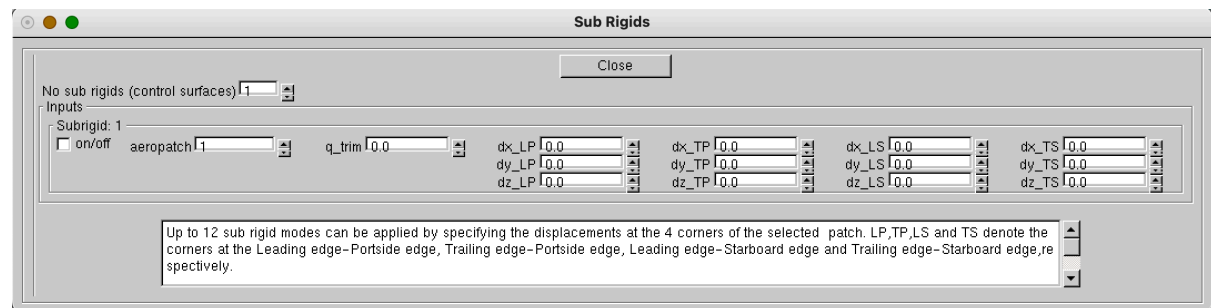
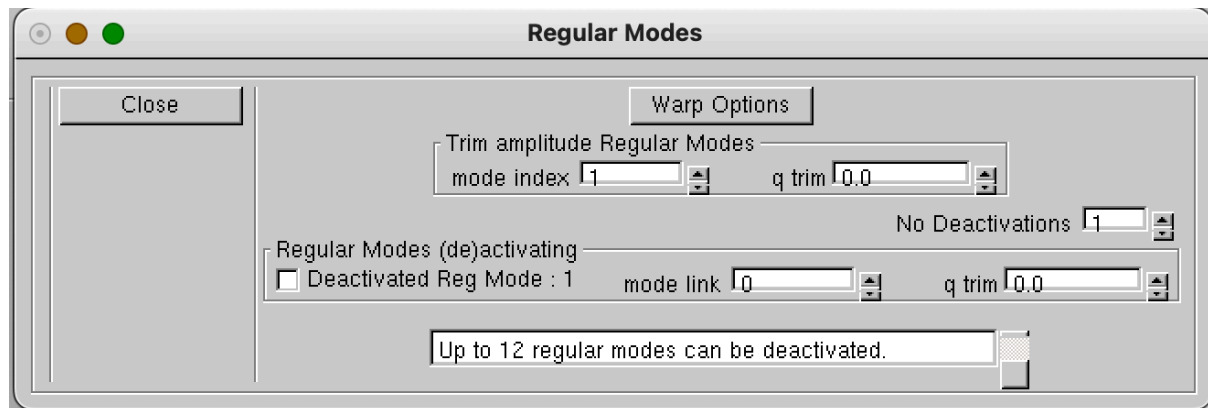


Figure 40 The sub rigids

corners at the Leading edge-Portside edge, Trailing edge-Portside edge, Leading edge-Starboard edge and Trailing edge-Starboard edge, respectively (Figure 40).  $q_{trim}$  denotes the mean setting activated in steady calculations.

### *Regular modes button > Regular Modes Window*

The regular modes are in generally obtained from a FEM calculation on an unstructured



**Figure 41 Regular Modes**

mesh. They are warped to the patches with the methods accessible in the warping window after pressing the warp options button. The modes can be applied with a mean setting for steady calculations. Also, modes (maximal 12) can be deactivated.  $q\_trim$  denotes the mean setting activated in steady calculations.

## Warp options button > Warp options window

Figure 42 presents the window associated with respect to the warping of the unstructured

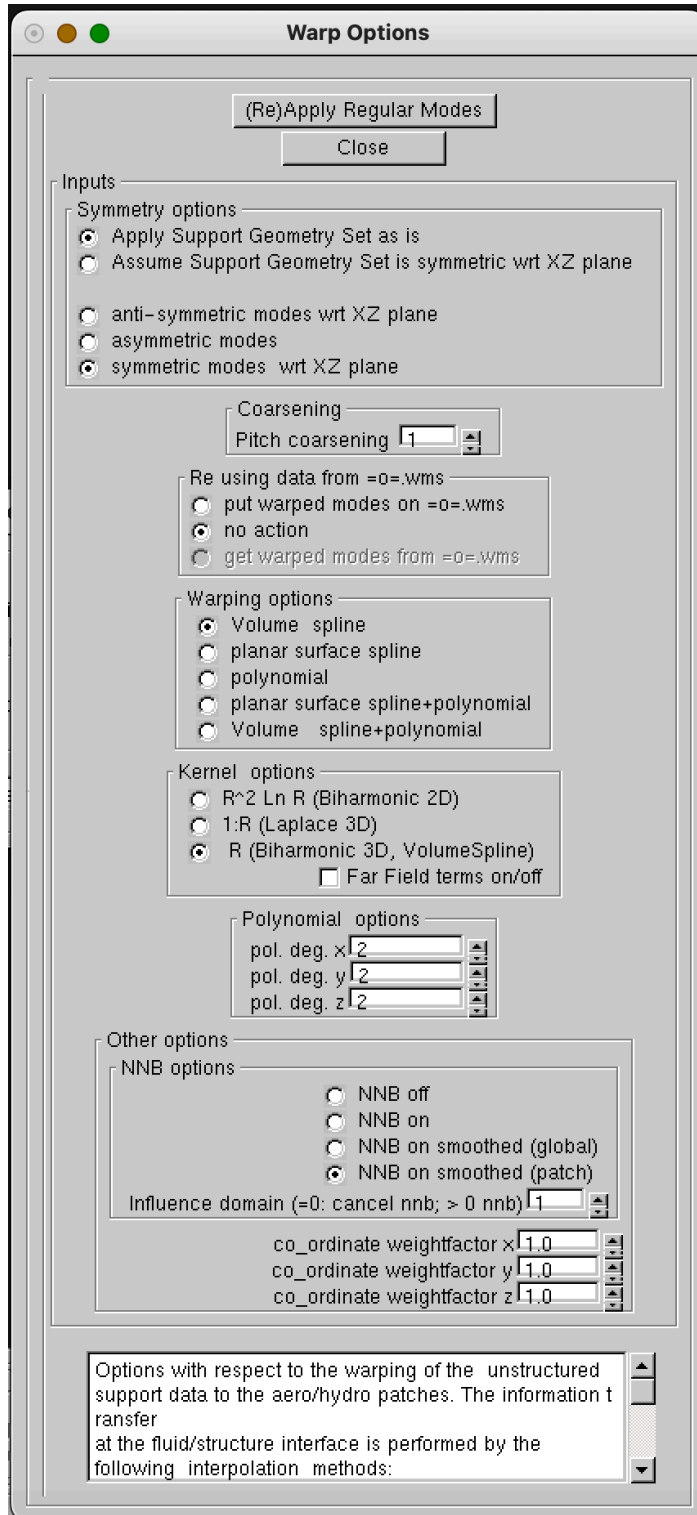


Figure 42 Warp Options Window

support data to the aero/hydro patches. Symmetry options with respect to the geometry and the modes can be set.

Computational work can be reduced by setting the pitch value > 1;

A restart option is provided.

Various warping options for the regular and special modes can be selected to accommodate accuracy and/or efficiency of the warping of the unstructured support data to the aero patches: Volume spline, Planar surface spline and Least Squares Polynomial (LSP) approximation.

Both spline can be applied in a combined hybrid way with LSP enabling a noise-free interpolation with respect to algebraic type of motions.

The kernel can be selected, the far field behavior and the order of the LSP.

Various nearest neighbors strategies are available to reduce computational work. The *smoothed* global and patch NNB are advised. These take care of local and trends of the support data (a variant of the mollifier/VSIC method(see [The mollifier or the VSIC method](#)))

A coordinate transformation can be applied to set additional weight factors to improve the warping.

### Polynomial modes button > Polynomial Modes Window

The polynomial modes are in generally used in pre design studies or academic studies. Also These modes can be applied with a mean setting for steady calculations. Modes (maximal 12) can be deactivated. Polynomial modes can be (de-)activated and interactively prescribed (see Figure 43 and Figure 44. The polynomials are defined along local patch coordinates.

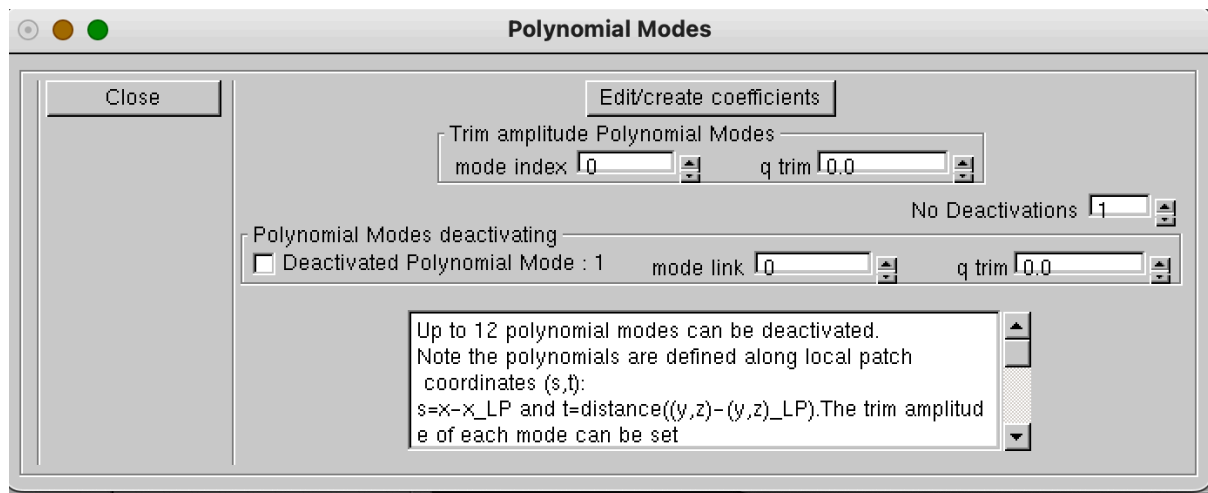


Figure 43 Polynomial modes

### Edit/create coefficients button > Edit Polynomial Modes Window

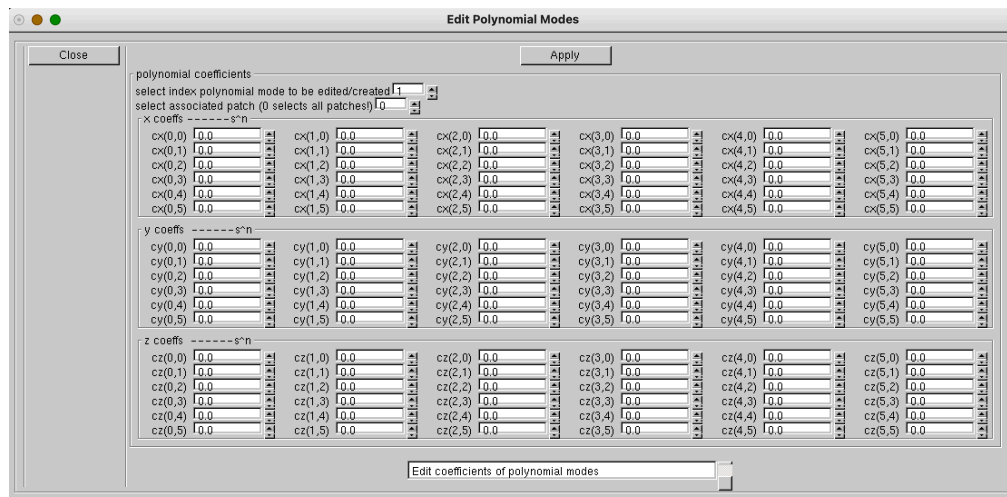


Figure 44 Coefficients of the polynomial displacements

Polynomial modes can be prescribed. The polynomials are defined along local patch coordinates.



### Special Modes button > Special Modes Window

Special modes can be applied by specifying the displacements at arbitrary points (Figure 45).

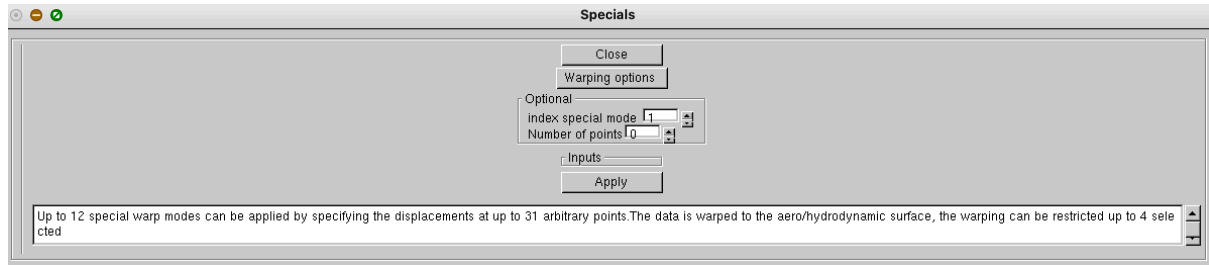


Figure 45 The special modes window

The data is warped to the aerodynamic surface, the warping can be restricted to selected aerodynamic patches. The warping options can be selected by pressing the Warping options button.

### Gusts Button> Gusts window

Harmonic gust modes can be applied (Figure 46), harmonic variation ( $g+ik$ ) in  $x$  (invariant in  $y, z$ ), amplitude is linear varying in  $|y|$  and  $|z|$ .

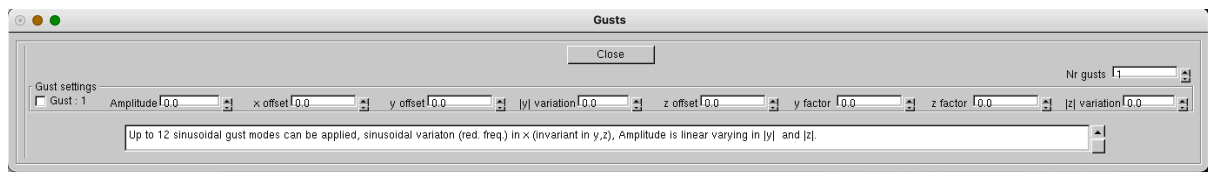


Figure 46 Adding/Creating Gust modes

### Wave Button> WAVES window

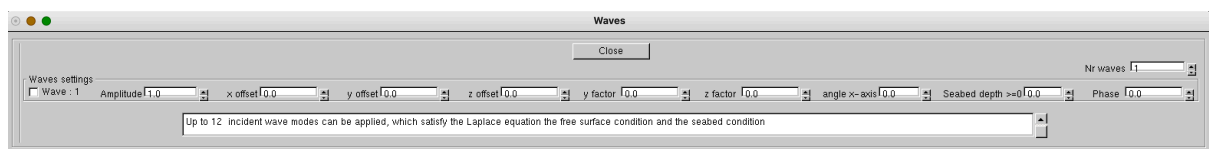
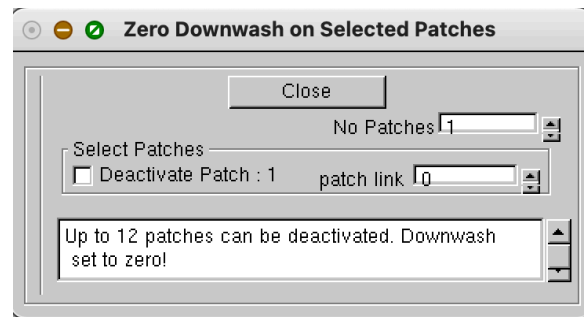


Figure 47 Adding/Creating Wave modes

Harmonic wave modes can be applied (Figure 47), harmonic variation satisfying the free surface condition and the sea bed condition.

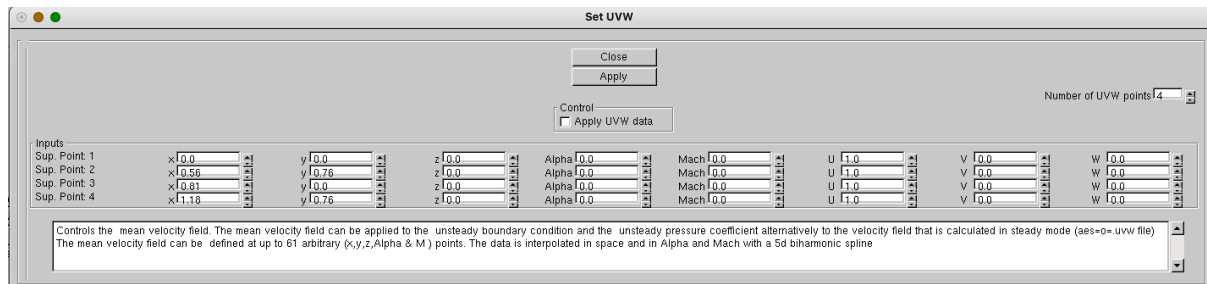
*Deadbeat patch Button> Zero Downwash on Selected Patches Window*

The downwash on selected patches can be set to zero (hard wall) (Figure 48)



**Figure 48** The deadbeat patch window

*Mean velocities Button> set UVW window.*



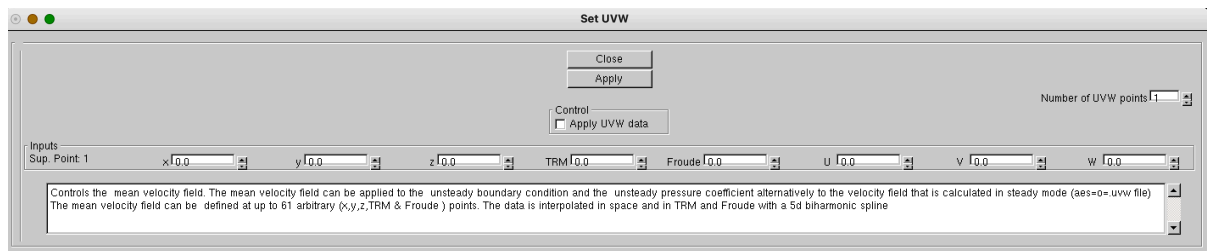
Controls the mean velocity field. The mean velocity field can be applied to the unsteady boundary condition and the unsteady pressure coefficient alternatively to the velocity field that is calculated in steady mode (aes=0=uvw file). The mean velocity field can be defined at up to 61 arbitrary (x,y,z,Alpha & M) points. The data is interpolated in space and in Alpha and Mach with a 5d biharmonic spline

Figure 49 UVW Window

In some cases, it is worthwhile to add the effect of the mean flow on the unsteady solutions. One can perform a steady simulation or alternatively create a velocity field by entering velocities in space for a number of points at selected Mach numbers and angle of attacks (Figure 49). A 5D biharmonic spline is applied to interpolate the data to the boundaries.

*Mean velocities Button> set UVW window.*

In some cases, it is worthwhile to add the effect of the mean flow on the unsteady solutions.



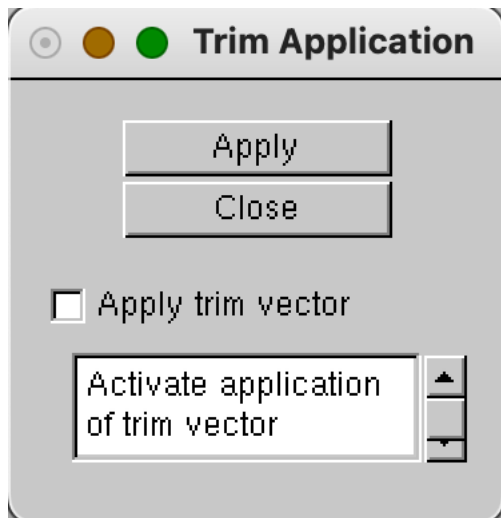
Controls the mean velocity field. The mean velocity field can be applied to the unsteady boundary condition and the unsteady pressure coefficient alternatively to the velocity field that is calculated in steady mode (aes=0=uvw file). The mean velocity field can be defined at up to 61 arbitrary (x,y,z,TRM & Froude) points. The data is interpolated in space and in TRM and Froude with a 5d biharmonic spline

Figure 50 UVW Window

One can perform a steady simulation or alternatively create a velocity field by entering velocities in space for a number of points at selected Froude numbers and TRIM, SINKAGE (Figure 50). A 5D biharmonic spline is applied to interpolate the data to the boundaries.

*Trim Button> set TRIM Application window.*

The trim vector (Figure 51) is the change of geometry due to a steady state setting of the displacement modes. It is also possible to perform calculations with a trimmed state of the geometry defined on the file aes=o=.trm which should be conform with the same number of points as the geometry.



**Figure 51 Activation of a trim vector**

*BL Button> Boundary Layer Correction window.*

Controls the application of geometry corrections by means of adding Boundary Layer Thickness (Figure 52). This allows a corrected prediction of pressures in zones where the prediction

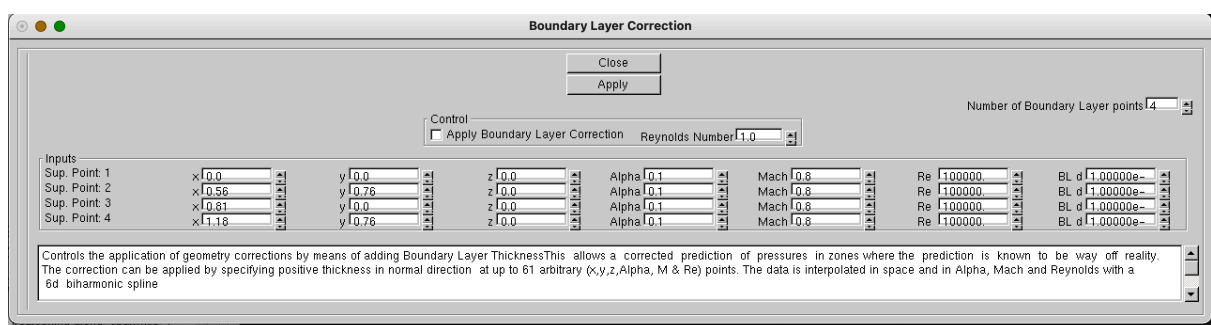


**Figure 52 Boundary Layer Correction Window**

is known to be way off reality (effectors). The correction can be applied by specifying positive thickness in normal direction at up to 61 arbitrary (x,y,z,Alpha, Mach number & Reynolds number) points. The data is interpolated in space and in Alpha, Mach and Reynolds with a 6D bi harmonic volume spline.



*BL Button> Boundary Layer Correction window.*

Controls the application of geometry corrections by means of adding Boundary Layer Thickness (Figure 53). This allows a corrected prediction of pressures in zones where the

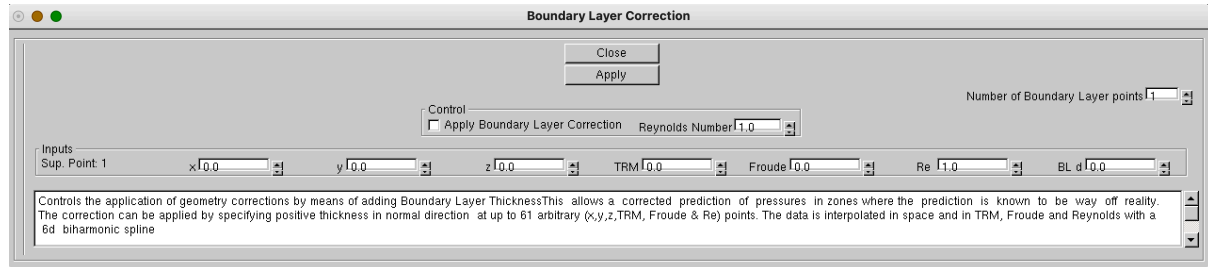


Figure 53 Boundary Layer Correction Window

prediction is known to be way off reality (effectors) . The correction can be applied by specifying positive thickness in normal direction at up to 61 arbitrary (x,y,z,TRIM, Froude number & Reynolds number) points. The data is interpolated in space and in TRIM, Froude and Reynolds with a 6D bi harmonic volume spline.

*Pressure correction Button> Gains window.*

The calculated pressure distribution can be factored with a correction (Mach number, frequency and position dependent) to accommodate transonic, boundary layer and edge

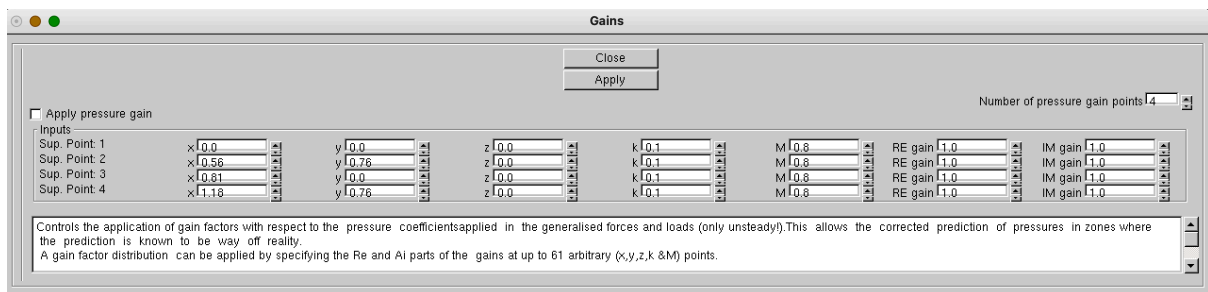


Figure 54 Gains Window

effects (Figure 54). These corrections are defined on a few support points and will be interpolated to the aerodynamic patches with a hyperspace biharmonic spline

Pressure correction Button> Gains window.

The calculated pressure distribution can be factored with a correction (Froude number,

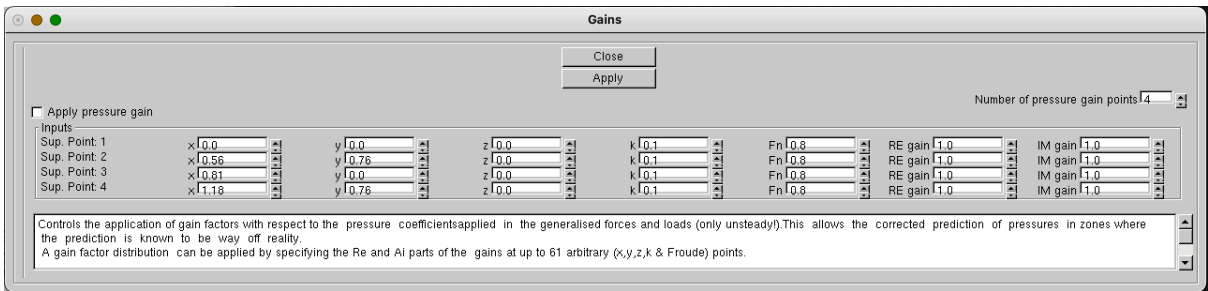


Figure 55 Gains Window

frequency and position dependent) to accommodate transonic, boundary layer and edge effects (Figure 55). These corrections are defined on a few support points and will be interpolated to the aerodynamic patches with a hyperspace biharmonic spline

Impedance Button> Impedance window.

The impedance can be globally set by means of a 5D bi-harmonic hyperspace spline based on

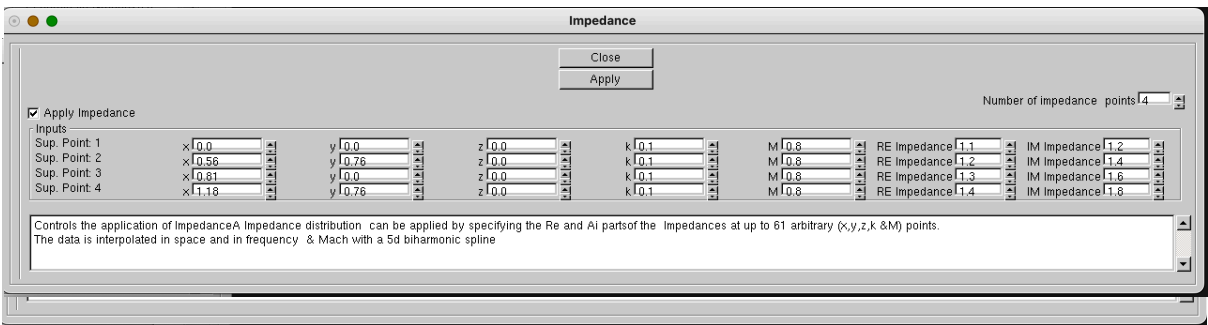


Figure 56 Impedance window

support points in space, Mach number and frequencies (Figure 56).

Incident Fields Button> Incident Fields window.

Incident fields can be set by means of a set of singularities (Figure 57).

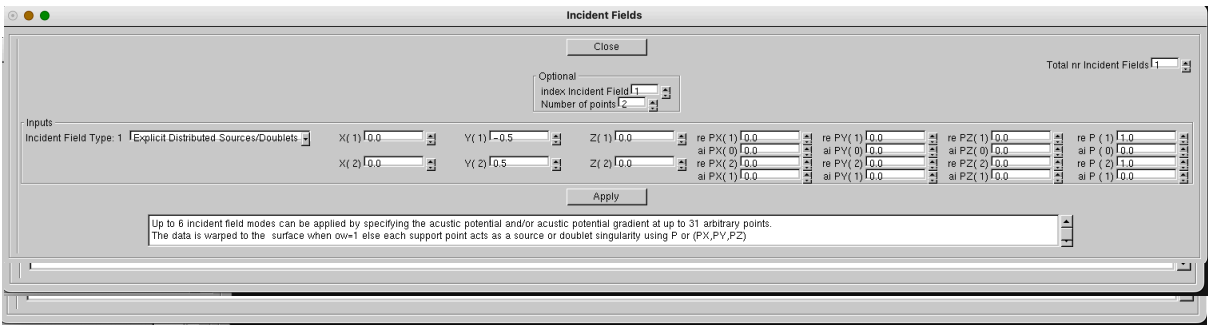
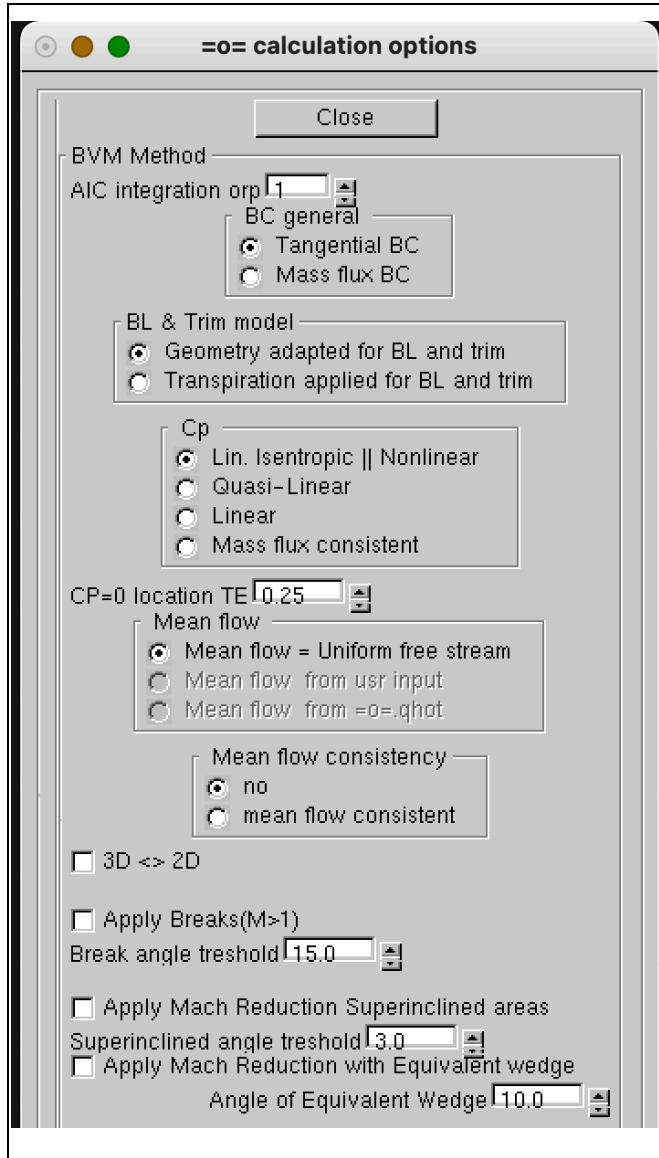


Figure 57 Incident fields window

*BVM Button* > *=o= calculation options window.*

Upon pressing the BVM Button a window (Table 16) opens where you can set options with regards to the modelling of the aerodynamics.



### Set options for the BVM modelling

#### Accuracy:

- 0: low; 1: modest; 2 good; 3 very good et cetera,
- -1 (semi analytical, only  $M > 1$ ).

#### Set BC (boundary condition)

A) linear small disturbance boundary or B) mass-flux boundary condition.

The effect of BL thickness and/or the trim\ can be modelled as A) transpiration or B) geometry change.

Cp is calculated with 4 forms: A) linear isentropic or nonlinear formula (steady). B) quasi linear small disturbance formula (compares best with slender body theory). D) consistent with mass-flux boundary condition. Use A or B for flows with strong cross-derivatives. The TE parameter controls the Cp behavior at the trailing edge (Kutta).

The mean flow can be set Uniform, from user input or from a steady AES=O= calculation.

Mean flow consistency means that steady velocities are forced tangential to the body surface.

The calculation can be applied to a 2D section of the first patch at its portside.

In supersonic flow geometric discontinuities in chordwise direction (breaks) for full body discretization's can get a special treatment. The break is recognized when the change in angle is larger as the break threshold.

Super inclined panels are per default eliminated. Optionally the local Mach number at these panels can be reduced and/or an equivalent wedge angle from which a global corrected Mach number is employed so that they are no longer super inclined.;

Table 16 BVM Window

*BVM Button> =o= calculation options window.*

Upon pressing the BVM Button a window (Table 17) opens where you can set options with regards to the modelling of the hydrodynamics.

<div> <span></span> <span></span> <span></span> <span>=o= calculation options</span> </div>	<div>Set options for the BVM modelling</div>
<div> <div>Close</div> <div> <div>BVM Method</div> <div> <div>AIC integration ord</div> <div>1</div> <div></div> </div> <div> <div>BC general</div> <div> <input checked="" type="radio"/> not           <input type="radio"/> +Geometry adapted for TRIM &amp; SNKG         </div> </div> <div> <div>BL &amp; Trim model</div> <div> <input checked="" type="radio"/> Geometry adapted for BL and trim           <input type="radio"/> Transpiration applied for BL and trim         </div> </div> <div> <div>Cp</div> <div> <input checked="" type="radio"/> Lin. Isentropic    Nonlinear           <input type="radio"/> Quasi-Linear           <input type="radio"/> Linear         </div> </div> <div> <div>Cp Wave</div> <div> <input checked="" type="radio"/> Both           <input type="radio"/> Scattered Wave Part           <input type="radio"/> Incident Wave Part (Froude/Krilov)         </div> </div> <div> <div>Cp Hydrostatic</div> <div> <input checked="" type="radio"/> On           <input type="radio"/> Off           <input type="radio"/> Only Hydrostatic         </div> </div> <div> <div>CP=0 location TE</div> <div>0.25</div> <div></div> </div> <div> <div>Mean flow</div> <div> <input checked="" type="radio"/> Mean flow = Uniform free stream           <input type="radio"/> Mean flow from usr input           <input type="radio"/> Mean flow from =o=.qhot         </div> </div> <div> <div>Mean flow consistency</div> <div> <input checked="" type="radio"/> no           <input type="radio"/> mean flow consistent         </div> </div> </div> </div> <td data-bbox="957 465 1417 1776"> <p><i>Accuracy:</i> Increasing accuracy with increasing absolute values, 0: low; -1, 1: modest ; -2, 2 good; -3, 3 very good accuracy et cetera,)</p> <p><i>Set BC (boundary condition)</i> A) tangential boundary or B) geometry adapted for TRIM and SINKAGE. The effect of BL thickness and/or the trim\ can be modelled as A) transpiration or B) geometry change.</p> <p>Cp is calculated with 3 forms: A) linear isentropic or nonlinear formula (steady).B) quasi linear small disturbance formula (compares best with slender body theory ). Use A or B for flows with strong cross-derivatives. The pressure contribution induced by a wave</p> <p>The scattered part or the incident part of the pressure or both can be calculated.</p> <p>The hydrostatic contribution can be added to the pressure</p> <p>The TE parameter controls the Cp behavior at the trailing edge (Kutta). The mean flow can be set Uniform, from user input or from ae steady calculation. Mean flow consistency means that steady velocities are forced tangential to the body surface.</p> </td>	<p><i>Accuracy:</i> Increasing accuracy with increasing absolute values, 0: low; -1, 1: modest ; -2, 2 good; -3, 3 very good accuracy et cetera,)</p> <p><i>Set BC (boundary condition)</i> A) tangential boundary or B) geometry adapted for TRIM and SINKAGE. The effect of BL thickness and/or the trim\ can be modelled as A) transpiration or B) geometry change.</p> <p>Cp is calculated with 3 forms: A) linear isentropic or nonlinear formula (steady).B) quasi linear small disturbance formula (compares best with slender body theory ). Use A or B for flows with strong cross-derivatives. The pressure contribution induced by a wave</p> <p>The scattered part or the incident part of the pressure or both can be calculated.</p> <p>The hydrostatic contribution can be added to the pressure</p> <p>The TE parameter controls the Cp behavior at the trailing edge (Kutta). The mean flow can be set Uniform, from user input or from ae steady calculation. Mean flow consistency means that steady velocities are forced tangential to the body surface.</p>

Table 17 BVM Window Hydrodynamic mode

Upon pressing the BVM Button a window (Table 18) opens where you can set options with regards to the modelling of the aeroacoustics.



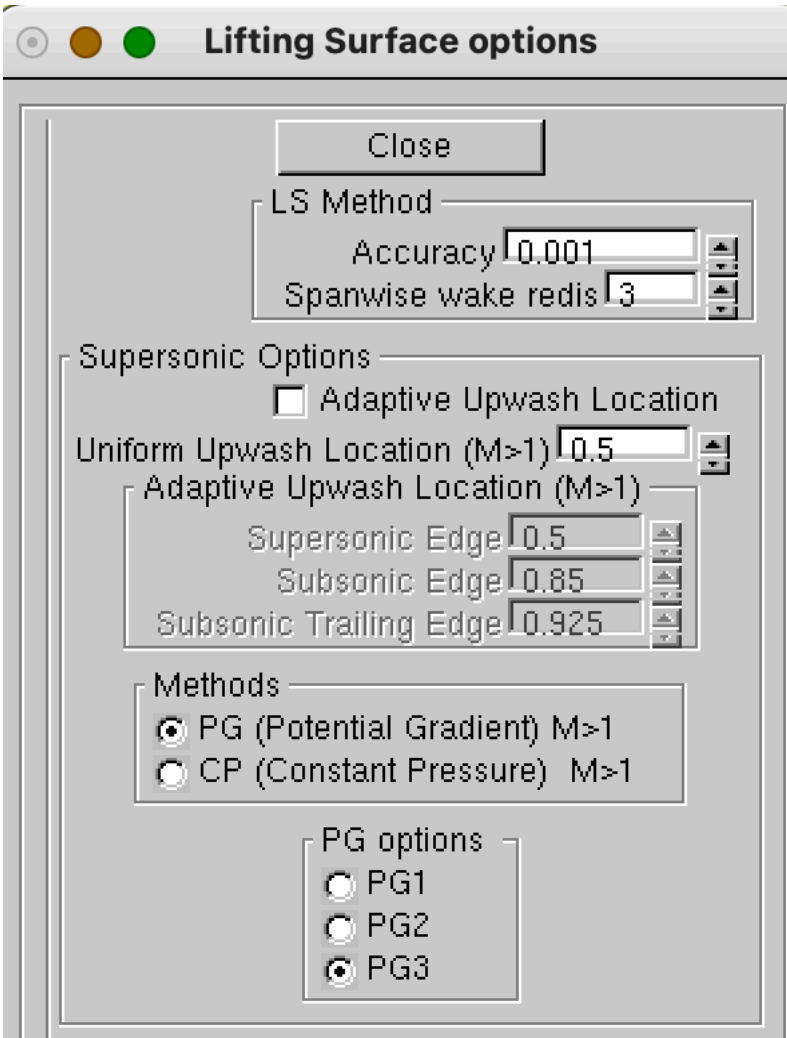


	<p>Set options for the BVM modelling</p> <p><i>Accuracy:</i> Increasing accuracy with increasing values: 0: low; 1: modest : 2 good: 3 very good accuracy et cetera,)</p> <p>The impedance in the BC</p> <p>The effect of BL thickness and/or the trim\ can be modelled as A) transpiration or B) geometry change. (steady)</p> <p>Cp is calculated with 3 forms: A)linear isentropic or nonlinear formula (steady).B) quasi linear small disturbance formula) linear small disturbance formula (compares best with slender body theory ). Use A or B for flows with strong cross-derivatives.</p> <p>The scattered part or the incident part of the pressure or both can be calculated.</p> <p>The TE parameter controls the Cp behavior at the trailing edge (Kutta).</p> <p>The pressure The scattered part contribution can be added to the pressure</p> <p>The mean flow can be set Uniform, from user input or from ae steady calculation.</p> <p>Mean flow consistency means that steady velocities are forced tangential to the body surface.</p>
--	---

Table 18 BVM Window aeroacoustics mode

*LS Button > LS options window.*

Upon pressing the LS Button a window (Table 19) opens where you can set options with regards to the modelling of the lifting surface (AES=3= type) aerodynamics.

 <p style="text-align: center;"><b>Lifting Surface options</b></p> <p>Close</p> <p>LS Method</p> <p>Accuracy 0.001</p> <p>Spanwise wake redis 3</p> <p>Supersonic Options</p> <p><input type="checkbox"/> Adaptive Upwash Location</p> <p>Uniform Upwash Location (M&gt;1) 0.5</p> <p>Adaptive Upwash Location (M&gt;1)</p> <p>Supersonic Edge 0.5</p> <p>Subsonic Edge 0.85</p> <p>Subsonic Trailing Edge 0.925</p> <p>Methods</p> <p><input checked="" type="radio"/> PG (Potential Gradient) M&gt;1</p> <p><input type="radio"/> CP (Constant Pressure) M&gt;1</p> <p>PG options</p> <p><input type="radio"/> PG1</p> <p><input type="radio"/> PG2</p> <p><input checked="" type="radio"/> PG3</p>	<p>Set accuracy</p> <p>Set number of parabolic integrations for DL and CP</p> <p>Set the upwash location for supersonic/hypersonic flow</p> <p>Adaptive to leading edge type or invariant.</p> <p>DL applies the 75% location.</p> <p>DL is default subsonic.</p> <p>Set the supersonic</p> <p><b>PG:</b> low reduced frequencies &amp; high supersonic Mach</p> <p><b>CP:</b> high reduced frequencies &amp; low supersonic Mach for High Mach</p> <p>Set numerics AIC calculation</p> <p>PG method</p> <p><b>PG0/PG1:</b> low reduced frequencies and moderate to high supersonic Mach. In between use PG2/PG3</p>
--	--

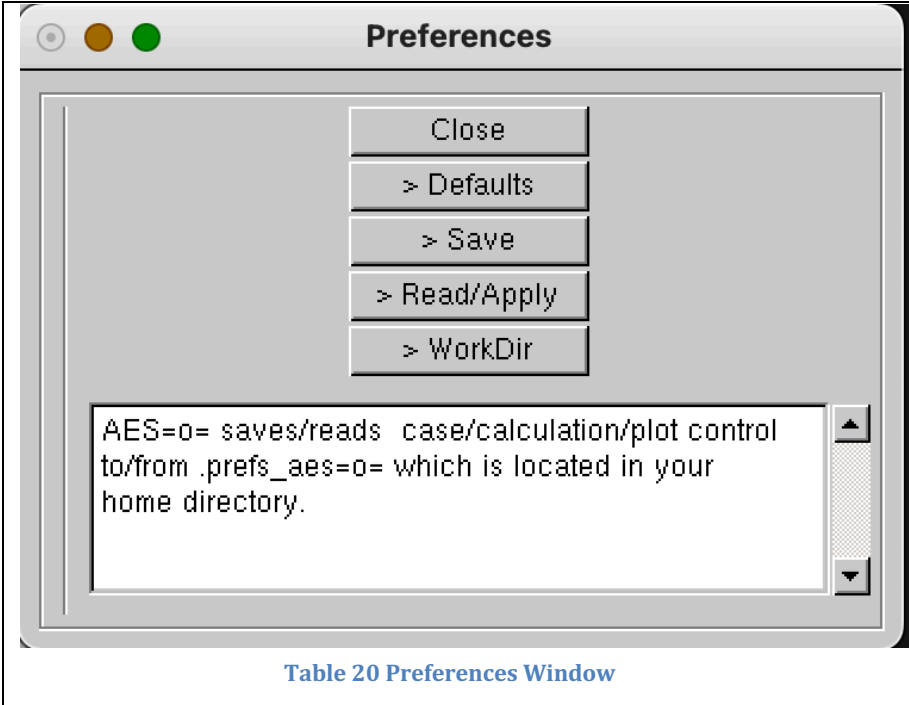
**Table 19 Lifting Surface Window**

## Left Sidebar Bottom

The left sidebar bottom deals with general aspects of the aes=o= method such as:

- setting, saving and/or reading of the .prfs\_aes=o= file and the working directory (Table 20).
- setting, saving and/or reading of the aes=o=.cnf file and the selection of the geometry, regular modes and polynomial modes files, respectively (Figure 58).
- Licence activation, description of inputs and outputs (Figure 59, Figure 60).
- The disclaimer.

### Preferences Button > Preferences window.

 <p style="text-align: center;"><b>Table 20 Preferences Window</b></p>	<p>Apply default preferences Save the preferences Read and apply the precedences Set the working directory</p>
---	--

## Configuration Button> Configuration window.

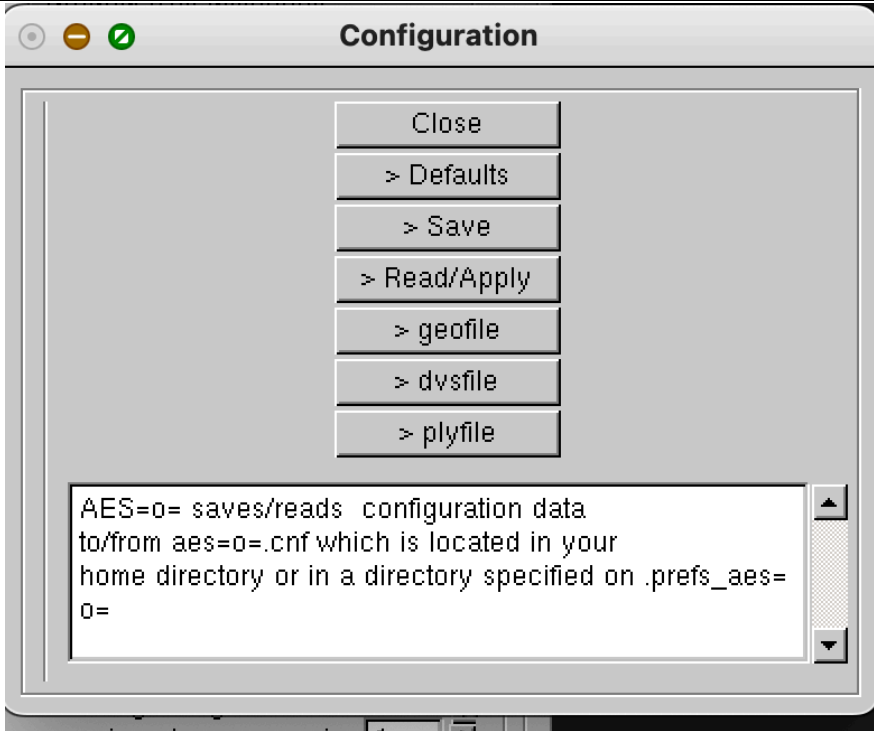


Figure 58 Configuration Window

Apply default configuration  
Save the configuration  
Read and apply the configuration  
Select geometry file

Select a regular modes file  
Select a polynomial file

## Info Button> Info window.

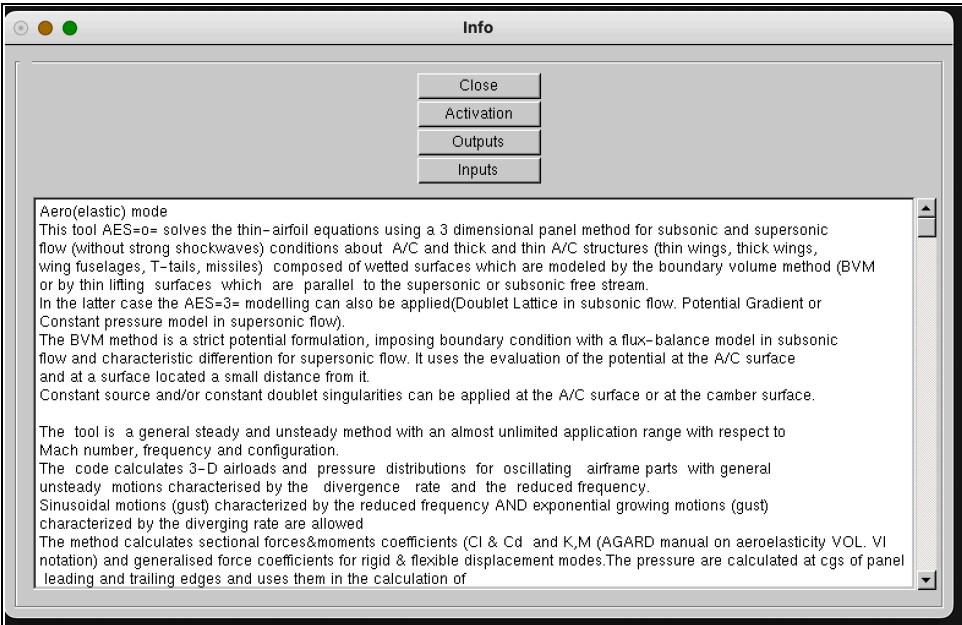
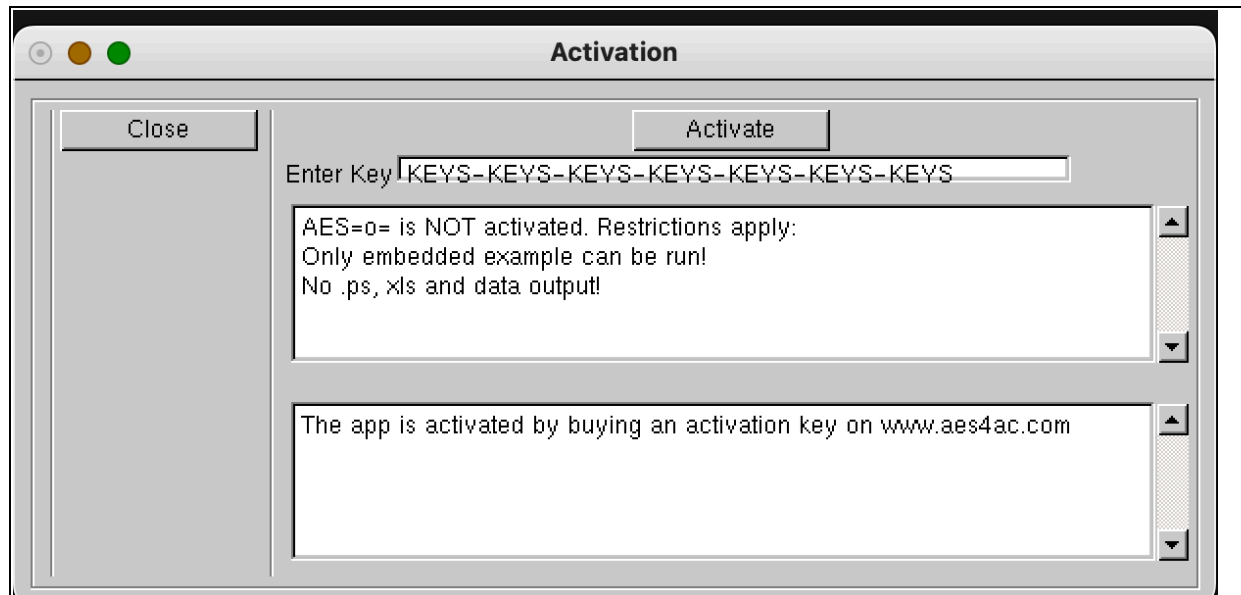


Figure 59 Info Window

Sets Licence activation,  
and describes  
Inputs and  
Outputs



*Activation Button> Activation window.*



**Figure 60 Activation Window**

## Bottom bar

The bottom bar right row (Figure 61) deals with calculation aspects:

- Perform steady calculations
- Perform unsteady calculations
- Restart options
- Create & Save Output files
- H continuation

The bottom bar mid row (Figure 62, Figure 63) deals with control of the curve's ranges of the 2D graphics pics:

- Select range and pitch of case parameters (Mach et cetera)
- Select range and pitch of patches and patch strips

### Bottom bar right row

On the bottom bar right row on can activate the run, select the type of the run, select restart

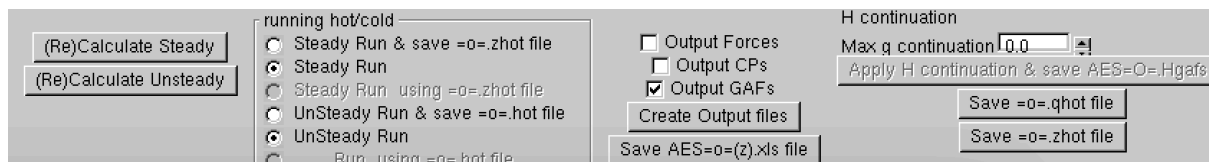


Figure 61 Bottom bar right row

options, select the type of file outputs, activate H continuation and saving of the restart files. In aeroacoustics mode the steady calculation is meant to generate a steady flow field which might have a purpose in the boundary conditions and pressure formulae

### Bottom bar mid row (Aerodynamics&Aeroacoustics)

On the bottom bar mid row, a group of controls deals with the selection of two dimensional

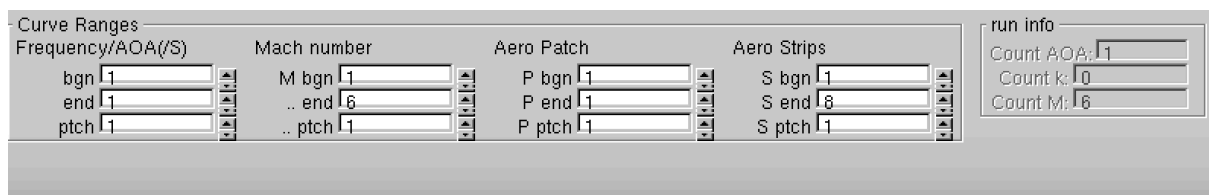


Figure 62 Bottom Bar mid row

graphics. One can set the range and pitch of (g+ik, angle of attack , Mach number, the patches and the sectional strips of the patches. Also, the right columns presents info with respect to the execution.

### Bottom bar mid row (Hydrodynamics)

On the bottom bar mid row, a group of controls deals with the selection of two dimensional

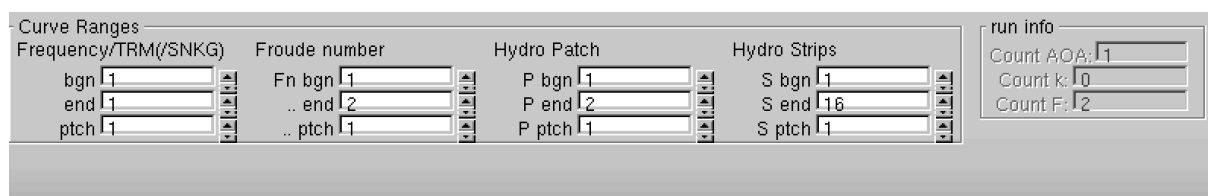


Figure 63 Bottom bar mid row



graphics. One can set the range and pitch of (ik, TRIM, SINKAGE, Froude number, the patches and the sectional strips of the patches. Also, the right columns presents info with respect to the execution ( $AOA=TRIM/SINKAGE$ ).

## Right sidebar

The right sidebar deals with the 2D and 3D graphics inspection/analysis of panelling, trim state (static deformation & effector settings), displacement modes, pressure & velocity, distribution & warping. Basically:

- 3D visualization of:
  - Geometry (Table 27, Table 28)
  - Boundary Layer Thickness (Table 30)
  - Trimmed geometry (Table 31)
  - Displacements/Gusts/Waves/Fields (Table 29)
  - Pressure Coefficients/gains (Figure 64, Figure 65)
  - Velocities( Figure 66)
- 2D steady plots ( Table 21, Table 22) of:
  - Strip Forces
  - Patch Forces
  - Overall Forces
  - Pressure
  - Geometry
- 2D unsteady plots (Table 23, Table 26) of
  - Strip Forces
  - Patch Forces
  - Overall Forces
  - Pressure
  - Displacements
  - Generalized Forces
- 3D graphics control (Table 32)
- 2D graphics control (Table 21 bottom):





	<p>Select 2D graphics or 3D visualization</p> <p>Select 3D options</p> <p><i>Steady rollout</i></p> <p>Select curves versus Mach or Versus Angle of Attack/Slip</p> <p>Select Forces, pressure or Geometry</p> <p>Select Strip forces versus AOA or Mach Select Strip forces versus SPAN Select Patch Forces Select Global Forces Select Forces versus Drag.</p> <p>Select SPAN: j index,y,z,S</p> <p>Scale X with chord</p> <p>Select the forces,</p> <p><i>Graphics options rollout</i></p> <p>Zoom in/out</p> <p>Number of Ticmarks Allow rounding Use curve tags. Redo Create a PostScript file</p>
--	---

Table 21 The right sidebar with steady graphics rollout

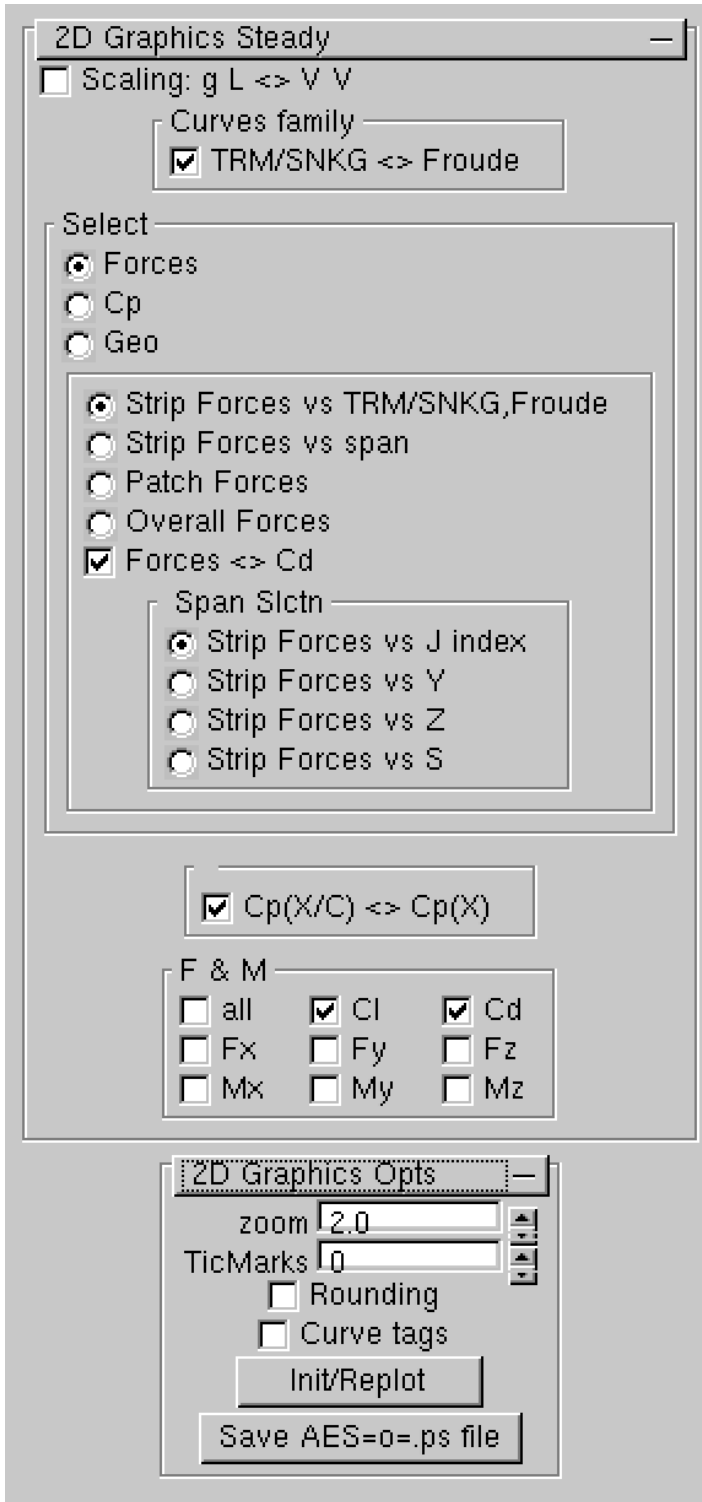
	<p><i>Steady rollout</i></p> <p>Select curves versus Froude or Versus TRIM/SINKAGE</p> <p>Select Forces, pressure or Geometry</p> <p>Select Strip forces versus TRIM/SINKAGE or Froude Select Strip forces versus SPAN Select Patch Forces Select Global Forces Select Forces versus Drag.</p> <p>Select SPAN: j index,y,z,S</p> <p>Scale x with chord</p> <p>Select the forces,</p> <p><i>Graphics options rollout</i> Zoom in/out Number of Ticmarks Allow rounding Use curve tags.</p> <p>Redo Create a PostScript file</p>
--	--

Table 22 The right sidebar with steady graphics rollout



	<p><i>2D Unsteady rollout</i></p> <p>Select Vertical Axis: Real, Imaginary, Magnitude/Phase</p> <p>Select Axis</p> <p>Select curves versus frequency or Mach Number</p> <p>Select Forces, pressure, Generalised Forces or Displacements</p> <p>Select Strip forces versus frequency or Mach Select Strip forces versus SPAN Select Patch Forces Select Global Forces</p> <p>Select SPAN: j index,y,z,S</p> <p>Scale X with chord In aeroacoustic mode an additional option is provided to present the pressure in SPL</p> <p>Select the forces, K and M in AGARD notation</p> <p>Select the Generalised aeroforces (Table 24)</p> <p>Select the modes (Table 25)</p>
--	--

Table 23 2D Graphics Unsteady Rollout

Mode Selector Button> Modes window

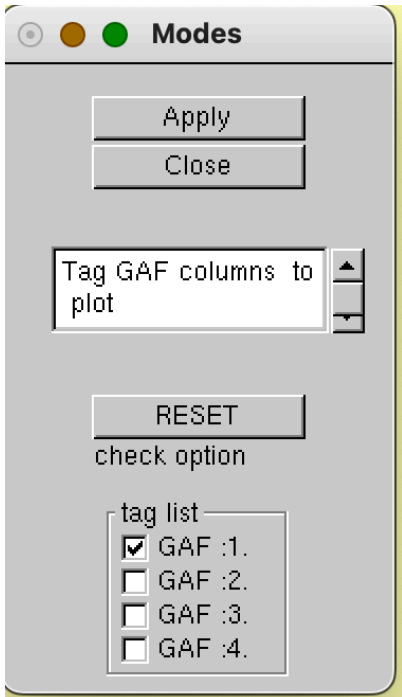
	<p>Selects all or none</p> <p>Make a selection</p>
--	--

Table 24 GAF (GHF) Selection Window

GAF Selector Button> GAF window

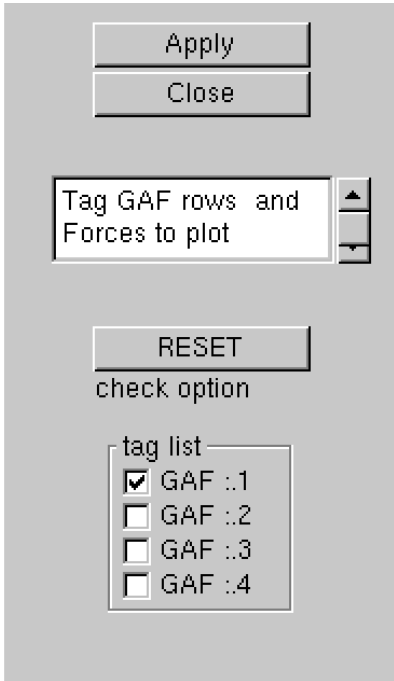
	<p>Selects all or none</p> <p>Make a selection</p>
---	--

Table 25 Select the active mode



2D Graphics Unsteady

Vertical Axis

☒ Real Part/ Mgntd

☒ Imaginary Part/Phs

Axis

☒ Re & Im

☐ Polar

☐ Mg & Ph

Curves family

☒ Red.Fr. <=> Froude

☐ Scaling: g L <=> V V

Select

☒ Forces

☐ Cp

☐ Generalised Forces

☐ Displacements

☐ Strip Forces vs k, Fn

☐ Strip Forces vs span

☐ Patch Forces

☒ Overall Forces

Span Slctn

☒ Strip Forces vs J index

☐ Strip Forces vs Y

☐ Strip Forces vs Z

☐ Strip Forces vs S

☒ Cp(X/C) <=> Cp(X)

F & M

☐ all

☐ K

☐ M

☐ Fx

☐ Fy

☐ Fz

☐ Mx

☐ My

☐ Mz

GHFS

☐ GHFS <=> added mass/damp

☐ all

☒ Diagonal

GHF selector

Modes

☒ all

Mode selector

*2D Unsteady rollout*

Select Vertical Axis Real, Imaginary, Magnitude/Phase

Select Axis  
Select curves versus frequency or Mach Number

Select scaling

Select Forces, pressure, Generalised Forces( GHF) or Displacements

Select Strip forces versus frequency or Froude  
Select Strip forces versus SPAN  
Select Patch Forces  
Select Global Forces

Select SPAN: j index,y,z,S

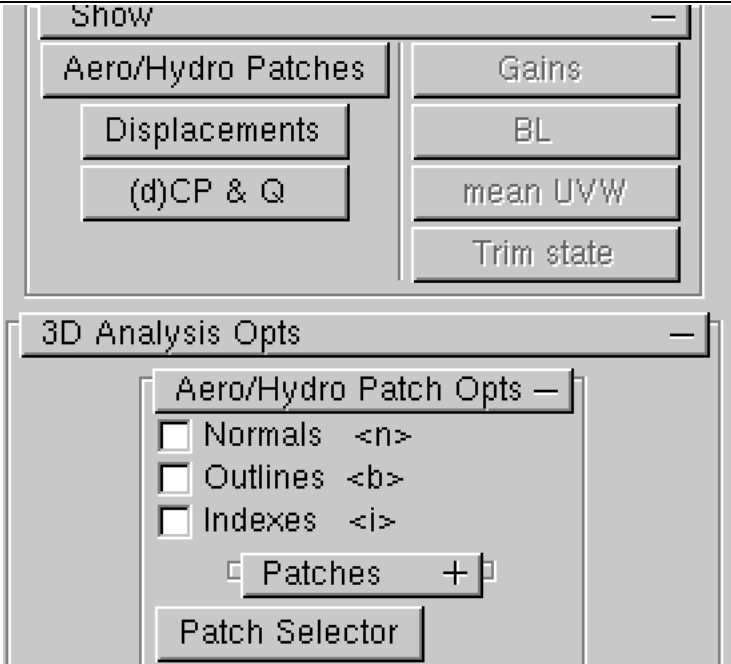
Scale X with chord

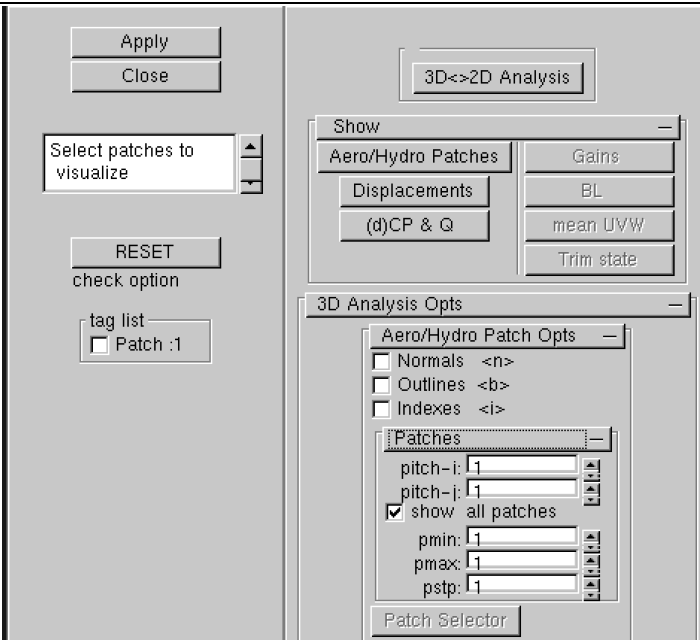
Select the forces, K and M in AGARD notation

Select the Generalized Hydro force/GHFS or added mass/damping. Added mass =  $\text{Re}(\text{GAF})/\omega/\omega$ , Added damping= $-\text{Im}(\text{GAF})/\omega$

Select the modes

Table 26 2D Graphics Unsteady rollout in hydrodynamic mode

 <p><b>Table 27 Rollout dealing with the visualisation of the geometry</b></p>	<p>Selects the quantities of interest to be visualised (depending on the calculation) Pressing the Aero/Hydro patches shows the patches selected in the Aero/Hydro Patch Rollout.</p> <p>Selection of normals, outlines and indices</p> <p>Selection of patches. The patch selector opens a patch select window</p>
--	---

<p>The window is activated by pressing Patch selector button. Select all or none patches</p> <p>Select patches</p>	 <p><b>Table 28 Rollout dealing with the visualisation of the geometry</b></p>	<p>Reduces number of visualised points in i and j direction</p> <p>Sets a patch range</p>
--	---	---



Pressing the Displacements button shows the selected displacements on selected patches. The displacements can be viewed as deformation, as contour lines, vectors and vector outlines. Pressing the modes selector you can select the active modes (rigids, sub rigids, regular modes, waves, field modes et cetera) and also the options to show the original support data of the modes.

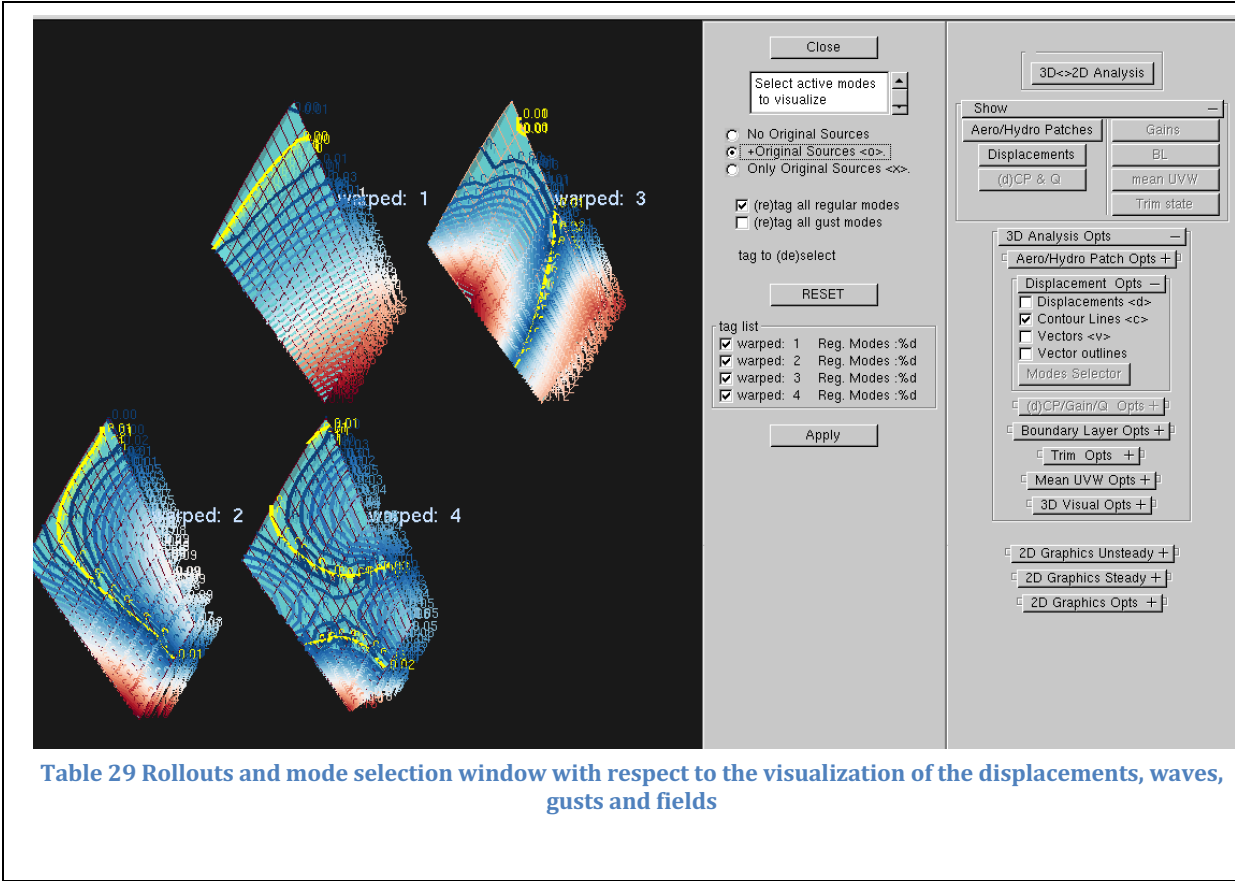


Table 29 Rollouts and mode selection window with respect to the visualization of the displacements, waves, gusts and fields

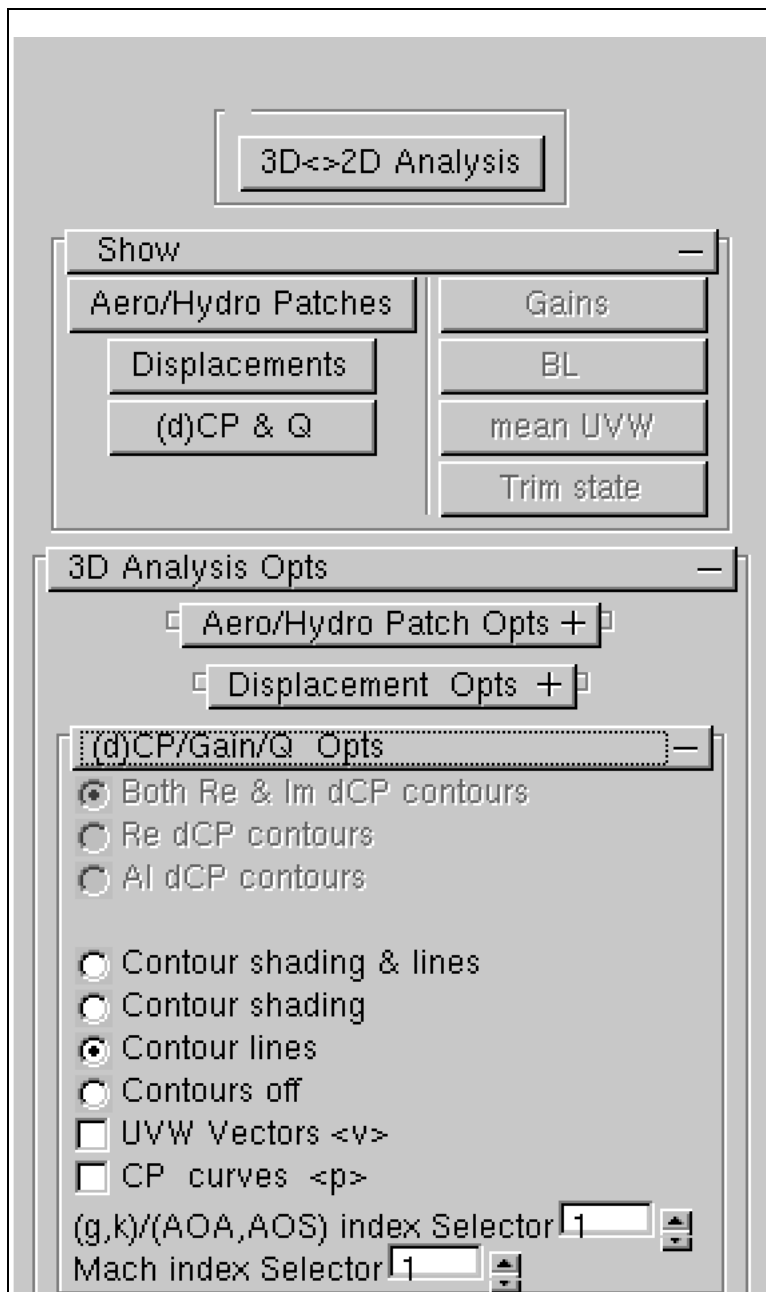


Figure 64 Rollouts with respect to the visualization of the pressures, gains, impedance & uvw

Pressing the (d)CP & Q button or the Gains button (Pressure correction) shows the pressure coefficients (or gains) and velocities displacements (steady) on selected patches together with the displacements.

The real part and the imaginary part of the pressures (or gains) can be viewed together or separate.

In aeroacoustic mode the impedance field can be viewed and the pressure can be in SPL

The pressures (or gains) can be viewed as contour lines, contour shading, and in the steady case with curves put offset normal to the patches.

The UVW vectors apply only for the steady case.

The real part is visualised together with a displacement at its max position  
The real part at its mean position

The pressure (or gains) is selected for a frequency/AOA,AOS,Mach number combination



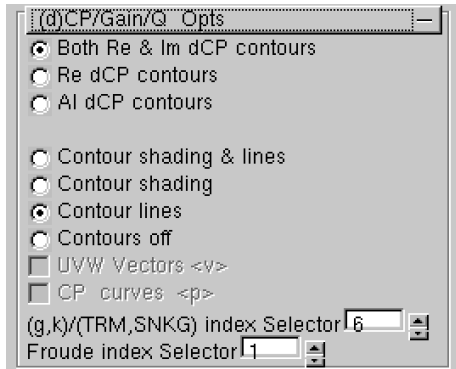


**Figure 65 Rollout with respect to the visualization of the pressures and waves**

Pressing the (d)CP & Q button or the Gains button (Pressure correction) shows the pressure coefficients (or gains) and velocities displacements (steady) on selected patches together with the displacements.

The real part and the imaginary part of the pressures (or gains) can be viewed together or separate.

The pressures (or gains) can be viewed as contour lines, contour shading, and in the steady case with curves put offset normal to the patches. Further the free surface is deformed with the elevation and the elevation can also be viewed with curves put offset normal to the free surface patches

The UVW vectors apply only for the steady case.

The real part is visualised together with a displacement at its max position

The real part at its mean position

The pressure (or gains) is selected for a frequency/TRIM/SINKAGE, Froude number combination

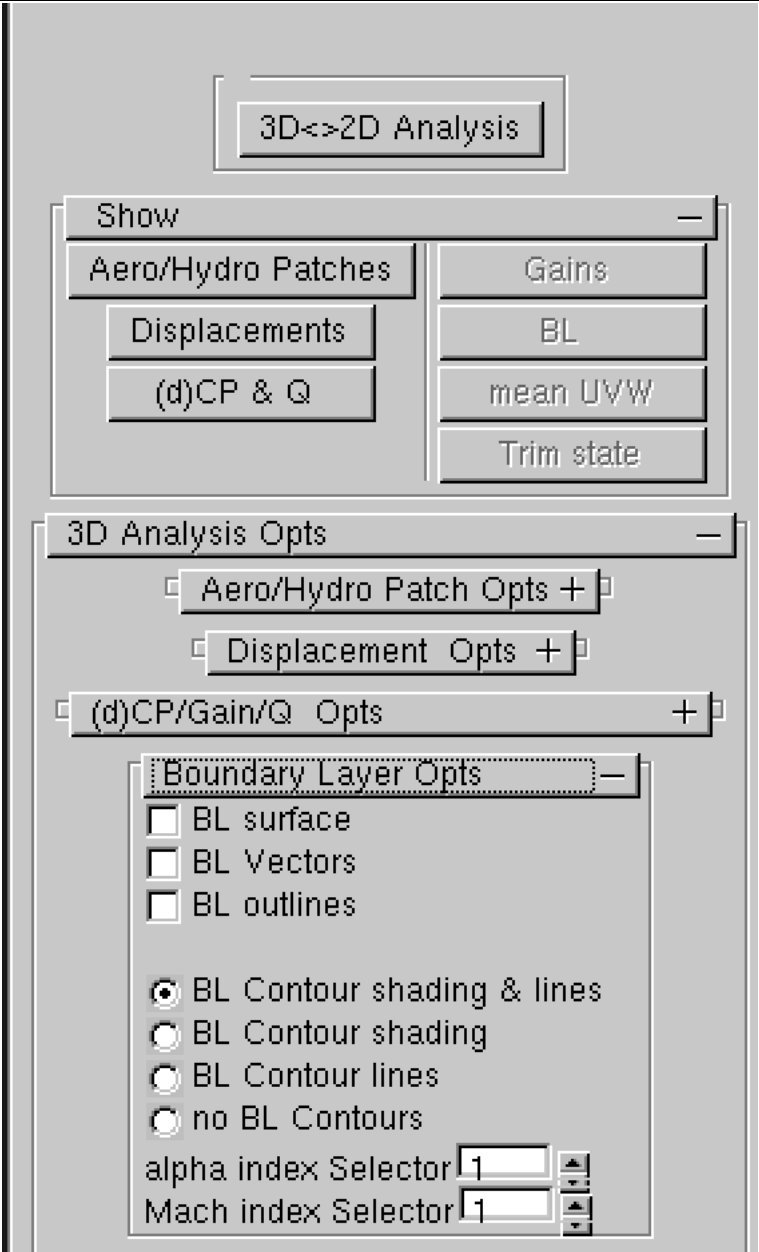
 <p>The screenshot shows a software interface for 3D&lt;-&gt;2D Analysis. At the top is a button labeled "3D&lt;-&gt;2D Analysis". Below it is a "Show" section with a minus sign, containing a "Aero/Hydro Patches" button and a column of four buttons: "Displacements", "(d)CP &amp; Q", "Gains", "BL", "mean UVW", and "Trim state". Below the "Show" section is a "3D Analysis Opts" section with a minus sign, containing three expandable options: "Aero/Hydro Patch Opts +", "Displacement Opts +", and "(d)CP/Gain/Q Opts +". The "(d)CP/Gain/Q Opts +" section is expanded, showing a "Boundary Layer Opts" section with a minus sign. This section contains several options: three checkboxes for "BL surface", "BL Vectors", and "BL outlines"; four radio buttons for "BL Contour shading &amp; lines" (selected), "BL Contour shading", "BL Contour lines", and "no BL Contours"; and two index selectors, "alpha index Selector" and "Mach index Selector", both set to "1".</p>	<p>Pressing the BL button shows the Boundary Layer visualisation options on selected patches.</p> <p>The BL can be visualised as a surface, vectors and as an outline.</p> <p>Contour shading and Contour lines can be applied.</p> <p>The BL is selected for a AOA,AOS,Mach number combination</p>
--	---

Table 30 Rollout with respect to the visualization of the boundary layer thickness



<div><div>3D&lt;&gt;2D Analysis</div><div><div>Show</div><div><div>Aero/Hydro Patches</div><div>Displacements</div><div>(d)CP &amp; Q</div></div><div><div>Gains</div><div>BL</div><div>mean UVW</div><div>Trim state</div></div></div><div><div>3D Analysis Opts</div><div><div>Aero/Hydro Patch Opts +</div><div>Displacement Opts +</div><div>(d)CP/Gain/Q Opts +</div><div>Boundary Layer Opts +</div><div><div>Trim Opts</div><div><div><input checked="" type="checkbox"/> Trm surface</div><div><input checked="" type="checkbox"/> Trm Vectors</div><div><input type="checkbox"/> Trm outlines</div><div><div><input checked="" type="radio"/> Trim Contour shading &amp; lines</div><div><input type="radio"/> Trim Contour shading</div><div><input type="radio"/> Trim Contour lines</div><div><input type="radio"/> no Trim Contours</div></div></div></div></div></div></div>	<p>Pressing the TRIM state button shows the trimmed geometry visualisation options on selected patches.</p> <p>The trimmed surface can be visualised as a surface, vectors and as an outline.</p> <p>Contour shading and Contour lines can be applied.</p>
--	--

Table 31 Rollout with respect to the visualization of the trimmed state



Figure 66 Rollout with respect to the visualization of the explicit velocity field

The mean UVW velocity field can be visualized for selected patches and AOA/AOS Mach number combinations



	<p>Pressing the 3D visual Opts Button opens a rollout for controlling the visualization.</p> <p>Select wireframe, mirrors</p> <p>Set scale</p> <p>Draw axes on/off</p> <p>Text on/off</p> <p>Contour labels on/off</p> <p>Select the projection</p> <p>Change projection</p> <p>Select mouse for rotation or translation</p> <p>Zoom in/out</p> <p>Save a ppm file of the visualisation.</p>
--	--

Table 32 Controller of the 3D Graphics

## Running AES=O=

1. Open a terminal.
2. Go to your run directory.
3. Run `aes=o=`.

The main input file is `aes=o=.cnf` which together with `.prefs_aes=o=` controls the calculation. The `.prefs_aes=o=` data is also written at the end of the `aes=o=.cnf` file.

The `aes=o=.cnf` file is created/updated upon saving in the configuration menu.

The save operation expands control, case and bulk information to the `aes=o=.cnf` file. When one is satisfied with the `aes=o=.cnf` file and need to change only the bulky data (geometry and downwash) it is sufficient by specifying the new bulky file names at the begin of the `aes=o=.cnf`. These names should be different from the names stored in the expansion area of `aes=o=.cnf` to expand the new bulky file data in the `aes=o=.cnf` file and can be used to perform calculations without having to change control et cetera.

When starting up the code without any files, the code will use its embedded data for the AGARD wing 445.6

By pressing the steady or the unsteady calculate button the calculation is performed using the specified Mach number range and angle of attack (or [TRIM](#)) & angle of slip range (or [SINKAGE](#)) and reduced frequency distribution and activated downwash modes et cetera in combination with the selected calculation method. The solution matrices can be stored for [reuse](#) accommodating follow on stages of your design & certification cycle (mode shape changes). Also note the possibility to coarsen the paneling to reduce turn around time.

The results (forces, pressures, velocities & applied downwash) can be extensively analyzed by using the analysis accessible in the right sidebar together with control at the mid bottom. The calculated pressure distributions can be visualized simultaneously with their exiting modes shapes.

The calculation can also be performed in batch by setting the first parameter on `.prefs_aes=o=` to one

### The Input files

#### The `.prefs_aes=o=` file

The `.prefs_aes=o=` file is expected/created in the home directory. Below an example is shown.



0 7	The first value (0,1,2) selects, normal, immediate calculation and batch calculation, respectively The second value sets the mode (0= aerodynamic , 1= hydrodynamic, 2..6=TBD, 7=acoustic
./	specifies the working directory
# case orps	
0.00000 4.00000 0.00000 0.00000 0.00000 0.00000 0.00000 0.00000 0.100000E-02 0.200000E-01 0.00000 0.00000 0.00000 0.00000	
6 1 6 1	
0	
0.00000 0.00000	
0.00000 0.00000	
0.00000 0.00000	
0.00000 0.00000	
0.00000 0.00000	
# method orps	
0.500000 0.850000 0.925000 0.100000E-02	
0 0 2 3	
0.250000 15.0000 3.00000 0.500000E-01	
0 0 0 1 0 0 0 0 1 0 0 0	
1 1	
0 0	
0	
0	
0.00000	
# warping Orps regulars	
2 0 3 2 2 2 2 0 1 3 1 1	

1.00000 1.00000 1.00000	
# warping Orps specials	
2 0 3 2 2 2 2 0 1 3	
1.00000 1.00000 1.00000	
# plot 2D orps	
1 0 0 0 0 1 0 1 0	
1 0 0 0 0 0 0 0	
1 1 0 1 0 0 0	
1 6 1 1 1 1	
1 1 1 1 10 1	
1 0 0 0	
1 0 0 0 0 0 0 0	
32	
00000000000000000000000000000000	
10000000000000000000000000000000	
# data outputs	
0 0 1	
# physics	
315.000000 1.000000 ! sosinf rhoinf	SPL!
# init workbench	
1920 1200 1 2	
0.69 1.25 1.00 0.00	
1.00 1.00 0.69 1.00 0.10 0.10 0.10 0.90	
0 0 0 240 0 130 30 60 255 250 60 60 230 220 50 240 130 40 0 220 0 127 127 127	

**Table 33 .prefs\_aes=o= file**

### The aes=o=.cnf file

The first 3 records on the aes=o=.cnf file specify the filenames associated with geometry, regular vibration modes and polynomial vibration modes, respectively. The data on these files will be expanded to the associated sections on the aes=o=.cnf when these filenames are different from the filename recorded in the latter sections. Otherwise the existing data on the sections is applied.





## Outputs

$(d)C_p$	pressure (difference) coefficient, nondimensionalised with $q$ the dynamic pressure
$C_l$	Lift coefficient,
$C_d$	Drag coefficient.
$K$	normal force coefficient, (Agard notation [28]).
$M$	moment coefficient about quarter chord axis, (Agard notation [28], positive nose down).
$F_x$	force coefficient along x axis
$F_y$	force coefficient along y axis
$F_z$	force coefficient along z axis
$M_x$	Moment coefficient about the x axis
$M_y$	Moment coefficient about the y axis
$M_z$	Moment coefficient about the z axis
$GAF_{ij}$	generalised aerodynamic force coefficients in mode $j$ as a result of mode $i$ , nondimensionalised with dynamic pressure
$GHF_{ij}$	generalised hydrodynamic force coefficients in mode $j$ as a result of mode $i$ , nondimensionalised with dynamic pressure, also added mass = real part $(GHF_{ij})/\omega/\omega$ and added damping is imaginary part $(-GHF_{ij})/\omega$

**Table 34 The outputs**

The sectional unsteady force coefficients  $K$  are nondimensionalised with  $q$ , local chord and  $\pi$ .

The sectional unsteady moment  $M$  coefficients are nondimensionalised with  $q$ , local chord<sup>2</sup> and  $\pi/2$ .

The sectional steady force coefficients are nondimensionalised with  $q$  and local chord.

The sectional steady moment coefficients are nondimensionalised with  $q$  and local chord<sup>2</sup>.

Reference lengths are not applied.

Sound pressures can be presented in SPL requiring the speed of sound and density.

## An aerodynamic demo application

In the present report some applications with respect to the features of AES=O= will be demonstrated. For the verification of the underlying models we refer to references [21] [22] [24] [32] [24] [1].

The objective of this example is to demonstrate AES=O= for a simple configuration. AES=O= is hardly limited in applications and can easily support design and certification of A/C and watercrafts. For demonstration purposes a panelling of wing 445.6 is already hardwired in the app and also vibration mode data of wing 445.6 is hardwired in the app. The vibration modes are defined on an unstructured mesh and can be warped to the panelling. Running the app AES=O= ab initio will use the hardwired example and generate automatically the preferences file *.prefs\_AES=O=* and the configuration file *AES=O=.cnf* in your home directory. These files might serve as templates for your own applications.

An on the fly made steady and unsteady example using AES=O= is presented in this section for the paneling, the warping of the vibration modes and the calculated loads and pressure distribution.

After starting the code, the workbench shows up (see Figure 67)). First, we set the case parameters (see Figure 68 ).

We select the case parameters for the steady calculations as follows:

6 Mach number in the range 0.5--0.9

6 Angles of Attack in the range 0.0--30 deg

We select the case parameters for the unsteady calculations as follows:

6 Mach number in the range 0.5--0.9

6 Reduced Frequencies in the range 0--1.0

The control that is applied is depicted in Figure 69, Figure 70, Figure 71 and Figure 72.

Next, we enter the paneling window and the embedded initial thick geometry of wing 445.6 is depicted in Figure 73. We enter the displacement window and the visualization of the embedded displacement modes shows up in Figure 74. Next, we drill down to the edit window ( Figure 75 )where we made 3 changes:

- We increase the thickness with 100% (doubling);
- We change the y coordinate of the starboard leading edge to 0.3;
- Finally, we change the x coordinate of the portside trailing to 0.7661.and

The resulting geometry is depicted in Figure 76 and shows a geometry with a gothic delta wing signature.

As the displacement modes for the new geometry, we apply the same embedded data set for wing 445.6 which is automatically warped to the new configuration. The warped data together with the support data is depicted in Figure 77

By pressing the steady or unsteady calculate button the calculation is performed using the specified case parameters and activated model data (Mach number, Angle of Attack and



reduced frequency distribution and activated vibration modes for the modified geometry and warping.

The steady results are presented in Figure 78, Figure 79, Figure 80, Figure 81, Figure 82 and Figure 83. To generate these pictures the graphics control shown at the Right Sidebar has been applied after pressing the steady calculate button. The time it takes to perform the calculations is barely noticeable on today's laptops.

- Figure 78 Depicts the overall forces versus angle of attack for constant Mach number curves
- Figure 79 Depicts the overall forces versus Mach number for constant angle of attack curves
- Figure 80 Depicts the overall forces versus Drag for constant angle of attack curves
- Figure 81 Depicts the overall forces versus Drag for constant Mach number curves
- Figure 82 Shows a contour plot visualization of the pressure coefficient together with pressure coefficient curves at Mach number is 0.5 and angle of attack 30 deg.
- Figure 83 Shows a contour plot visualization of the pressure coefficient together with pressure coefficient curves and at Mach number is 0.9 and angle of attack 30 deg.

The unsteady results are presented in Figure 84, Figure 85, Figure 86, Figure 87, Figure 88, Figure 89 and Figure 90. Again, to generate these pictures the graphics control shown at the Right Sidebar is applied after pressing the steady calculate button. The time it takes to perform the calculations is again barely noticeable on today's laptops.

Figure 84	Depicts Unsteady Overall Forces versus Reduced Frequency, Constant Mach number curves
Figure 85	Depicts Unsteady Overall Forces versus Mach number, Constant Reduced Frequency Curves
Figure 86	Depicts Diagonal Generalised Forces versus Mach number, Constant Reduced Frequency Curves
Figure 87	Depicts Generalised Forces versus Mach Number, Constant Reduced Frequency Curves. AES=V= can be directly used to perform flutter analysis with the data.
Figure 88	Shows a contour plot visualization of Real (left) and Imaginary part of the unsteady pressure coefficient distribution combined with the extreme position of the generating first mode at Mach number 0.9 and Reduced Frequency 1.0. Note that the geometry is deformed according to the mode shapes.
Figure 89	Shows a contour plot visualization of Real (left) and Imaginary part of the unsteady pressure coefficient distribution combined with the extreme position of the generating fourth mode at Mach number 0.9 and Reduced Frequency 1.0
Figure 90	Shows a contour plot visualization of Real and Imaginary parts of the unsteady pressure coefficient distribution for the four modes modes at Mach number 0.9 and Reduced Frequency 1.0

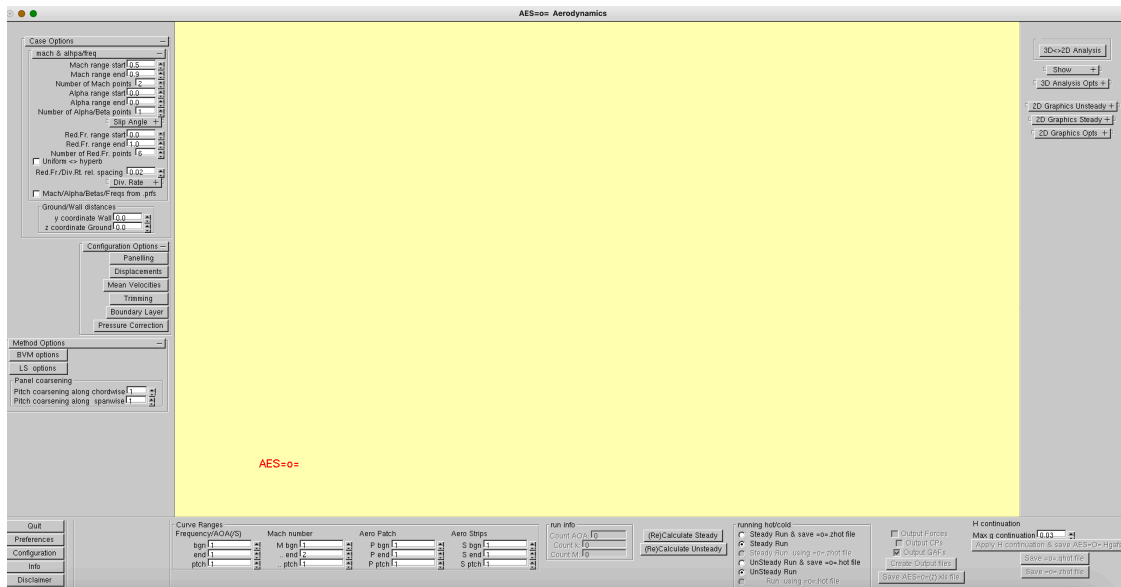


Figure 67 Workbench AES=0= at startup in aerodynamic mode

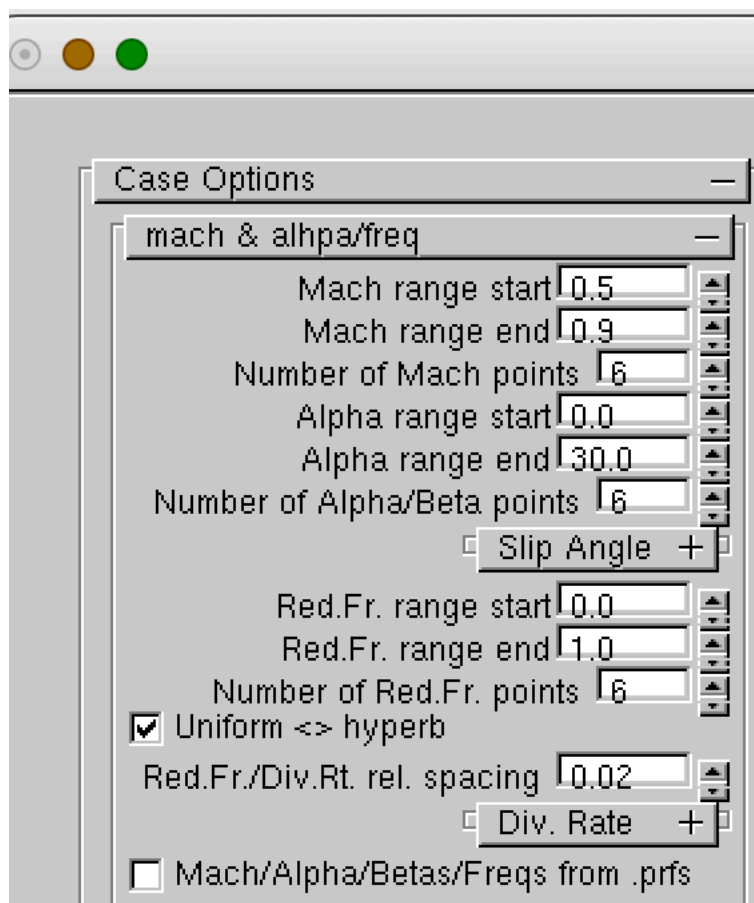


Figure 68 Setting the case parameters

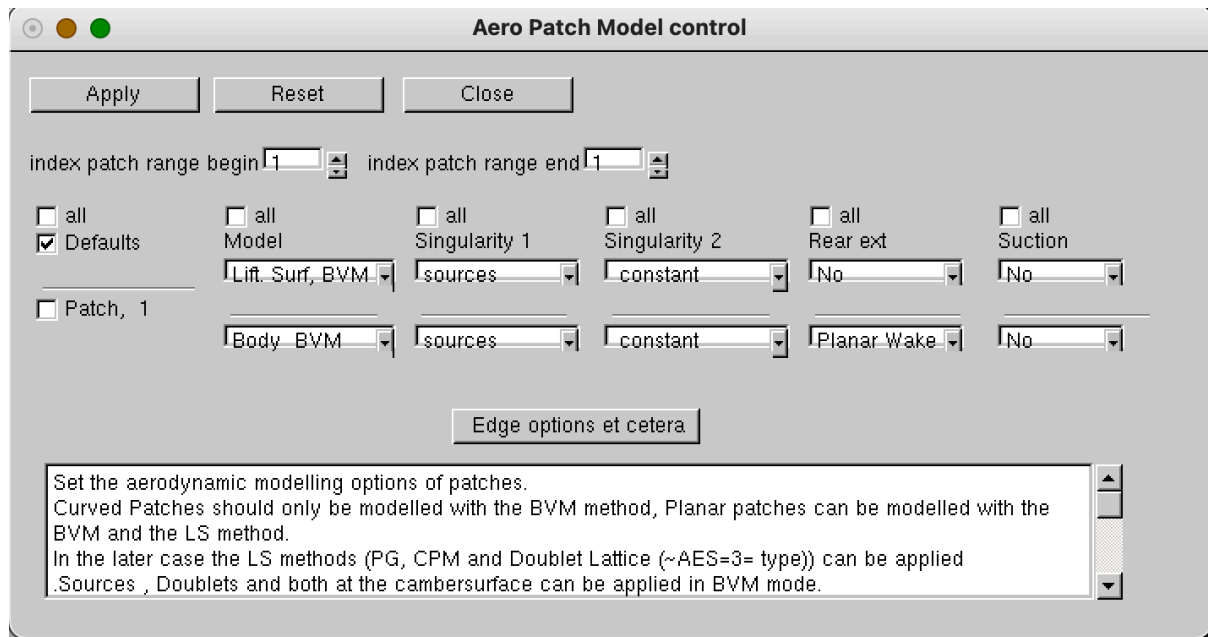


Figure 69 The applied primary patch model control

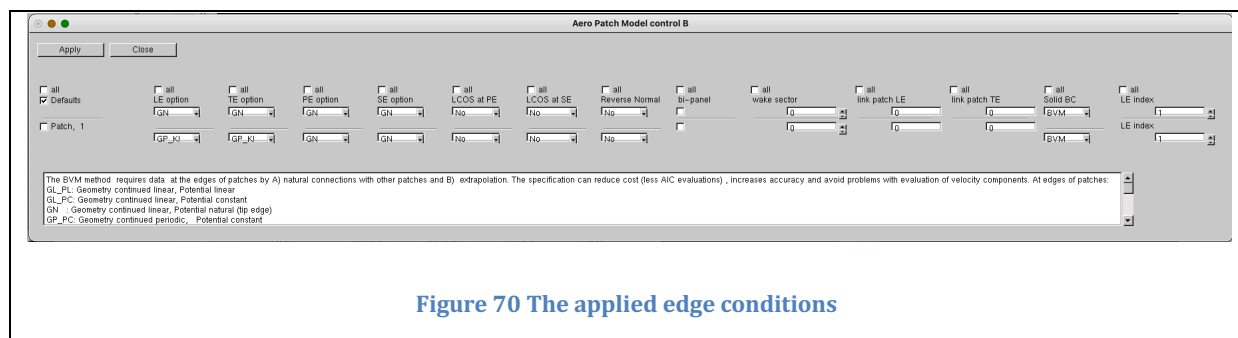


Figure 70 The applied edge conditions

**=o= calculation options**

Close

BVM Method

AIC integration orp

BC general

☒ Tangential BC

☐ Mass flux BC

BL & Trim model

☒ Geometry adapted for BL and trim

☐ Transpiration applied for BL and trim

Cp

☒ Lin. Isentropic || Nonlinear

☐ Quasi-Linear

☐ Linear

☐ Mass flux consistent

CP=0 location TE

Mean flow

☒ Mean flow = Uniform free stream

☐ Mean flow from usr input

☐ Mean flow from =o=.qhot

Mean flow consistency

☒ no

☐ mean flow consistent

☐ 3D <> 2D

☐ Apply Breaks(M>1)

Break angle treshold

☐ Apply Mach Reduction Superinclined areas

Superinclined angle treshold

☐ Apply Mach Reduction with Equivalent wedge

Angle of Equivalent Wedge

Figure 71 The applied BVM model options



**Warp Options**

(Re)Apply Regular Modes

Close

Inputs

Symmetry options

- ☒ Apply Support Geometry Set as is
- ☐ Assume Support Geometry Set is symmetric wrt XZ plane
- ☐ anti-symmetric modes wrt XZ plane
- ☐ asymmetric modes
- ☒ symmetric modes wrt XZ plane

Coarsening

Pitch coarsening

Re using data from =0=.wms

- ☐ put warped modes on =0=.wms
- ☒ no action
- ☐ get warped modes from =0=.wms

Warping options

- ☒ Volume spline
- ☐ planar surface spline
- ☐ polynomial
- ☐ planar surface spline+polynomial
- ☐ Volume spline+polynomial

Kernel options

- ☐  $R^2 \ln R$  (Biharmonic 2D)
- ☐ 1:R (Laplace 3D)
- ☒ R (Biharmonic 3D, VolumeSpline)

☐ Far Field terms on/off

Polynomial options

pol. deg. x

pol. deg. y

pol. deg. z

Other options

NNB options

- ☐ NNB off
- ☐ NNB on
- ☐ NNB on smoothed (global)
- ☒ NNB on smoothed (patch)

Influence domain (=0: cancel nnb; > 0 nnb)

co\_ordinate weightfactor x

co\_ordinate weightfactor y

co\_ordinate weightfactor z

Figure 72 Applied warping options

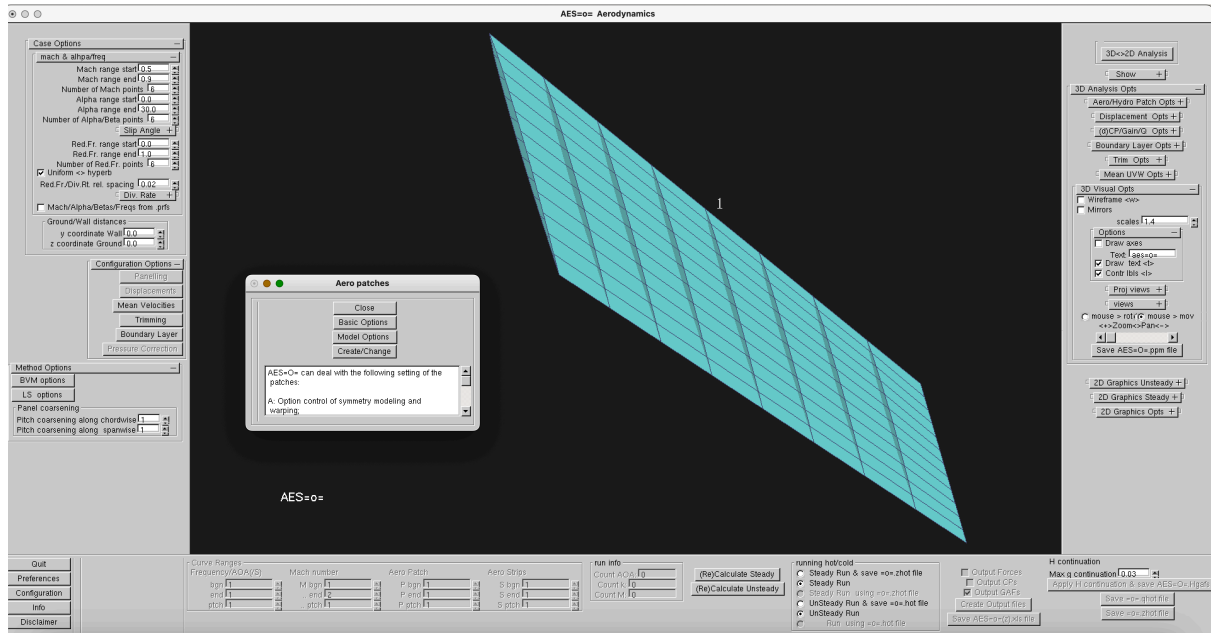


Figure 73 Opening the panel window

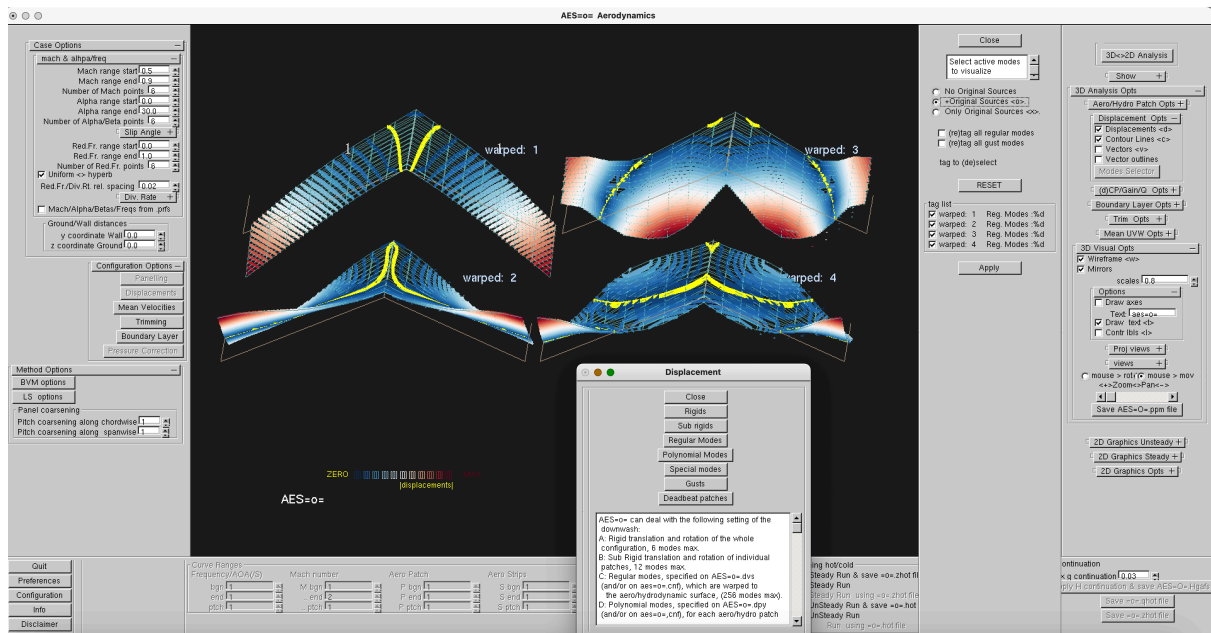


Figure 74 Opening the Displacement Window



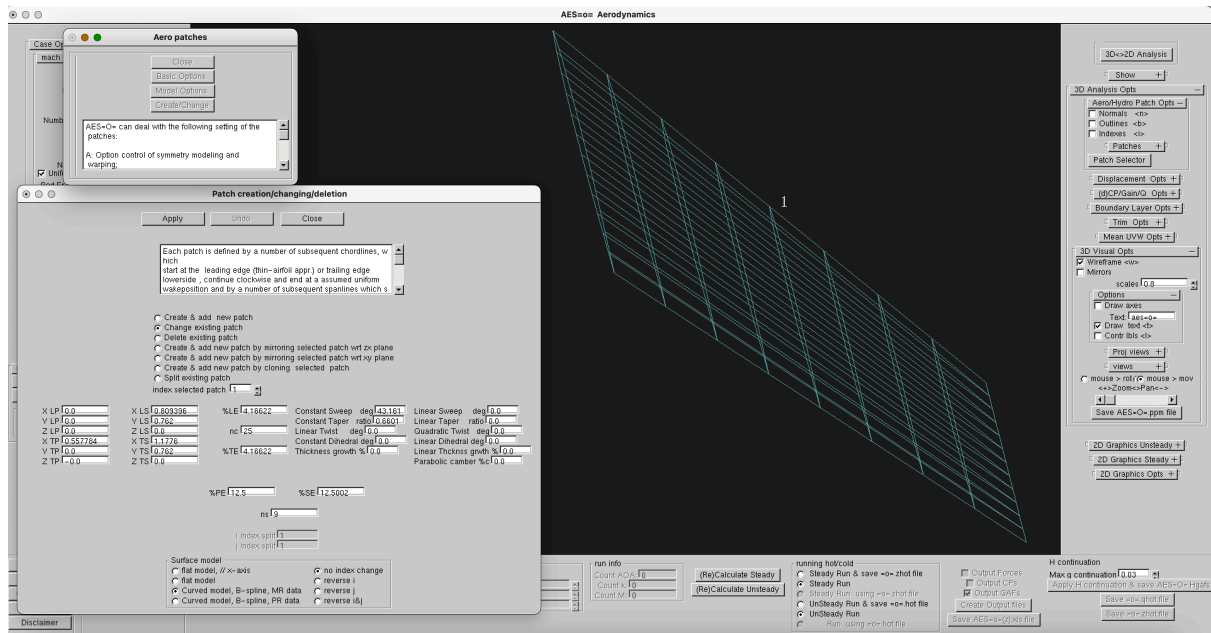


Figure 75 Opening the patch create et cetera window

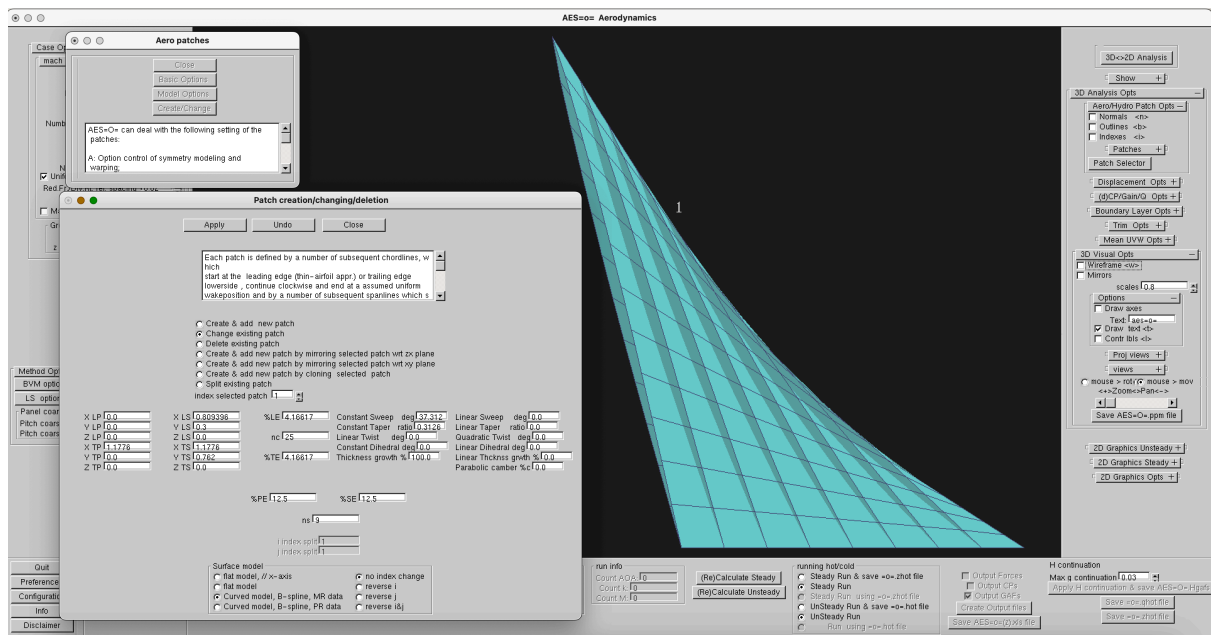


Figure 76 Changing wing 445.6 to a wing with gothic signature

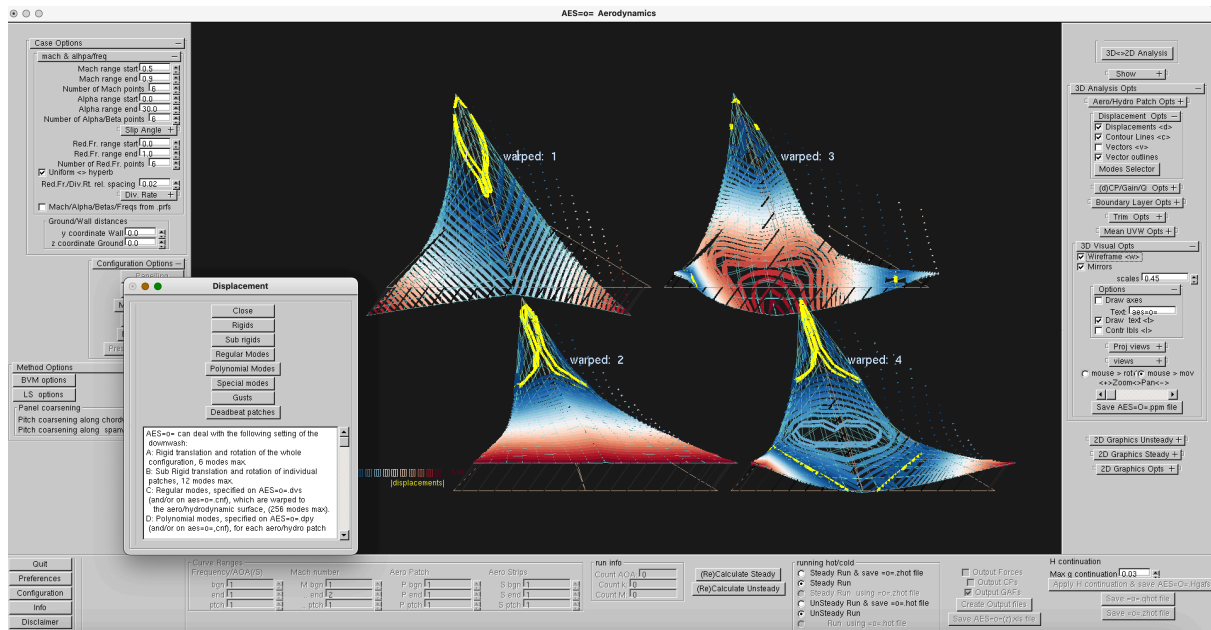


Figure 77 Automatic warping of wing445.6 modes on the Gothic platform

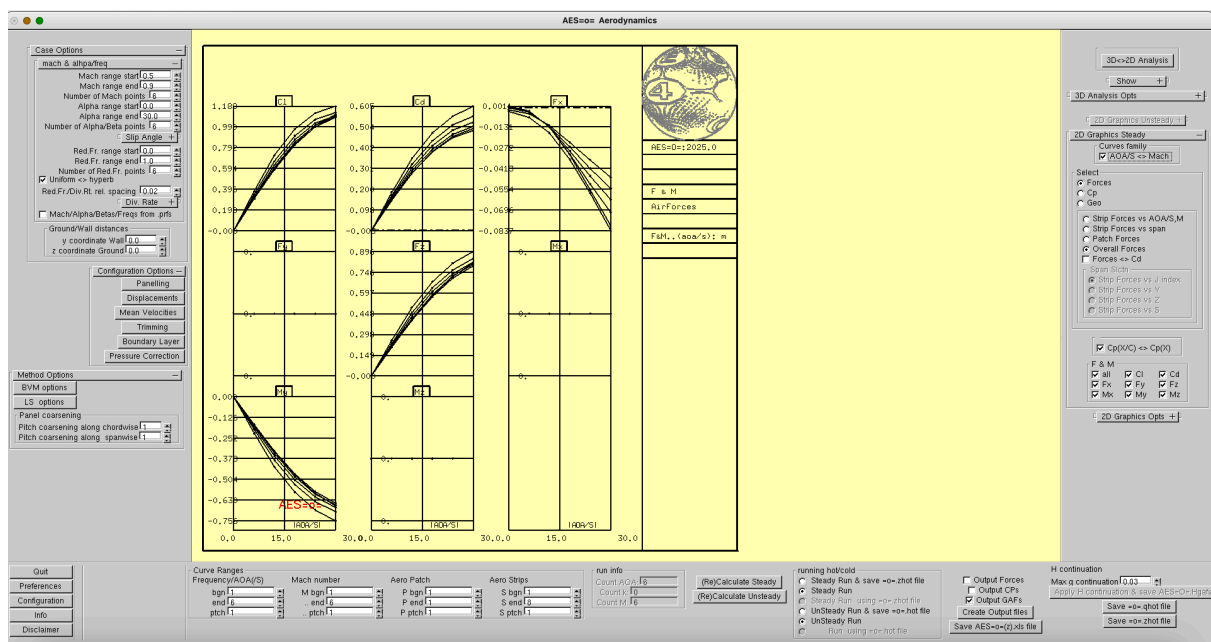


Figure 78 Overall Forces versus Angle of Attack, Constant Mach Curves

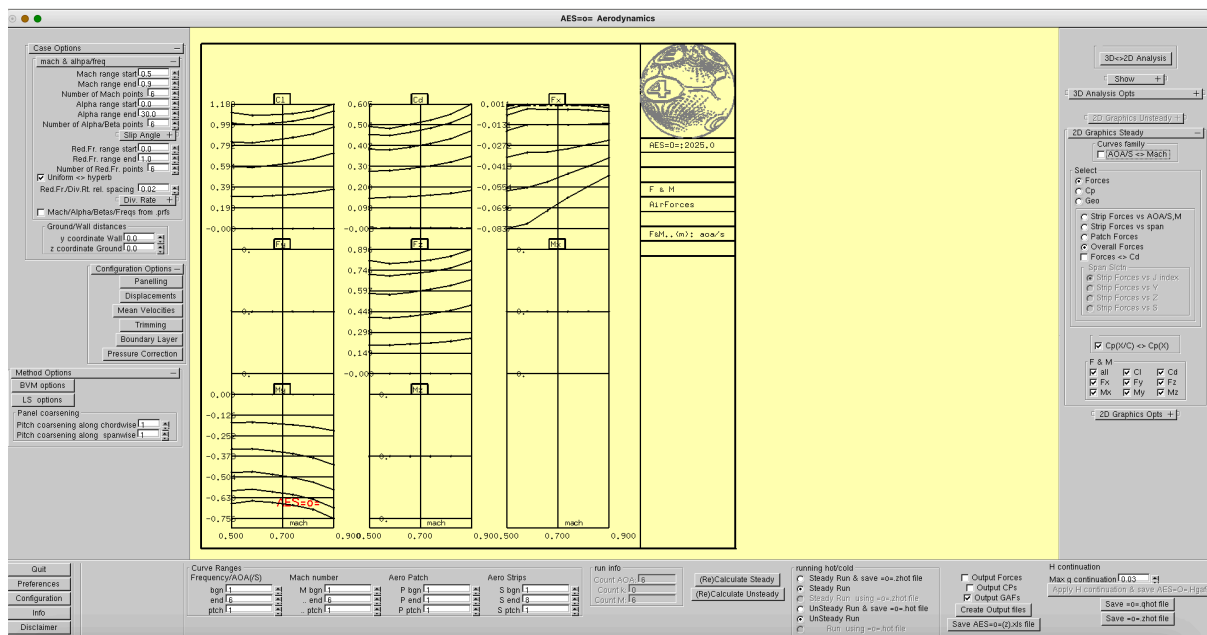


Figure 79 Overall forces versus Mach number, Constant Angle of Attck curves

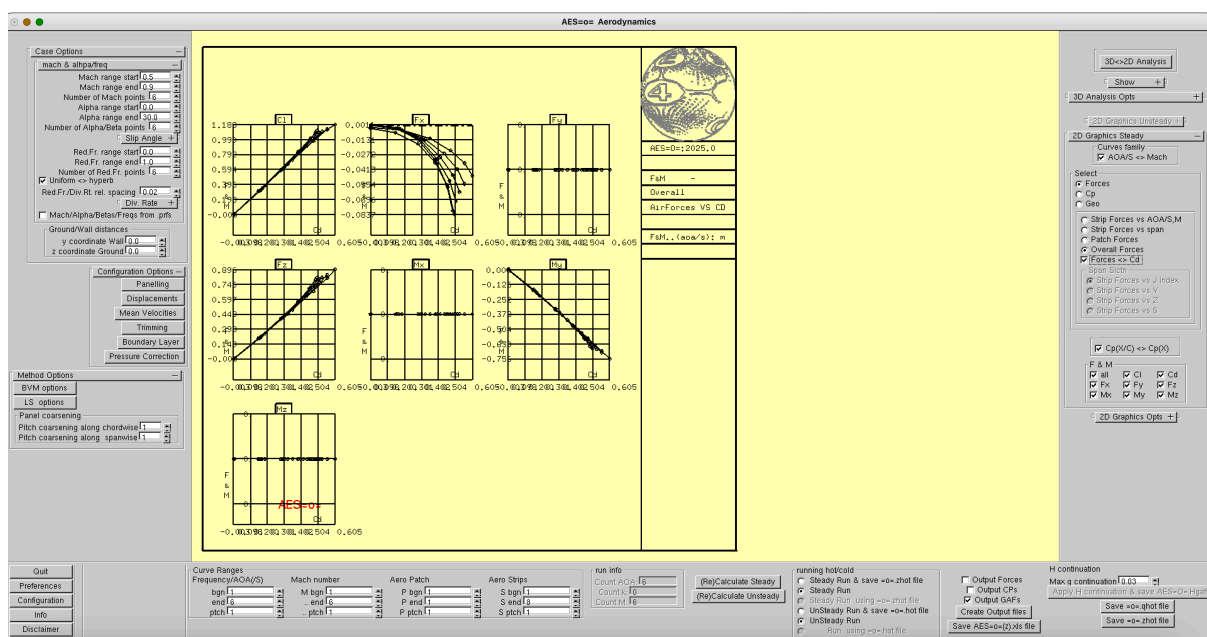


Figure 80 Overall Forces versus Cd, Constant Angle of Attack curves

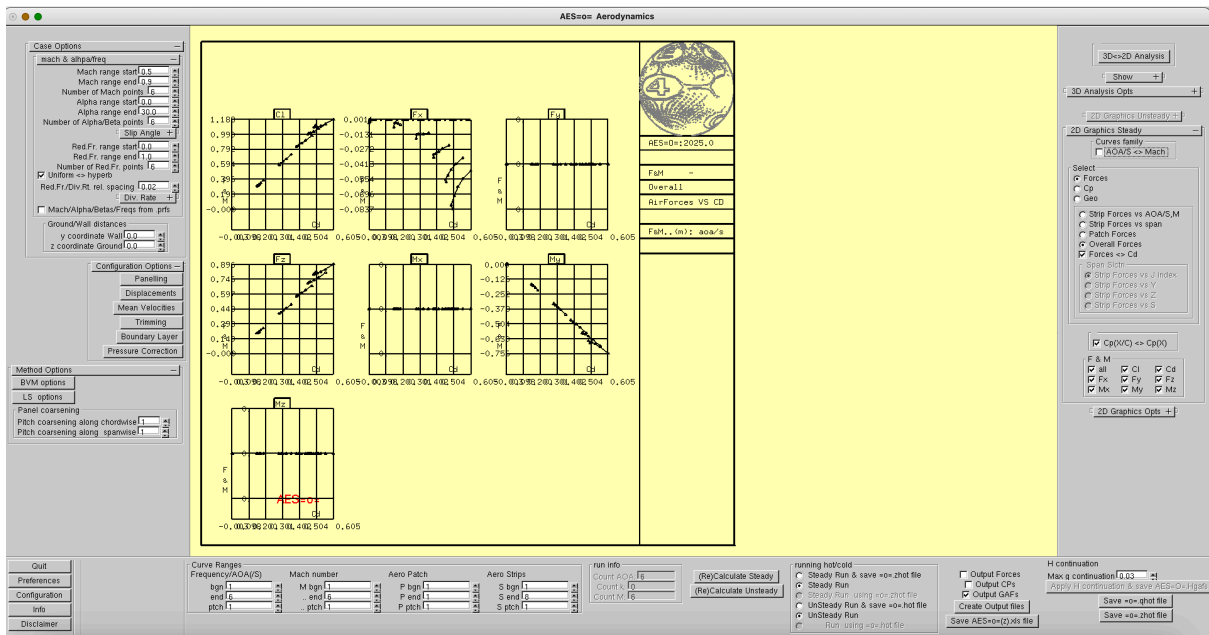


Figure 81 Overall Forces versus Cd, Constant Mach number curves

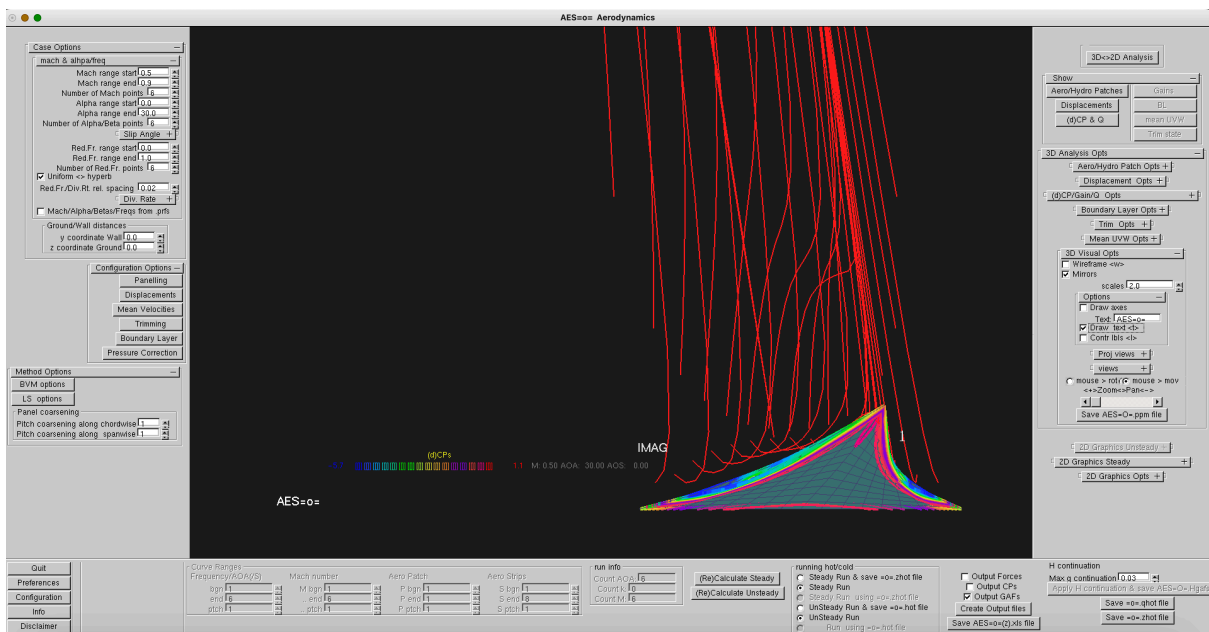


Figure 82 Visualisation of the Pressure Coefficient at Mach number is 0.5 and Angle of Attack 30 deg

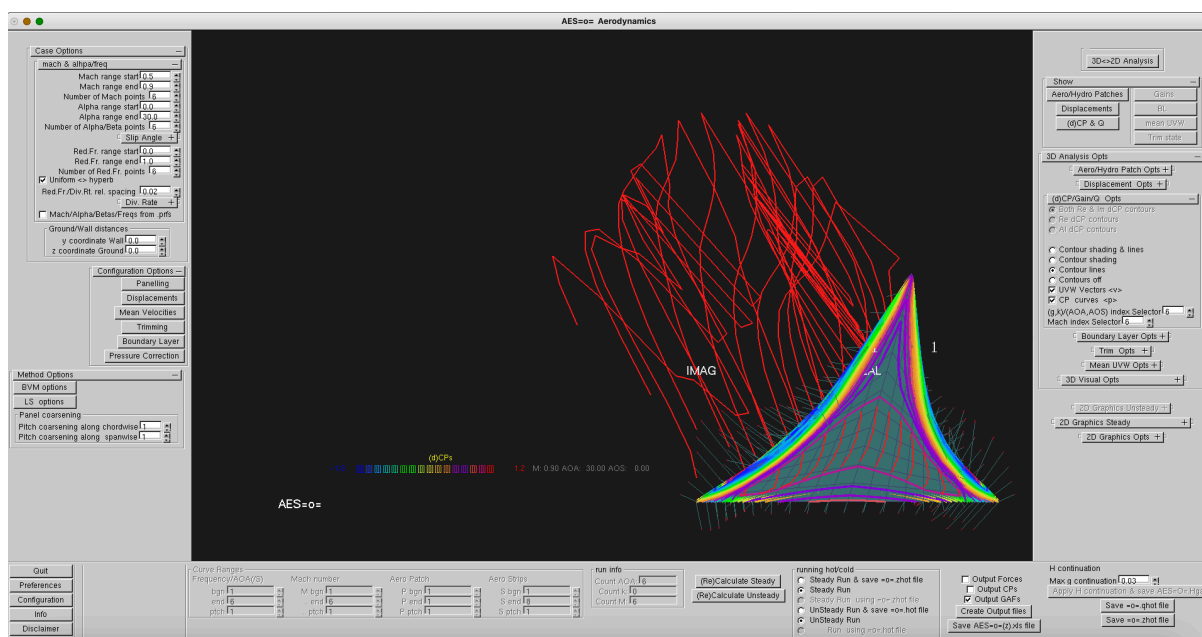


Figure 83 Visualisation of the Pressure Coefficient distribution and the velocities at Mach number is 0.9 and Angle of Attack is 30 deg

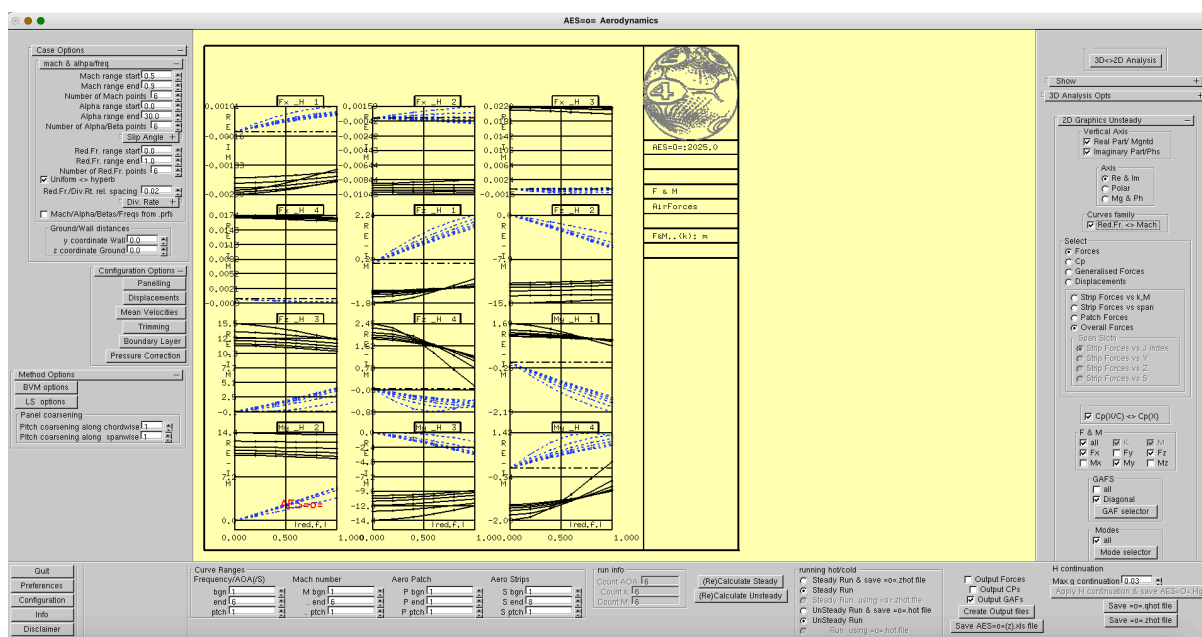


Figure 84 Unsteady Overall Forces versus Reduced Frequency, Constant Mach number curves

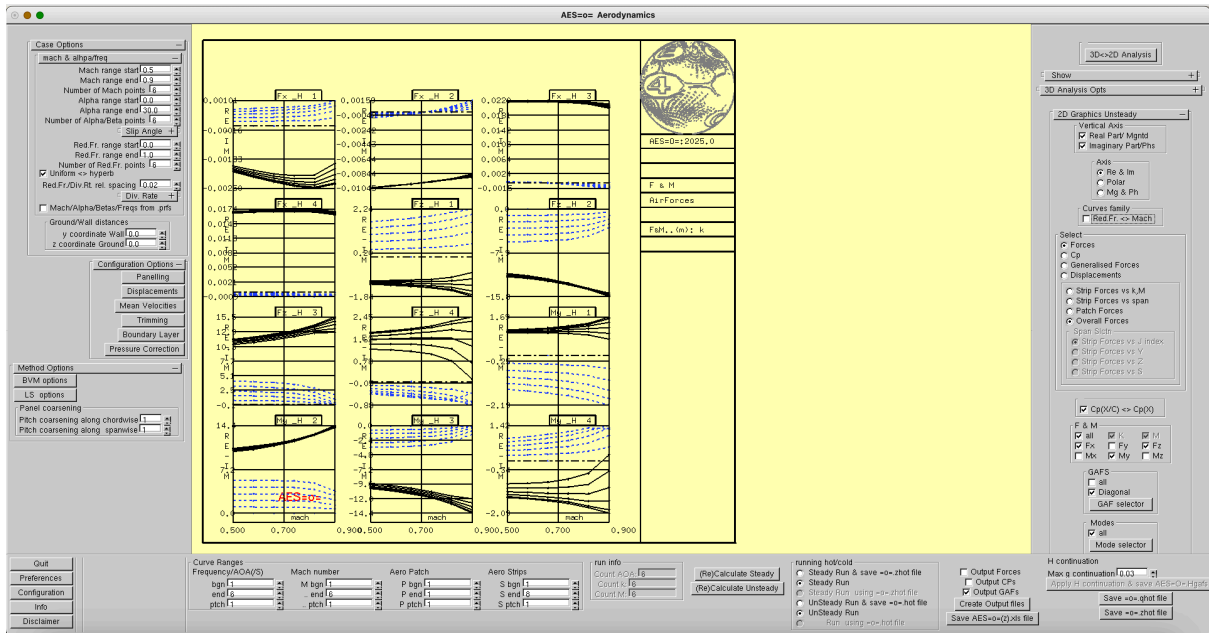


Figure 85 Unsteady Overall Forces versus Mach number, Constant Reduced Frequency Curves

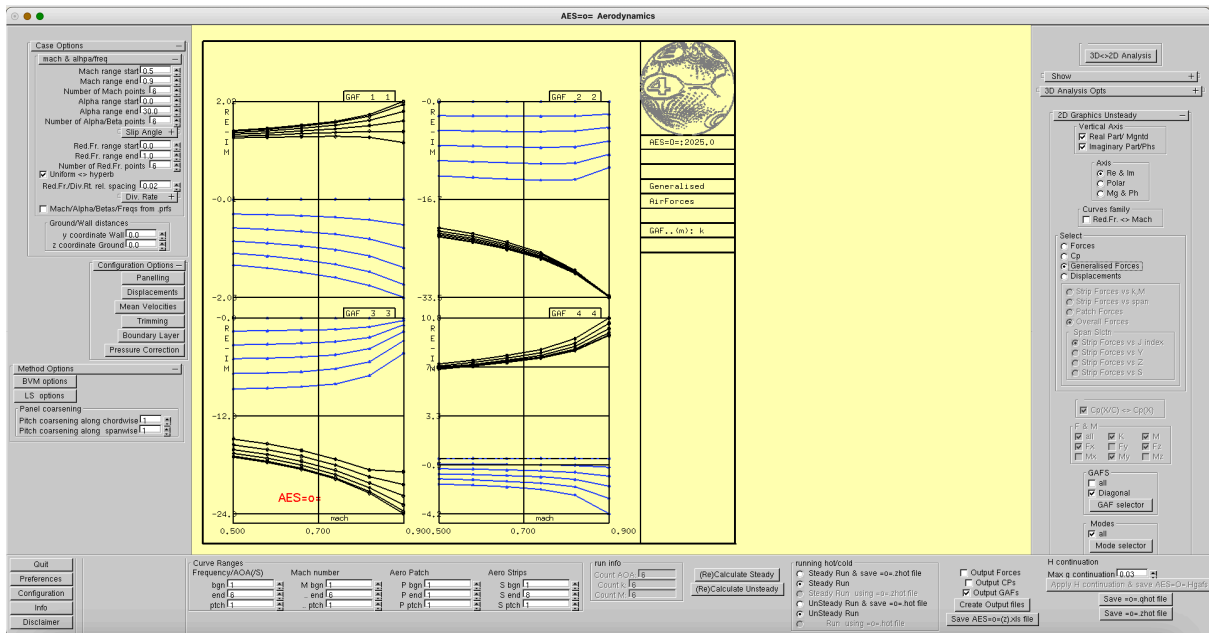


Figure 86 Diagonal Generalised Forces versus Mach number, Constant Reduced Frequency Curves

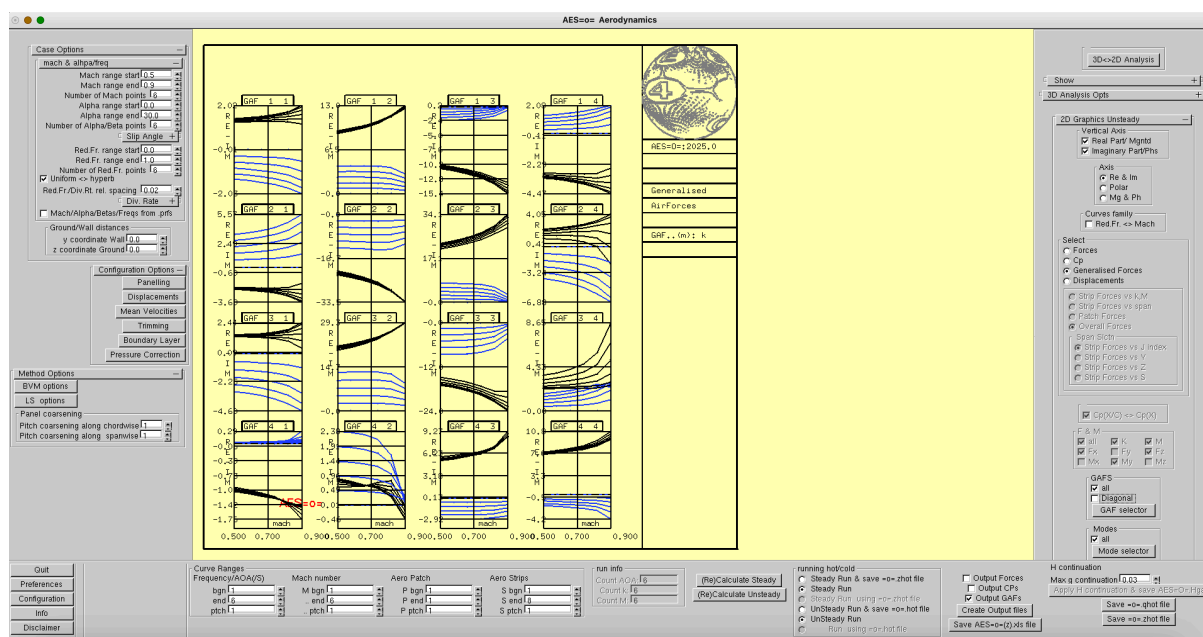


Figure 87 Generalised Forces versus Mach Number, Constant Reduced Frequency Curves

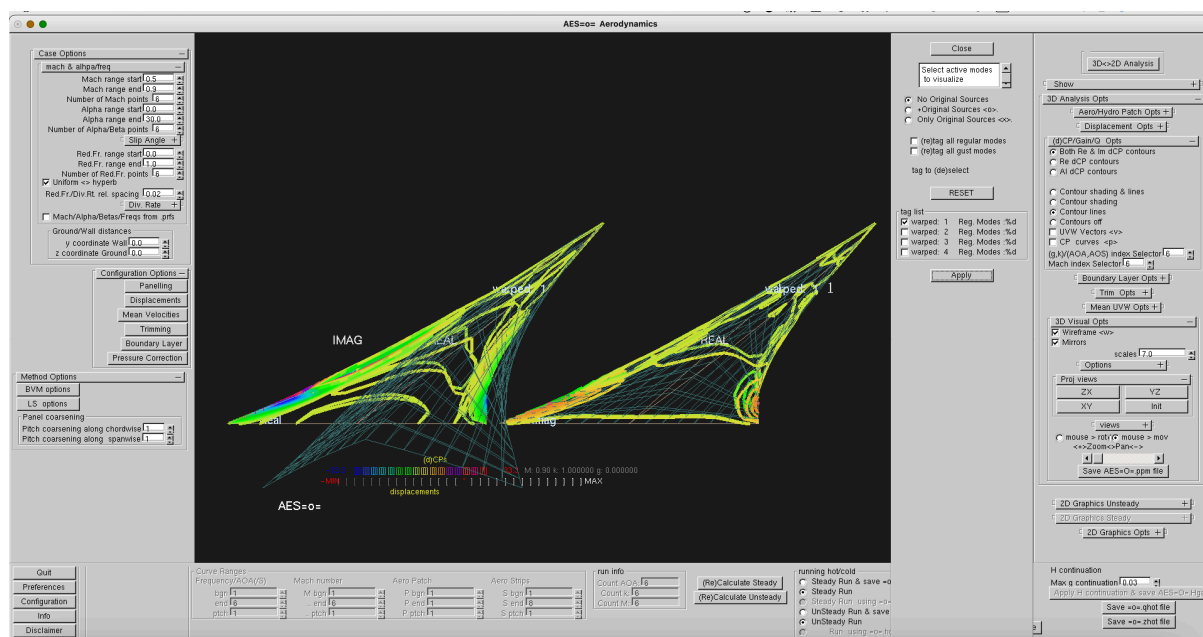


Figure 88 Real (left) and Imaginary part of the unsteady pressure coefficient distribution combined with the extreme position of the generating first mode at Mach number 0.9 and Reduced Frequency 1.0



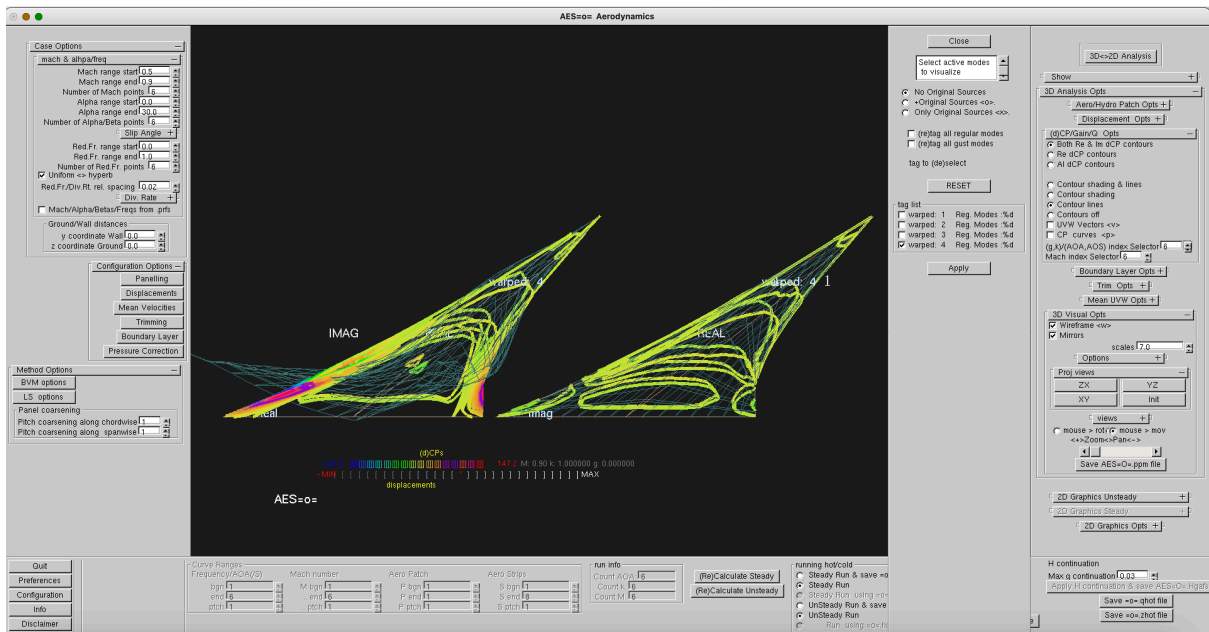


Figure 89 Real (left) and Imaginary part of the unsteady pressure coefficient distribution combined with the extreme position of the generating fourth mode at Mach number 0.9 and Reduced Frequency 1.0

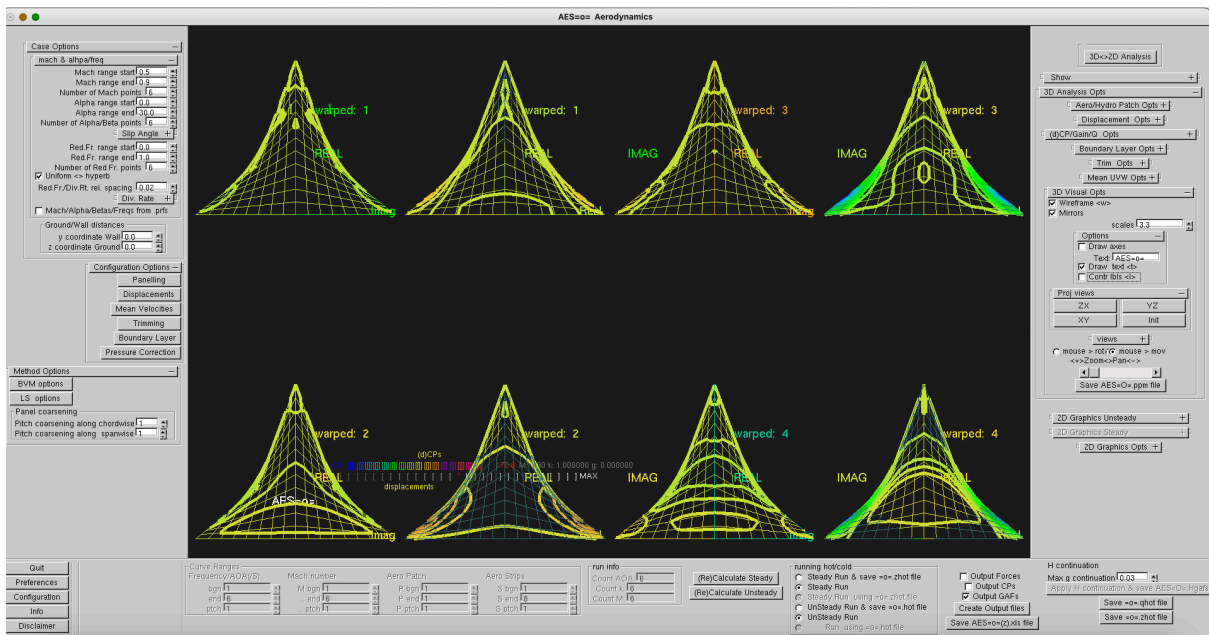


Figure 90 Real and Imaginary parts of the unsteady pressure coefficient distribution for the four modes at Mach number 0.9 and Reduced Frequency 1.0





## Conclusions

This report has described the detailed formulations and usage of the aerodynamic /hydrodynamic and acoustic calculation methods embedded in AES=O=. Steady and unsteady surface pressure and loads distributions of complete aircraft/watercraft can be predicted effortlessly with AES=O= and might form the basis of a design generation or a second opinion.

AES=O= incorporates a very flexible panel method avoiding unacceptably large turn-around times, especially when dealing with design, certification and qualification studies and modifications/installation effects reckoning with aerodynamic, hydrodynamics, aeroacoustics, and aeroelastic applications and a low level of effort at work-floor level.

AES=O= deals with simple three-dimensional shapes (wings) to complete fixed wing aircraft/watercraft and arbitrary two-dimensional shapes (airfoils and arbitrary cross sections). The applications are easy to use for engineers, the processes are easily repeatable, robust and fast.

As a bonus, the mollifier/VSIC method has been described in detail and demonstrated.

## Bibliography

- [1] M. H. L. Hounjet, "Calculation of unsteady subsonic and supersonic flow about oscillating wings and bodies by new panel methods," in *IFASD*, Aachen, 1989.
- [2] M. H. L. Hounjet, "Transonic panel method to determine loads on oscillating airfoils with shocks," *AIAA Journal*, vol. 19, no. 5, pp. 559-566, 1981.
- [3] M. H. L. Hounjet, "Installation and Compact Userguide AES=3=," Le Cannet des Maures, March 2023.
- [4] V. Bertram, "A Rankine Source Method for the Forward-Speed Diffraction Problem," Technische Universität Hamburg-Harburg, Hamburg, 1990.
- [5] J. R. Hoff, "Three-dimensional Green Function of a Vessel with Forward Speed in Waves," Dr. Ing thesis, Division of Marine Hydrodynamics, Norwegian Institute of Technology, Trondheim, Norway, 1990.
- [6] B. Kim and Y.-S. Sliin, "Steady Flow Approximations in Three-Dimensional Ship Motion Calculation," *Journal of Ship Research*, pp. pp. 229-249, Vol.51, No. 3, September 2007.
- [7] M. H. L. Hounjet and B. J. G. Eussen, "Prospects of time-linearized unsteady calculation methods for exponentially diverging motions in aeroelasticity," in *SDM/Dynamic Specialist*, Dallas, April 1992.
- [8] M. H. L. Hounjet, "Verification of H flutter analysis," *Journal of Aircraft*, vol. 47, no. 6, 2010.
- [9] M. H. L. Hounjet, "Evaluation of Elastomechanical and Aerodynamic Data Transfer Methods for Non-planar Configurations in Computational Aeroelastic Analysis," in *International Forum on Aeroelasticity and Structural Dynamics*, Manchester, 1995.
- [10] M. H. L. Hounjet and et al, "Efficient AeroElastic Analysis," Amsterdam, 2003.
- [11] M. H. L. Hounjet, "Hyperbolic grid generation with BEM source terms," in *IABEM-90 Symposium of the International Association for Boundary Element Methods, October 15-19, 1990, Rome, Italy*, Rome, 1990 September.
- [12] J. C. F. Telles, "A self-adaptive co-ordinate transformation for efficient numerical evaluation of general boundary element integrals," *International journal for numerical methods in engineering*, vol. 24, pp. 959-973, 1987.
- [13] J. L. Hess, "Calculation of acoustic fields about arbitrary three-dimensional bodies by a method of surface source distributions based on certain wave number expansions," DAC 66901, 1968.
- [14] A. R. Dusto and M. A. Epton, "An advanced panel method of analysis of arbitrary configurations in unsteady subsonic flow," NASA CR 152323, 1980.



- [15] E. F. Ehlers, M. A. Epton, F. I. Johnson, A. E. Magnus and P. Ruppert, "An improved higher order panel method for linearized supersonic flow.," in *AAIA Paper 78-15*, 1978.
- [16] M. T. Landahl, *Unsteady transonic flow*, New York: Pergamon Press, 1961.
- [17] J. L. Sims, "Tables for supersonic flow around right circular cones at zero angle of attack," NASA SP-3004, 1964.
- [18] M. H. L. Hounjet, "Installation and Compact Userguide AES=3=," AES4AC, Le Cannet des Maures, March 2023.
- [19] W. E. Cummins, "The force and moment on a body in a time-varying potential flow," *Journal of ship research*, pp. pp. 7-18, pp. 54., April 1957.
- [20] E. Polhamus, "A concept of the vortex lift of a sharp-edge delta wings based on a leading-suction-suction analogy," NASA TN D-3767, December 1966..
- [21] M. H. L. Hounjet, "ARSPNS: A method to calculate steady and unsteady potential flow about fixed and rotating lifting and non-lifting bodies.," NLR, Amsterdam, October 1985.
- [22] M. H. L. Hounjet, "ARSPNSC: A method to calculate subsonic steady and unsteady potential flow about complex configurations.," NLR, Amsterdam, November 1986..
- [23] M. H. L. Hounjet, "FTRANS and FTRAN3: Methods ot calculate steady and time-linearized unsteady potential flow about wings in transonic flow.," NLR TR 87020 L, January 1987., Amsterdam, 1987.
- [24] M. H. L. Hounjet, "CAR 88 a method to calculate subsonic and supersonic, steady and unsteady, potential flow about complex configurations," NLR TR 88154 U, 1988.
- [25] R. N. Desmarais, "An accurate and efficient method for evaluating the kernel of the integral equation relating pressure to normal wash in unsteady potential flow.," in *Structural Dynamics*, AIAA 82-687, May 1982.
- [26] W. P. Rodden, J. P. Giessing and T. P. Kalman, "New developments and applications of the subsonic doublet lattice methods for non-planar configurations.," AGARD CP-80-71, Part 2, No. ,4, 1971.
- [27] E. T. Copton, *asymptotic expansions*, Cambridge: Cambridge university press, 1965.
- [28] AGARD, "Manual on aeroelasticity Volume 6," AGARD, 1971.
- [29] M. H. L. Hounjet and et al, "Outline and application of the NLR aeroelastics imulation method.," in *ICAS Paper 94-5.8.2 also NLR TP 94422*, September 1994..
- [30] R. L. Harder and R. N. Desmarais, "Interpolation using surface splines," *Journal of Aircraft*, vol. 9, no. 2, pp. 189-191, feb. 1972.
- [31] M. H. L. Hounjet and et al, "Experiences in Aeroelastic Simulation Practices," in *EUROMECH colloquium 349*., Gottingen, 1996.

- [32] M. H. L. Hounjet, "Aeroacoustic simulations of the ERICA tilt-rotor during descent flight," NLR CR-2007-845, Amsterdam, 2007.
- [33] M. H. L. Hounjet, "Meshing around with AES=V=," AES4AC, Berg en Terblijt, 2021.
- [34] O. L. Dieterich, Hounjet M. H. L. and et al, "HeliNOVI: Current Vibration Research Activities," in *31st European Rotorcraft Forum*, Florence, Italy, 2005.
- [35] H. H. L. Van Tongeren, Hounjet, M. H. L. and et al, "Development pf a fighter aircraft aeroelastic model based on a existing global-stress model," in *IFASD IFASD-2009-036*, Seattle, 2009.
- [36] M. H. L. Hounjet, "Aeroelastic Application of AES=V=," AES4AC, Berg en Terblijt, 2020.
- [37] W. Gordon and C. Hall, "Construction of curvilinear coordinate systems and application to mesh generation," *International Journal for Numerical Methods in Engineering*, vol. 4, no. 7, p. 461–477, 1973.
- [38] M. H. L. Hounjet, "An application of AES=3=," AES4AC B.V., Berg en Terblijt, 2017.
- [39] J. M. J. Journee, "Experiments and Calculations on 4 Wigley Hull Forms in Head Waves," Delft, 1992.
- [40] R. Coene, "A slender deltawing oscilating in surface waves. An example in unsteady propulsion,," Technische University Delft, department of aerospace engineering,, Delft, 1977.
- [41] E. C. J. Yates, "AGARD standard aeroelastic configurations for dynamic response.I-wing 445.6," AGARD, 1988.
- [42] M. H. L. Hounjet, "De golfweerstand van een deltavleugel,," TUD Ingenieursverslag sept. 1975., Delft, 1975.
- [43] M. Lagally, " Berechnung der Kräfte und Momente, die stromende Flüssigkeiten auf ihre Begrenzung ausüben," *Zeitschrift fur angewandte Mathematik und Mechanik*, p. Vol. 2, 1922.
- [44] D. D. Liu and e. al, "From Piston Theory to a Unified Hypersonic-Supersonic Lifting Surface Method," *Journal of Aircraft*, vol 34, no 3, 1997.
- [45] B. B. Prananta and M. H. L. Hounjet, "Computational Unsteady Aerodynamics in Aeroelastic Simulations," in *ICAS*, Melbourne, 1998.



## Appendix AES4AC B.V.

AES4AC B.V. ([www.aes4ac.com](http://www.aes4ac.com)) provides expert assistance and software in aero-elasticity and flutter speed prediction for Subsonic, Transonic, Supersonic and Hypersonic operations.

The followings methods are available:

- AES=2=: Calculates 2D unsteady aerodynamic forces & pressures on (partly(effectors)) oscillating flat plates in frequency domain, Incompressible, subsonic, sonic and supersonic/Hypersonic
- AES=W=: Calculates 2D unsteady aerodynamic. forces & pressures on (partly(effectors)) oscillating flat plates. The flat plate is placed in between upper and lower walls.
- AES=3=: Calculates 3D unsteady aerodynamic. forces&pressures on oscillating surfaces in incompressible, subsonic and supersonic/Hypersonic flow.
- AES=V=: Aeroelastic Pre and Postprocessor for geometry, warping & mollifying, Grid generation and flutter & time trace analysis.
- AES=O=: Prediction & analysis of 2D & 3D steady & unsteady aerodynamic/hydrodynamic pressures/forces on platforms (thick & flat surface panel methods. Incompressible, subsonic (~transonic) and supersonic/hypersonic

Also flutter support based on linear and nonlinear unsteady CFD methodology (Full Potential, Euler, Reynolds Averaged Navier Stokes(URANS), Thin Layer Reynolds Averaged Navier Stokes(TLNS), Baldwin Lomax and Spalart Allmaras turbulence models). True surface and transpiration boundary conditions.

AES4AC B.V. performs very fast and efficient A/C flutter analysis and calculation of generalised airforces by means of its aero-elastic workbench importing generalised mass, stiffness, node coordinates and mode shapes obtained from FEM applications.

Contact: [michael.hounjet@gmail.com](mailto:michael.hounjet@gmail.com)

247 Chemin Saint Clair  
83340 Le Cannet des Maures  
France

+33 6 69 48 39 30

Linkedin	<a href="http://www.linkedin.com/pub/michael-hounjet/7/995/9b">www.linkedin.com/pub/michael-hounjet/7/995/9b</a>
Academia	<a href="https://independent.academia.edu/MichaelHounjet">https://independent.academia.edu/MichaelHounjet</a>
Researchgate	<a href="https://www.researchgate.net/profile/Michael_Hounjet/2">https://www.researchgate.net/profile/Michael_Hounjet/2</a>
AES4AC	<a href="http://www.aes4ac.com">www.aes4ac.com</a>

## List of Figures

Figure 1 The datasets of the mollifier procedure. Left top the data to be injected. Left bottom the baseline data. Right top the resulting composed data.....	48
Figure 2 The datasets of the mollifier procedure. Bottom the baseline data. Top the resulting composed data .....	48
Figure 3 The datasets of the mollifier procedure. Left top the injected scattered data to be injected visualised after triangularization. Left bottom the baseline data. Right top the resulting composed data. ....	49
Figure 4 Contour plots of the datasets of the mollifier procedure. Left bottom the data to be injected. Left bottom the baseline data. left top the resulting composed data.....	49
Figure 5 Calculated steady pressure coefficient and velocity distributions on a set of donuts at a subsonic Mach number and relatively high angles of attack and sideslip .....	61
Figure 6 Calculated steady pressure coefficients and velocity distribution on a set of payloads at a relatively high subsonic Mach number. Mach is 0.9, Angle of Attack 30° and Angle of Sideslip 30° for a set of 8 payloads. ....	61
Figure 7 Inspection/generation panelling (changing dihedral & thickness of a thick wing)...	62
Figure 8 Warping on a F4 wing body.....	62
Figure 9 Unsteady pressure distributions on an oscillating rectangular wing in a transonic flow condition Mach number 0.875 and reduced frequency 1.0. ....	63
Figure 10 Inspection of calculated steady Cp distribution at upper side of a thick wing at Mach = 0.9 and AOA=20°.....	64
Figure 11 Inspection of calculated steady Cp distributions at spanwise sections of a thick wing at Mach = 0.9 and AOA=0.83°.....	64
Figure 12 Inspection of calculated Cl-Cd curves at Mach number =0.2 .. 0.9 of a thick 445.6 AGARD wing.....	65
Figure 13 Inspection of calculated real part of unsteady Cp distribution at upper side of a thick wing at extreme position of the mode shapes at Mach 0.9 and reduced frequency=1... ..	66
Figure 14 Inspection of calculated generalized forces GAF11, GAF22, GAF33 and GAF 44 on thick wing 445.6 at Mach=0.9 .....	66
Figure 15 Unsteady pressure distributions due to the first mode on the thick 445.6 wing .....	67
Figure 16 Inspection of calculated Cp and wave elevation due to a Wigley hull moving at various Froude numbers .....	68
Figure 17 Inspection of calculated Cp and wave elevation due to a sphere moving at various Froude numbers and at various depths. Inspection of calculated Cp and wave elevation due to a sphere moving at various Froude numbers and at various depths. ....	69
Figure 18 Inspection of calculated Cp and wave elevation due to Coene's delta wing moving at various Froude numbers and angle of attack [40] .....	70
Figure 19 Inspection of calculated Cp and wave elevation due to a spheroid moving at various Froude numbers .....	71
Figure 20 Inspection of calculated forces (Drag, Lift and Moment) on a submerged ellipsoid .....	72
Figure 21 Comparison of calculated forces (Drag, Lift and Moment) on a submerged ellipsoid with results presented in [4]. The symbols are from [4]......	72
Figure 22 SPL levels on finite cylinder and observer plane.....	73
Figure 23 The start-up screen of AES=O= in aerodynamic mode .....	78
Figure 24 The start-up screen of AES=O= in hydrodynamic mode.....	78
Figure 25 The start-up screen of AES=O= in aeroacoustics mode .....	79
Figure 26 Activation.....	80
Figure 27 Panelling Window.....	87



Figure 28 Aero patch control.....	88
Figure 29 Left part aero/hydro patch control .....	88
Figure 30 Right part aero/hydro patch control .....	88
Figure 31 Model Options.....	89
Figure 32 Model Options.....	90
Figure 33 Edge Options.....	92
Figure 34 Left part edge options window.....	92
Figure 35 Right part edge options Window .....	93
Figure 36 The patch edit window .....	96
Figure 37 Main Displacement Window (Downwash and Inspection) .....	98
Figure 38 The Downwash Window.....	98
Figure 39 The rigids .....	99
Figure 40 The sub rigids.....	99
Figure 41 Regular Modes .....	100
Figure 42 Warp Options Window .....	101
Figure 43 Polynomial modes.....	102
Figure 44 Coefficients of the polynomial displacements .....	102
Figure 45 The special modes window .....	103
Figure 46 Adding/Creating Gust modes.....	103
Figure 47 Adding/Creating Wave modes .....	103
Figure 48 The deadbeat patch window.....	104
Figure 49 UVW Window .....	105
Figure 50 UVW Window .....	105
Figure 51 Activation of a trim vector .....	106
Figure 52 Boundary Layer Correction Window.....	106
Figure 53 Boundary Layer Correction Window.....	107
Figure 54 Gains Window.....	107
Figure 55 Gains Window.....	108
Figure 56 Impedance window .....	108
Figure 57 Incident fields window.....	108
Figure 58 Configuration Window .....	114
Figure 59 Info Window .....	114
Figure 60 Activation Window.....	115
Figure 61 Bottom bar right row.....	116
Figure 62 Bottom Bar mid row .....	116
Figure 63 Bottom bar mid row .....	116
Figure 64 Rollouts with respect to the visualization of the pressures, gains, impedance & uvw .....	126
Figure 65 Rollout with respect to the visualization of the pressures and waves .....	127
Figure 66 Rollout with respect to the visualization of the explicit velocity field .....	130
Figure 67 Workbench AES=O= at startup in aerodynamic mode.....	138
Figure 68 Setting the case parameters.....	138
Figure 69 The applied primary patch model control .....	139
Figure 70 The applied edge conditions .....	139
Figure 71 The applied BVM model options.....	140
Figure 72 Applied warping options.....	141
Figure 73 Opening the panel window .....	142
Figure 74 Opening the Displacement Window .....	142

Figure 75 Opening the patch create et cetera window.....	143
Figure 76 Changing wing 445.6 to a wing with gothic signature .....	143
Figure 77 Automatic warping of wing445.6 modes on the Gothic planform .....	144
Figure 78 Overall Forces versus Angle of Attack, Constant Mach Curves .....	144
Figure 79 Overall forces versus Mach number, Constant Angle of Attck curves.....	145
Figure 80 Overall Forces versus Cd, Constant Angle of Attack curves.....	145
Figure 81 Overall Forces versus Cd, Constant Mach number curves .....	146
Figure 82 Visualisation of the Pressure Coefficient at Mach number is 0.5 and Angle of Attack 30 deg.....	146
Figure 83 Visualisation of the Pressure Coefficient distribution and the velocities at Mach number is 0.9 and Angle of Attack is 30 deg .....	147
Figure 84 Unsteady Overall Forces versus Reduced Frequency, Constant Mach number curves.....	147
Figure 85 Unsteady Overall Forces versus Mach number, Constant Reduced Frequency Curves.....	148
Figure 86 Diagonal Generalised Forces versus Mach number, Constant Reduced Frequency Curves.....	148
Figure 87 Generalised Forces versus Mach Number, Constant Reduced Frequency Curves	149
Figure 88 Real (left) and Imaginary part of the unsteady pressure coefficient distribution combined with the extreme position of the generating first mode at Mach number 0.9 and Reduced Frequency 1.0 .....	149
Figure 89 Real (left) and Imaginary part of the unsteady pressure coefficient distribution combined with the extreme position of the generating fourth mode at Mach number 0.9 and Reduced Frequency 1.0 .....	150
Figure 90 Real and Imaginary parts of the unsteady pressure coefficient distribution for the four modes at Mach number 0.9 and Reduced Frequency 1.0 .....	150





## List of Tables

Table 1 Geometry file.....	51
Table 2 Connections .....	53
Table 3 Alternatives to BVM method .....	55
Table 4 Radiation Condition at free surface.....	55
Table 5 General Displacement File .....	56
Table 6 Polynomial file .....	57
Table 7 File outputs .....	59
Table 8 Left sidebar in aerodynamic mode .....	82
Table 9 Left Sidebar in hydrodynamic mode .....	83
Table 10 Left Sidebar in Aeroacoustics mode .....	84
Table 11 Main Case Parameters Rollout in aerodynamic/aeroacoustics mode.....	85
Table 12 Main Case Parameters Rollout in hydrodynamic mode .....	86
Table 13 Listbox options basic patch control.....	89
Table 14 Model listbox options .....	91
Table 15 Selectable edge options .....	95
Table 16 BVM Window .....	109
Table 17 BVM Window Hydrodynamic mode .....	110
Table 18 BVM Window aeroacoustics mode.....	111
Table 19 Lifting Surface Window .....	112
Table 20 Preferences Window.....	113
Table 21 The right sidebar with steady graphics rollout .....	119
Table 22 The right sidebar with steady graphics rollout .....	120
Table 23 2D Graphics Unsteady Rollout.....	121
Table 24 GAF (GHF) Selection Window.....	122
Table 25 Select the active mode .....	122
Table 26 2D Graphics Unsteady rollout in hydrodynamic mode.....	123
Table 27 Rollout dealing with the visualisation of the geometry.....	124
Table 28 Rollout dealing with the visualisation of the geometry.....	124
Table 29 Rollouts and mode selection window with respect to the visualization of the displacements, waves, gusts and fields.....	125
Table 30 Rollout with respect to the visualization of the boundary layer thickness .....	128
Table 31 Rollout with respect to the visualization of the trimmed state .....	129
Table 32 Controller of the 3D Graphics .....	131
Table 33 .prefs_aes=o= file .....	134
Table 34 The outputs .....	135